

MEASUREMENTS OF INTERFERENCE TO TELEVISION RECEPTION
CAUSED BY THE MOD-1 WIND TURBINE AT BOONE, NC

Technical Report No. 1

by

Dipak L. Sengupta, Thomas B.A. Senior
and Joseph E. Ferris

Radiation Laboratory
Department of Electrical and Computer Engineering
The University of Michigan
Ann Arbor, Michigan 48109

January 1981

Prepared for:

Midwest Research Institute
Solar Energy Research Institute
Golden, CO 80401

Work performed under Contract No. DE-SERI-XH-0-9263-1

ABSTRACT

Electromagnetic interference to television reception caused by the MOD-1 WT at Boone, NC, has been studied by measuring the ambient field strengths, static (blade) scattering and TV interference at a number of sites in the vicinity of the WT. The commercial TV signals available in the area were used as the RF sources. Tests were performed at the top and bottom of the WT tower, and at ten other sites chosen to represent the region around the WT.

The ambient field strengths were generally low at all ten sites on all of the available TV Channels. At the WT site, the field strengths were quite strong and about 30 to 40 dB higher than at the test sites. The equivalent scattering area of each blade determined from the static tests was very close to the 40 m^2 predicted on the basis of laboratory measurements of scale model MOD-0 blades. The static tests also showed that, under some conditions, the metallic walls of the nacelle housing can produce significant scattered signals. Dynamic measurements indicated varying amounts of TVI at all sites on all Channels. With a high performance antenna, the backward region interference observed was judged acceptable, showing that such an antenna can reduce and/or overcome the higher levels of interference that were found with a low quality antenna. Forward region interference extended further from the WT and, as expected, could not be reduced by using a high performance antenna. For both types of interference, the theoretical results were in good agreement with the measured data. Based on the results

obtained, it would appear that the forward region interference on Channel 5 can exceed the level of acceptability out to 5 or 6 km in a southeasterly direction from the MOD-1 WT at Boone.

NOTICE

This report was prepared as an account of work sponsored by an agency of the United States Government. Neither the United States nor any agency thereof, nor any of their employees, makes any warranty, expressed or implied, or assumes any legal liability or responsibility for any third party's use or the results of such use of any information, apparatus, product or process disclosed in this report, or represents that its use by such third party would not infringe privately owned rights.

ACKNOWLEDGEMENTS

It is a pleasure to acknowledge the assistance of various individuals in the completion of the measurement program. We are particularly grateful to Mr. J. Pond of the University of Michigan Radiation Laboratory, Mr. T. Lamb, Mr. J. Brown and Mr. T. Miller of the WT site group, and Mr. D. Garrelts of SERI, for their assistance during the measurements; and to Mr. J. Moretz, Ms. P. Grimes and Mr. O. Adams of BREMCO for providing us with the necessary help at the test sites.

Successful completion of the program would not have been possible without the coordinating efforts of Mr. N. Kelley of SERI, Mr. J. Collins of NASA Lewis and Mr. R. Bumgarner of BREMCO.

Our thanks are also due to Professor Ronkowski of the Physics Department, Appalachian State University, for the loan of a strip chart recorder; to the University for allowing us to conduct tests at the A.S.U. Water Treatment Plant, and to Dr. G. L. Resse, Mr. and Mrs. H. Folk, Mr. T. Miller, Mr. M. Miller and Mr. J. Brown for making their property available as test sites and providing the necessary power.

We wish to express our thanks to Ms. Wanita Rasey for her expert and patient typing of the report.

EXECUTIVE SUMMARY

Electromagnetic interference to television reception caused by the MOD-1 wind turbine (WT) at Boone, NC, has been studied by carrying out detailed measurements at a number of sites in the vicinity of the WT. The commercial TV signals available in the area were used as the RF sources during the measurements. Tests were performed at the top and base of the WT tower, and at ten other sites chosen to represent the region around the WT. For some TV Channels all of the sites were in the backward interference region of the WT, but with other Channels some of the sites were also in the forward interference region.

At each site some or all of the following types of measurement were performed on all of the available TV Channels: (i) Ambient Field Strength. With the WT stationary, the strength of the received signal was measured by rotating the main beam of the receiving antenna until the output was a maximum. The ambient field strength at the site was then determined from the data by eliminating the effects of the antenna and the associated system losses. This provided information about the expected quality of TV reception in the area, and also the field strengths of the various TV Channels at the WT relative to those at a test site, which play an important role in the TVI effects produced by the WT. (ii) Static or Blade Scattering. With the WT blades locked in a desired (usually vertical) position and their pitch set for maximum power, the WT was yawed in azimuth through 360°. By measuring the

TV signals received with the antenna pointed at the WT, the maximum blade-scattered signals were determined. From these results, the equivalent scattering area (A_e) of each blade was determined. These measurements were important because the interference caused by the WT is directly proportional to A_e . (iii) Dyanamic or Television Interference (TVI). These tests were performed with the WT rotating by recording the received signal vs. time with the antenna directed at the desired transmitter or at the WT, while observing the received picture on the TV screen for any video distortion. Video recordings were made whenever it was felt desirable to preserve the video effects for future evaluation. In addition, the received signal vs. antenna beam pointing direction was also obtained for each TV Channel. These measurements provided substantial information, and were used to judge the following: (a) the horizontal plane pattern of the antenna in the actual test environment, (b) the effect of the windmill and/or its blade rotation on the signal received from any direction, and (c) an estimate of the amount of signal modulation caused by the blade rotation.

The equipment setup and the measurement procedures were similar to those employed in our previous studies. A high performance receiving antenna (the Winegard) was used at all sites, and at one site two low performance antennas were also used to show the effect of antenna quality on the observed TVI.

The ambient field strength measurements indicated that in the city of Boone and its surrounding area the strengths of all of the TV signals are weak, and the quality of reception in the area is

generally poor to unacceptable even with a high performance receiving antenna. At the WT the field strengths were found to be 30 to 40 dB higher than those at all of the other sites.

The equivalent scattering area of each blade determined from static tests using two different Channels at one site and a third Channel at a second site was very close to the 40 m² predicted on the basis of laboratory measurements of scale model MOD-0 blades. The static tests also showed that, under some conditions, the metallic walls of the nacelle housing can produce significant scattered signals.

The dynamic measurements indicated that: (a) Varying amounts of TVI were produced at all sites and on all of the available TV Channels. (b) With the high performance antenna, most of the backward region interference produced video distortion that was judged to be acceptable. With a low performance antenna, however, the observed TVI was greater, and in some cases exceeded the acceptable level. (c) At a number of sites, forward region interference was observed on Channels 5, 8 and 11. In particular, the TVI on Channel 5 extended farthest from the WT, and as expected, these effects could not be reduced or overcome by using a high performance antenna. From an analysis of the Channel 5 data, it appears that unacceptable forward region interference could extend up to 5 km SE from the WT on this Channel.

The equipment setup and the measurement procedures were found to be adequate, and can be used for any future TVI measurements on WTs of this (or similar) type.

Generally, the agreement between experiment and theory was good, and the theory therefore constitutes a valid means for predicting the TV interference produced by horizontal axis machines. The key items of information required are the equivalent scattering area of a blade, and the ambient field strengths on all of the available TV Channels at the WT and at the receiving sites of interest. Given this information, our analysis of the test data obtained at Boone indicates that the TV interference effects can be predicted with adequate accuracy using the approximate theory that has been developed.

TABLE OF CONTENTS

	<u>Page</u>
NOTICE	i
ACKNOWLEDGEMENTS	ii
EXECUTIVE SUMMARY	iii
CHAPTER 1. INTRODUCTION	1
CHAPTER 2. BACKGROUND INFORMATION	3
2.1 Physical Environment	3
2.2 TV Stations	8
2.3 The Interference Phenomenon	14
2.4 Test Sites	21
CHAPTER 3. TEST EQUIPMENT AND PROCEDURES	28
3.1 Equipment	29
3.2 Antennas	35
3.3 Types of Measurement	54
3.4 Measured Antenna Response	64
CHAPTER 4. MEASURED AMBIENT FIELD STRENGTHS	71
4.1 Data Reduction	72
4.2 Signal Strengths at the WT	77
4.3 Signal Strengths at Sites A-J	79
4.4 Signal Strengths along the Road near Site A	83
4.5 Conclusions	86
CHAPTER 5. BLADE SCATTERING (STATIC TESTS)	88
5.1 Procedure	88
5.2 Results	89
5.3 Data Analysis	93
5.4 Discussion	96
CHAPTER 6. TELEVISION INTERFERENCE MEASUREMENTS (DYNAMIC TESTS)	98
6.1 Site A	98
6.1.1 Results Obtained with the Winegard Antenna	99
6.1.2 Results Obtained with the Channel Master Antenna	107

	<u>Page</u>
6.1.3 Results Obtained with a Half-Wave Dipole	107
6.1.4 Data Analysis	116
6.2 Site I	124
6.2.1 Discussion of the Results	124
6.2.2 Data Analysis	129
6.3 Summary of Results	135
CHAPTER 7. CONCLUSIONS	139
APPENDIX A: THEORETICAL CONSIDERATIONS	142
A.1 WT Blade Model and the Coordinate Systems	142
A.2 Received Scattered Field	147
A.3 Modulation Level	152
APPENDIX B: TEST PLAN	155
REFERENCES	159

CHAPTER 1. INTRODUCTION

In early 1979 a MOD-1 WT was erected on Howard Knob above the city of Boone, NC, and dedicated in July of that year. Its operation since that time has produced a number of problems one of which is the intermittent interference with TV reception at homes up to a mile or more from the WT. Almost from the very start, complaints of TV interference began, and records of these complaints have been kept. Preliminary investigations carried out in September 1979 and June 1980 confirmed that the WT was affecting TV reception to a degree that could, in some cases, be quite objectionable, but also indicated that the use of a high performance antenna could be helpful in reducing the interference. Such antennas were installed at selected locations, but since there was no detailed monitoring of the results achieved, it has not been possible to determine whether this approach represents an adequate solution to the interference problem.

Meanwhile, complaints continued to come in and these showed that the interference was even more widespread than had originally been thought. It was therefore decided to carry out a more comprehensive series of tests at a number of designated sites out to a mile or so from the WT to measure the nature and severity of the interference, and to assess the capability of a high performance antenna to reduce (or even suppress) the interference. The measurements were performed during the period 8-26 September 1980. It is the

purpose of this report to describe the measurement program and to document the results obtained.

CHAPTER 2. BACKGROUND INFORMATION

2.1 Physical Environment

Boone is a small city of about 9000 people in the northwest corner of North Carolina. It is the home of Appalachian State University (identified as Appalachian State Teachers College on Fig. 2-1) and nestles in a valley in the Blue Ridge Mountains. The higher mountains nearby form a ridge extending NNW from the city. The highest peaks are about 1500 ft above the city, and the most easterly one is Howard Knob at an elevation of 4420 ft. This peak is one mile north of the city center and the site of the WT.

A topographical map of the area is given in Fig. 2-1. It is a reproduction of part of the 1959 U.S. Geological Survey of the Boone Quadrangle and shows the concentration of homes around the road U.S. 421 and, to a lesser extent, U.S. 221. Since 1959, however, there has been some development of the area. In particular, the region around Buckeye Gap has become more built up, and there are now more homes along Rainbow Trail going NW from the Gap, as well as a few clusters of homes on the east, west and southwest flanks of Howard Knob. These are the regions from which most complaints of TV interference have come, and at a home here the most prominent feature on the horizon is the WT. Although there are homes to the south, either on Jonaluska Road winding up towards Howard Knob from Boone or within the city limits, which are as close to the WT, most of these have CATV service.

A more up-to-date depiction of the population density is Fig. 2-2 which was obtained by splicing together four sheets of the

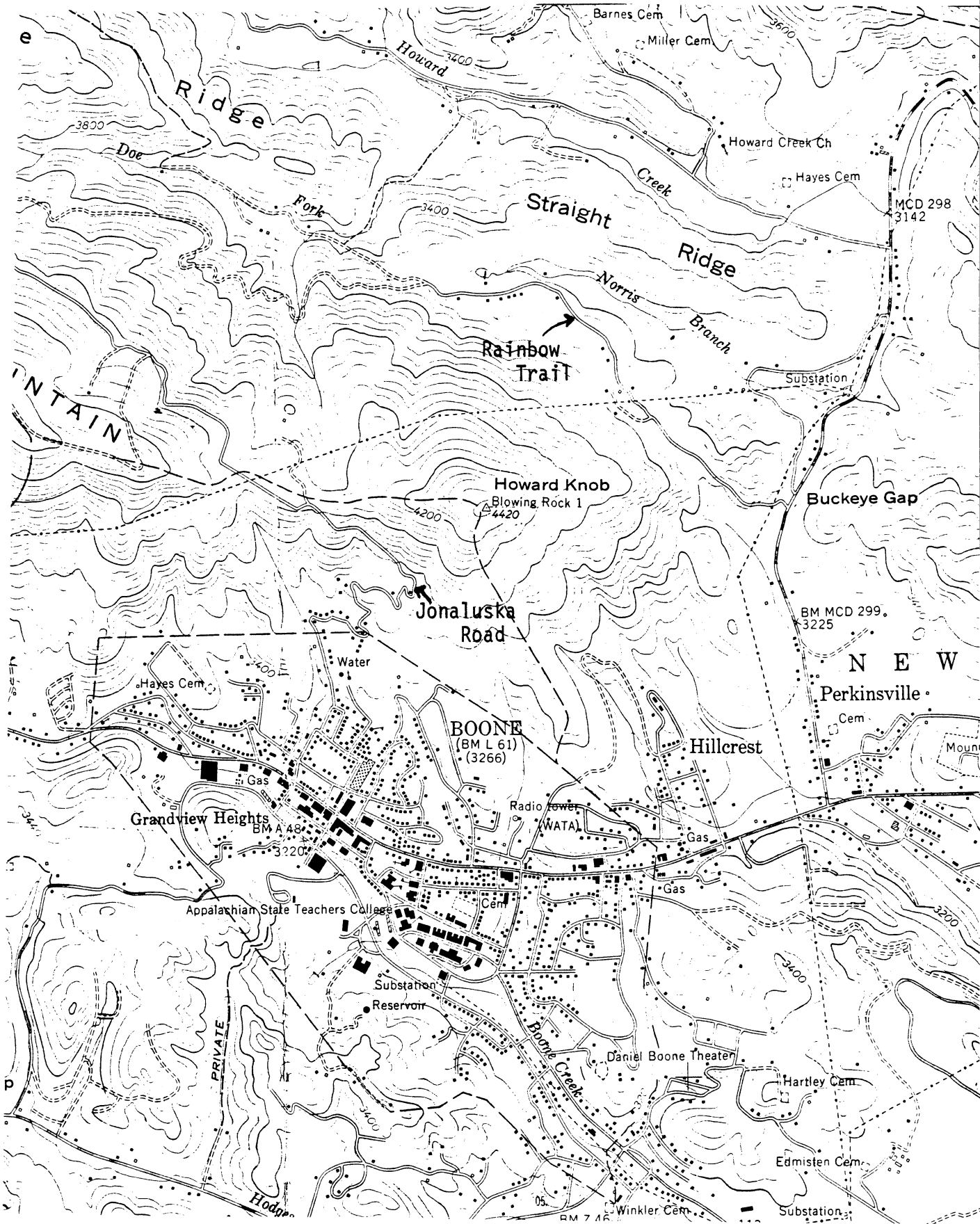


Fig. 2-1: Topographical map of the Boone area
(scale: 1 inch = 0.38 miles = 0.61 km).

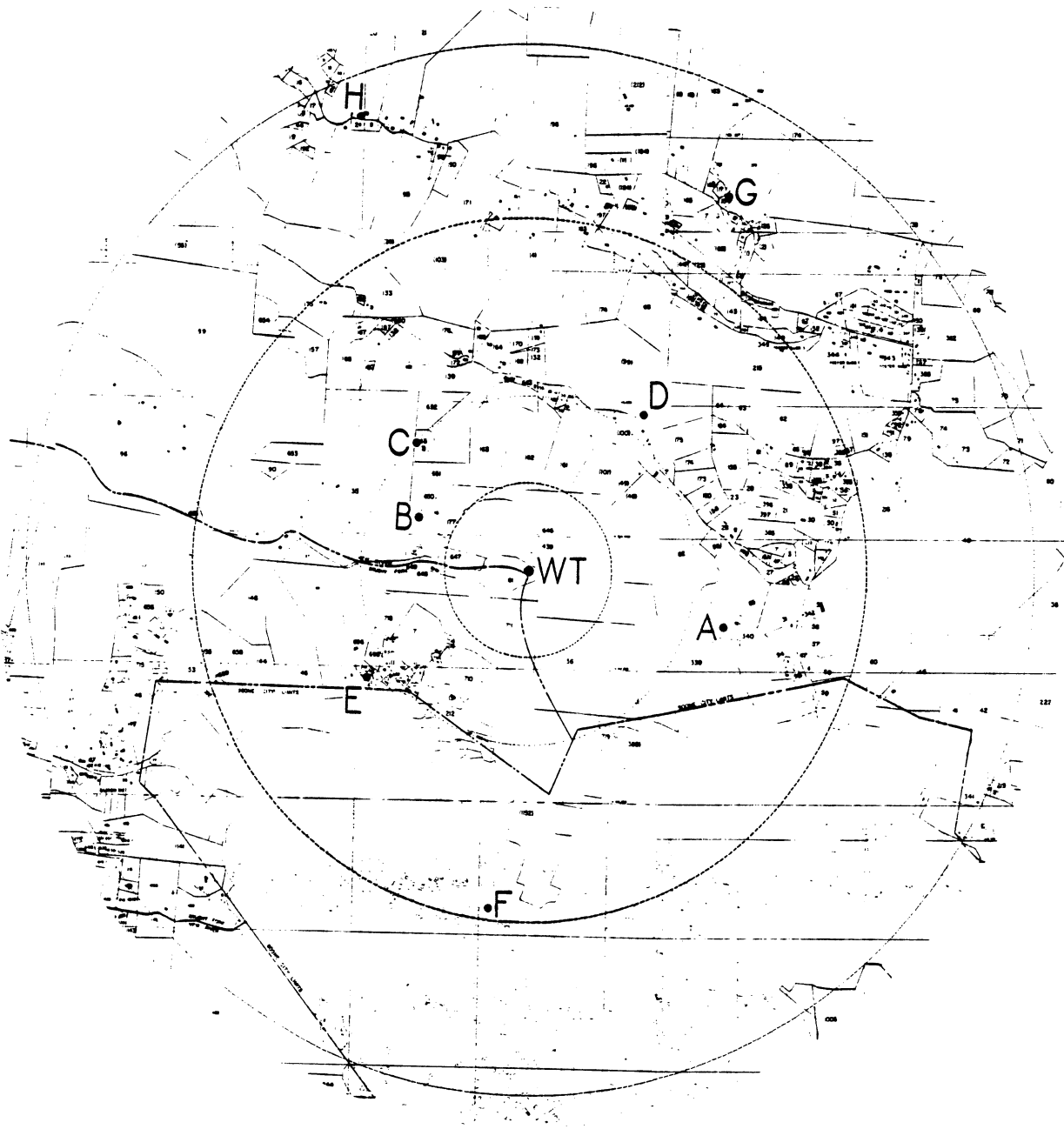


Fig. 2-2: Land ownership map of the Boone area showing dwellings. The broken lines are circles of radii 0.25, 0.5, 1.0 and 1.5 miles centered on the WT.

land ownership map prepared by the Tax Department in Watauga County, NC. Buildings which are believed to be private homes have been marked. The broken lines are circles of radii 0.25, 0.5, 1.0 and 1.5 miles centered on the WT. By actual count the numbers of homes within the various annuli but outside the city limits are as follows:

<u>Miles</u>		<u>Number of homes</u>
0 - 0.25	:	0
0.25 - 0.5	:	30
0.5 - 1.0	:	125
1.0 - 1.5	:	210

The sites at which the rests were performed (see §2.4) are indicated by the letters A through I in Fig. 2-2.

The MOD-1 WT is a two-bladed horizontal axis machine (see Fig. 2-3) designed and built by the General Electric Company [1]. The rated power output is 2 MW and is achieved at a rotor speed of 35 rpm in a 25 mph wind. The machine is tied into the power distribution system of the Blue Ridge Electric Membership Corporation (BREMCO), and the corporation is responsible for its operation. The height to the top of the tower (or, more precisely, the rotor axis) is 140 ft. The steel blades are 200 ft tip-to-tip with a coning angle of 9°, and are individually controlled. The machine cuts in when the wind speed reaches 11 mph and the blades are automatically feathered when the speed exceeds 35 mph.

For the last few years wind data have been collected on Howard Knob. At the height of 150 ft (45.7 m) above ground appropriate to the rotor axis of the WT, data for the period October 1978 through September 1979 show that the stronger winds tend to be from the NW and, to a lesser extent, SW. For wind speeds in the range 0-11, 0-22 and 0-40 mph



Fig. 2-3: View of the MOD-1 WT looking NE.

(i.e., 0-5, 0-10 and 0-18 m/s, respectively), corresponding roughly to the operating range of the WT, the wind rose showing the percent time the wind was in a given sector is shown in Fig. 2-4. The wind direction determines the pointing direction of the WT, and this in turn affects the TV interference at a given site.

2.2 TV Stations

There are nine TV Channels generally available in the Boone area. All are VHF and most of the transmitters are quite far away (see Fig. 2-5). The signals are therefore weak, and would be even without the shadowing produced by the surrounding hills.

Table 2-1 lists the nine Channels, their cities of origin, network affiliations, effective radiated (visual) powers, transmitting antenna locations (latitude and longitude), distances from the WT, and compass bearings. The distances are the great circle ones to the transmitters computed for a smooth spherical earth of radius 6370 km, and the directions are those from which the signals would be received in the absence of any perturbations produced by the terrain [2]. All of the radiated powers are the maxima, based on the antenna heights, allowed by the FCC (see FCC Rules and Regulations, Vol. III, Part 73, p. 277; 1972) for VHF transmitters in Zone II, which includes this part of the U.S.

At most homes in the area there are only a few Channels whose signals are sufficiently strong to provide a reasonable picture, and even with these it is necessary to use a high gain (fringe area) antenna. The particular Channels depend on the location, but most homes have

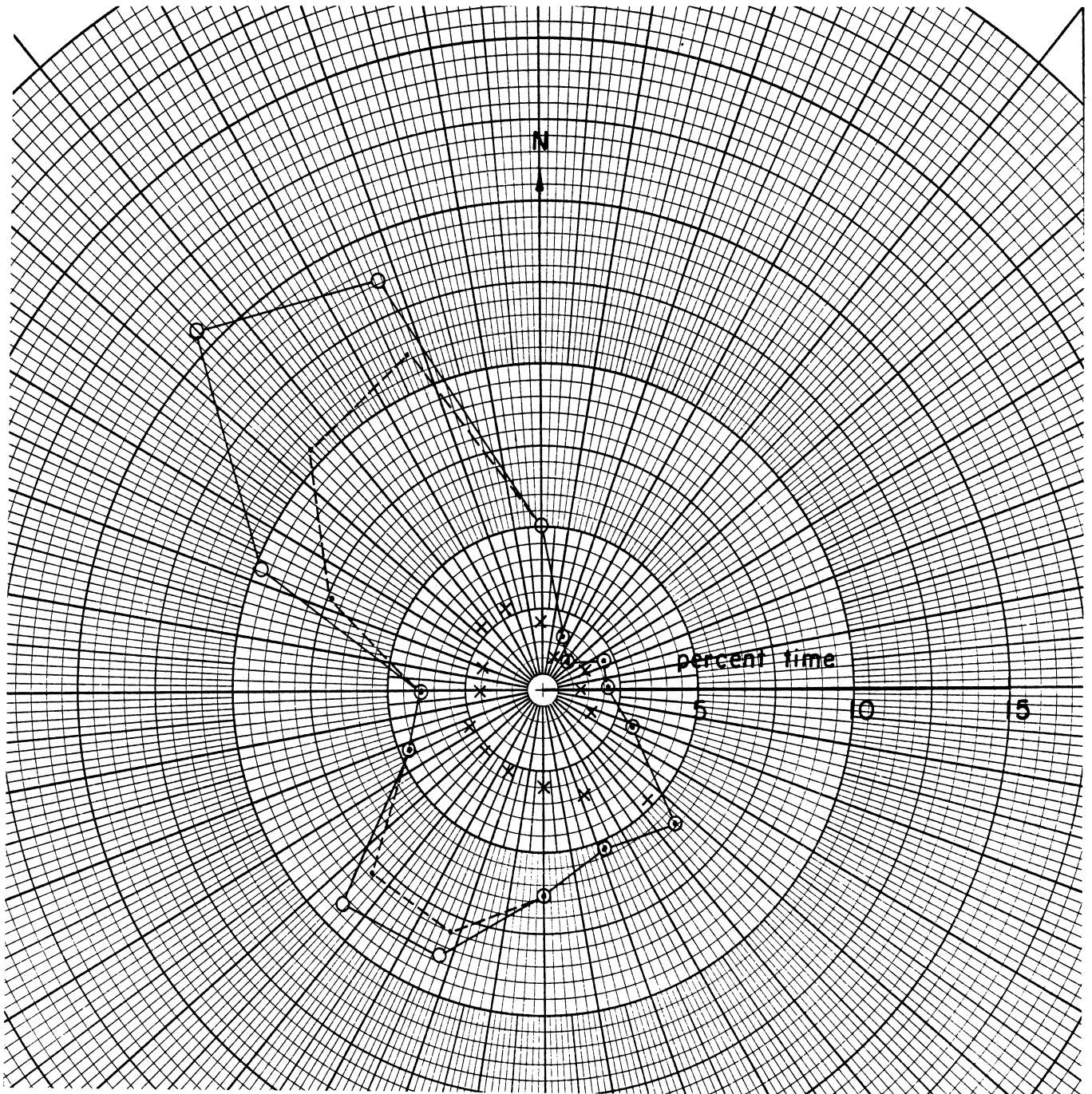


Fig. 2-4: Wind direction at a height 45.7 m above Howard Knob as a percentage of time for the period October 1978 to September 1979: xxx, 0.5 m/s; ..., 0-10 m/s; ooo, 0-18 m/s.

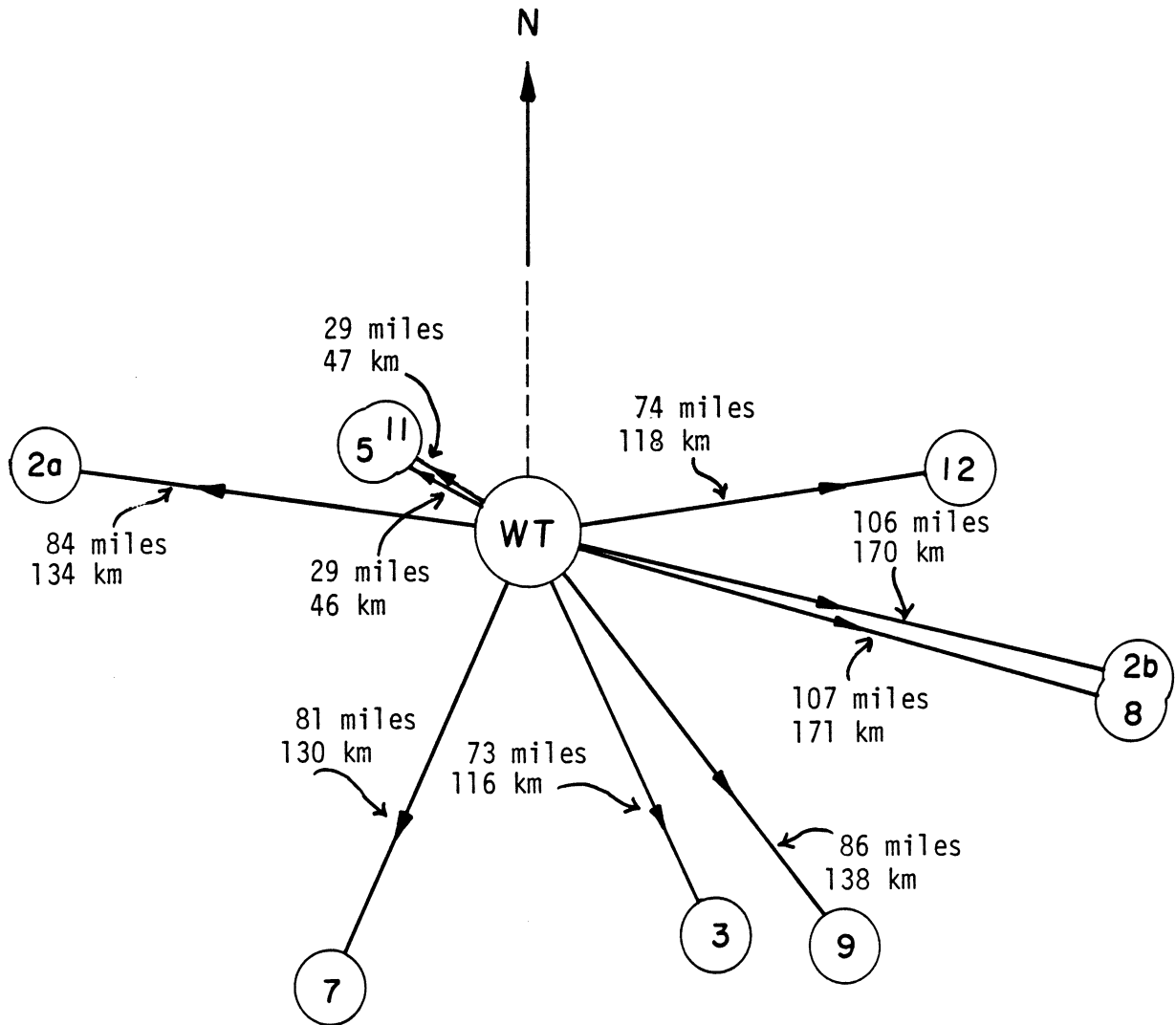


Fig. 2-5: TV Channels available in the Boone area. The vectors are to the corresponding transmitters, drawn to scale:
1 inch = 50.8 miles (1 cm = 20 km)

Table 2-1: TV Channels Available in the Boone Area

Channel	Station Location	Network Affil.	Effec. rad. visual power (kW)	Antenna Location		Distance from WT (in km)	Direction to Trans. (deg. from N)
				Latitude	Longitude		
2(a)	Sneedville, TN	ABC	100	36°22'52"	83°10'48"	134	278
2(b)	Greensboro, NC	CBS	100	35°52'13"	79°50'25"	170	103
3	Charlotte, NC	CBS	100	35°17'50"	81°6'53"	116	154
5	Bristol, VA	NBC	85.1	36°26'57"	82°6'31"	46	302
7	Spartanburg, SC	CBS	294.4	35°10'12"	82°17'26"	130	205
8	High Point, NC	none	316	35°48'47"	79°50'36"	171	105
9	Charlotte, NC	ABC	316	35°15'41"	80°43'38"	138	141
11	Johnson City, TN	CBS	245	36°25'55"	82°8'15"	47	299
12	Winston-Salem, NC	NBC	316	36°22'31"	80°22'27"	118	82

some access to each of the network transmissions, e.g., NBC via Channel 5 or 12. It would appear that the most commonly received Channels are 3, 5, 7 and 11, and, to a lesser degree, 8 and 12. The fact that two Channels 2 are listed in Table 2-1 may seem surprising, but both were picked up during our tests. However, the signals are quite weak throughout most of the area, and Channel 2(a) from Sneedville, TN, is only a viable option for residents to the west of the WT, whilst Channel 2(b) from Greensboro, NC, is a possibility for those to the east.

To provide good video reproduction the received video signal should produce [3] a minimum of 1 millivolt (mV) rms across the input terminals of a TV receiver presenting an impedance of 75Ω , and if the signal produces only 0.2 mV, the picture will be snowy and of generally poor quality. The corresponding video signal powers P_V at the input terminals of the receiver are 1.3×10^{-5} and 5.3×10^{-7} milliwatts (mW), i.e., -49 and -63 dBm respectively, where dBm denotes decibels above a milliwatt. We observe that 14 dBm encompasses the range from good to poor picture quality regardless of frequency (or TV Channel number), and though it is still possible to receive a picture when $P_V \approx -70$ dBm, the quality of the reproduction is then extremely poor.

P_V is the video power referred to in our measurements of ambient field strengths (see chapter 4), and is obtained from the output of a network analyzer. It is not directly a measure of the video carrier field strength E_V (in mV/m), but the latter can be obtained from P_V :

$$E_V = \frac{400 \pi}{\lambda_V} \sqrt{\frac{3P_V}{G}}, \quad (1)$$

where λ_V is the wavelength (in meters) of the video carrier signal, P_V is the power (in milliwatts), and G is the effective gain of the antenna, including any losses in the associated cabling. Because of the wavelength factor in (1), the field strengths needed for a given quality of picture must increase with frequency, and it is customary to cite values for Channels 2-6, 7-13 and 14-83 separately. Thus, for Grade A service (good reception) the minimum allowed* value of the median field strength is

Channels 2-6	:	$E_V = 2.51$ mV/m
7-13	:	$E_V = 3.55$ mV/m

whereas for Grade B service (fringe area reception), the minimum field strength is

Channels 2-6	:	$E_V = 0.224$ mV/m
7-13	:	$E_V = 0.631$ mV/m

With an average antenna such fields would provide the values of P_V that were quoted above.

By these standards the service available to most residents of the Boone area is Grade B (or worse), and except at sites near the tops of the mountains, e.g., at the WT itself or on neighboring Rich Mountain where the CATV antennas are located, none of the signals that were measured (see Section 4-3) approach those necessary for good

*The actual specification [4] of the grade of service is in terms of the median (electric) field strength of the video carrier signal at a height of 30ft (9.1m) above the ground, the median being defined as the value which is exceeded 50 percent of the time at the best 50 percent of the receiver locations.

reception. The low signals have led to the introduction of CATV service, used by most people in the city. Outside the city limits and/or at homes not on CATV, the residents have accustomed themselves to a quality of video reception below that typical in more urban areas, and because the signal levels are often close to the detection threshold of the receiver, even a small amount of interference can now convert the marginally acceptable picture into a virtually unintelligible one.

2.3 The Interference Phenomenon

The rotating blades of a horizontal axis WT can interfere with TV reception by producing video distortion. At a given distance from the WT the interference increases with increasing frequency, and is therefore worse on the upper VHF Channels than on the lower. It also decreases with increasing distance from the machine, but in the worst cases can still produce objectionable video distortion at distances up to a few kilometers. For ambient (primary) signals well above the noise level of the receiver, there is in general no significant dependence on the ambient field strength, and no audio distortion has been observed.

The interference is caused by the time-varying amplitude modulation of the received signal produced by the rotating blades. In a neighborhood of a WT the signals scattered by the blades combine with the primary signal to create a form of time-varying multipath, thereby amplitude modulating the total received signal. The modulation waveform consists of sync pulses, and since each blade of the MOD-1 machine contributes independently, the pulses (whose width is inversely proportional to the electrical length of a blade) repeat at twice the rotation frequency of the blades. If sufficiently strong, these

extraneous pulses can distort the received picture, whereas the audio information, being transmitted by frequency modulation, remains unaffected.

When the blades are stationary the scattered signal may appear on the TV screen as a ghost whose position (separation) depends on the difference between the time delays suffered by the primary and scattered signals. A rotation of the blades then causes the ghost to fluctuate, and if the ghost is sufficiently strong, the resulting interference can be objectionable. In such cases the received picture displays a horizontal jitter in synchronism with the blade rotation. As the interference increases, the entire (fuzzy) picture shows a pulsed brightening, and still larger interference can disrupt the TV receiver's vertical sync, causing the picture to roll over ('flip') or even break up. This type of interference occurs when the interfering signal reaches the receiver as a result of scattering, primarily specular, off the broad face of a blade, and is called backward region interference. As the angle ϕ (see Fig. 2-6) between the WT-transmitter and WT-receiver direction increases, the separation of the ghost decreases, and a somewhat greater interference is now required to produce the same amount of video distortion. In the forward scattering region when the WT is almost in line between the transmitter and the receiver, there is virtually no difference in the times of arrival of the primary and secondary signals. The ghost is then superimposed on the undistorted picture and the video interference appears as an intensity (brightness) fluctuation of the picture in synchronism with the blade rotation. In all cases, the amount of interference depends on the strength of the scattered signal relative to the primary one, and this decreases with increasing distance from the WT.

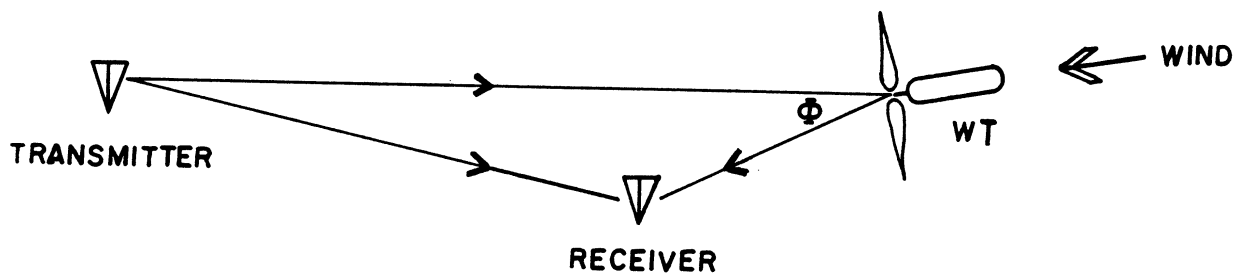


Fig. 2-6: Geometry of the WT blade scattering.

The backward region interference shows no significant dependence on the ambient signal strength and appears to be independent of the TV set if the signal is well above the noise level. Interference is observed only when a blade is positioned to direct the specularly reflected signal to the receiver. The azimuth and pitch angle of the blades are therefore key factors affecting the level of interference, and for any given transmitter and receiver locations, interference can occur only if the wind is such as to position the WT appropriately. In the forward region, however, the interference is less sensitive to the blade position but does depend on the ambient signal strength, and a receiver located in a low signal level area is more vulnerable to this type of interference.

The amount of video distortion depends on the ratio of the scattered (perturbing) and ambient field strengths at the input to the receiver, i.e., on the modulation index m of the total received signal, and the modulation threshold m_0 is defined to be the largest value of m for which the distortion is still judged to be acceptable. The threshold is obviously somewhat subjective, but as a result of laboratory simulations [5-7], scale model measurements [8], and field tests using the MOD-0 machines at Plum Brook [5,6] and on Block Island [9], it has been established [10] as 0.15 for $\phi = 0$ increasing uniformly to 0.35 for $\phi \approx 180^\circ$. The latter value is for a strong ambient signal and could be as small as 0.15 in a low signal area. With the WT blades oriented to direct the maximum scattered signal to the receiver, the region where $m > m_0$ is defined as the interference zone.

On the assumption of a smooth spherical earth and an omnidirectional receiving antenna, a method has been developed [10] for calculating the interference zone of a WT for any given TV Channel. The computation requires a knowledge of the effective length L_e and equivalent scattering area A_e of a WT blade, and for the MOD-1 machine the values [10] are $L_e = 25$ m, $A_e = 40$ m². Figure 2-7 shows the resulting interference zone for TV Channel 11 with transmitter 50 km from the WT. We observe that the backward region corresponding to specular scattering off the blades is approximately a cardioid centered on the WT with its maximum pointing towards the transmitter. There is also a narrow lobe directed away from the transmitter produced by forward scattering. The shape of an interference zone is only weakly dependent on the transmitter distance and TV Channel number, but its size increases markedly with increasing frequency (Channel number).

Such computations have no direct relevance to the situation in Boone where the mountainous terrain has a pronounced effect on the level of interference observed. In hilly country homes tend to be on the lower slopes or in the valleys where, due to shadowing, the ambient field strengths may be less than if the terrain were flat. A WT, on the other hand, must be exposed to the winds and would naturally be placed on the higher ground, as is the case in Boone. Because of the height-gain effect associated with the higher elevation, the illumination of the WT is stronger than it would be in flat terrain, thereby increasing the strength of the WT as a re-radiating source. The net effect is to aggravate the interference, and to increase the distance from the WT at which the video distortion could be unacceptable.

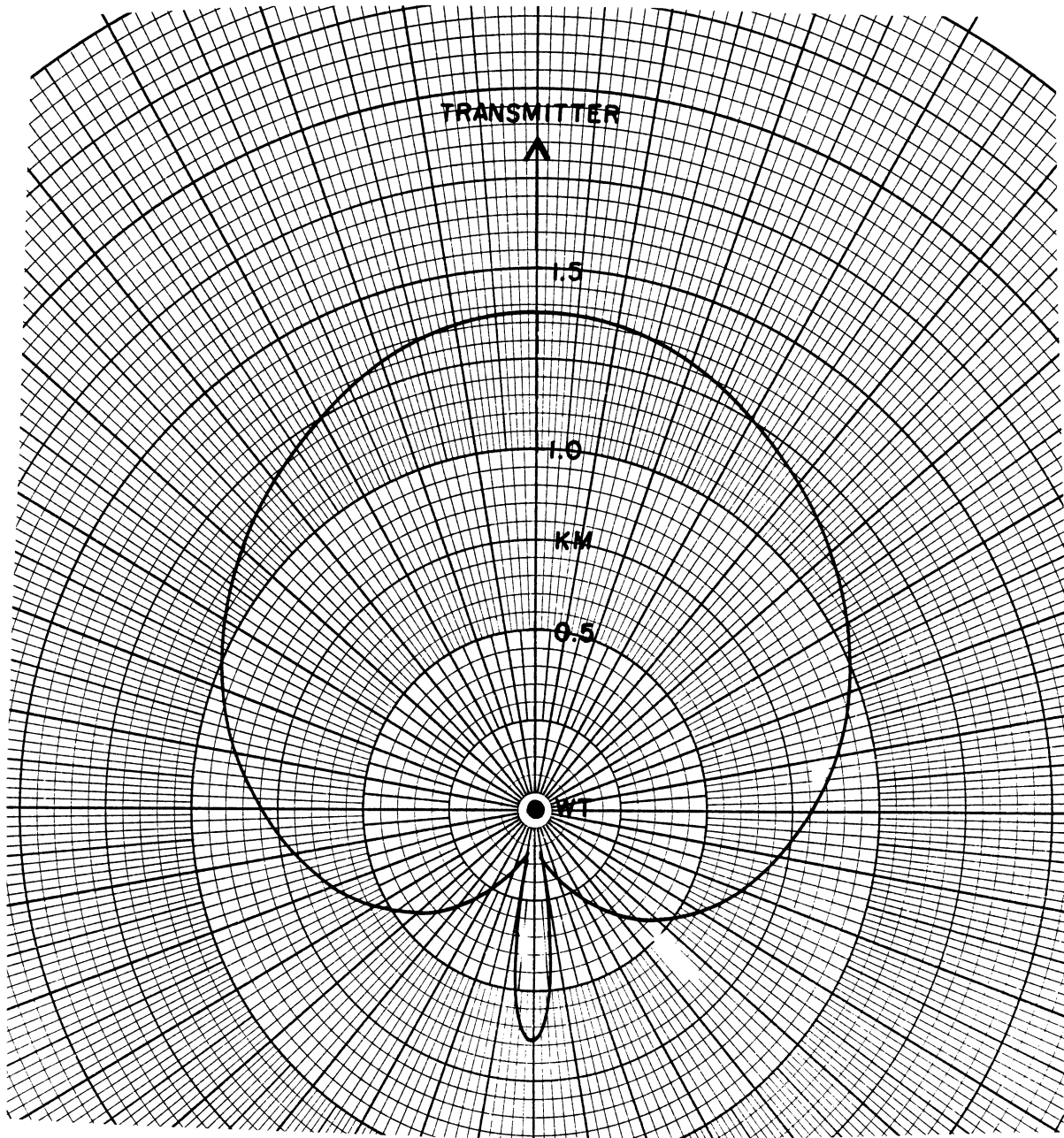


Fig. 2-7: Theoretical interference zone for TV Channel 11 with transmitter 50 km away.

However, there are also ameliorating factors. As previously remarked, the computation of an interference zone such as that in Fig. 2-7 is based on the assumption that the WT azimuth is appropriate for directing the maximum scattered signal to the receiver, and if the winds necessary to operate the WT are generally from (say) the NW or W, some portions of the zone could experience relatively little interference. In addition, there is the role played by the receiving antenna. Most residents of the Boone area find it necessary to have a fringe area antenna with a reasonably high gain, and it is then possible that the antenna can serve to discriminate against the unwanted interfering signal.

If, in Fig. 2-6, the main beam of the receiving antenna is pointed at the transmitter, the WT-scattered signal will be received via the side and back lobes of the antenna for most angles ϕ corresponding to the backward interference region, thereby reducing the observed interference. On the other hand, if the antenna is in the forward interference region of the WT, or that portion of the backward region where the direct and scattered signals are both received via the main beam, the antenna will lose most of its ability to provide discrimination.

With even a high performance VHF antenna such as the Winegard CH 8200 used in the present tests, the half width of the main beam is much greater than the half width of the forward peak of the interference zone. The discrimination that an antenna can provide is therefore limited by the pattern of the antenna and not by the nature of the interference zone, and since the discrimination is an important aspect of the present tests, it is convenient to define a modified

(expanded) forward scattering region as that portion of the zone where a high performance antenna will no longer produce any significant reduction in the interference. For the Winegard CH 8200 antenna the half width of the main beam measured at the -15 dB level is approximately 30° for Channels 2-6, decreasing to about 20° for Channels 7-13, and the side and back lobes are all below this level. Thus, for Channel 3, the antenna can significantly reduce (and may, in practice, suppress) the interference for $0 \leq \phi \leq 150^\circ$, but will be of relatively little help if $150^\circ < \phi \leq 180^\circ$. In the interests of simplicity and uniformity, we shall therefore take the half width of the modified forward scattering region to be 30° throughout the entire VHF band.

2.4 Test Sites

In preparation for the test program a handful of sites were designated where measured data for the ambient field strengths and interference levels would be obtained, and the ability of a high performance antenna to reduce (or even suppress) the interference would be explored. Factors which were taken into account in the selection of the sites were the areas from which complaints of TV interference had been received, the desire to sample a variety of electromagnetic situations, e.g., the backward and (modified) forward scattering regions for several TV Channels, and the availability of a power supply. This last restricted us to the roads in the area. To ensure that adequate data were collected even if the weather and/or wind conditions were bad for much of the time allotted to the tests, a ranking was assigned to the five sites, but this turned

out to be unnecessary. All of the designated sites were covered and because of the excellent conditions during the latter part of the program, measurements were also made at five other sites. The ten sites will be identified by the letters A through J and, apart from the last two which are beyond 1.5 miles from the WT, these are indicated in Fig. 2-2. See also Fig. 2-8 where all the sites are shown.

Table 2-2 gives some information about the sites. The distances from the WT are the horizontal ones obtained from the full size version of Fig. 2-2. The approximate heights below the WT axis were found by subtracting the site elevations determined from the elevation contours through the sites (see Fig. 2-8) from 4560 (=4420 + 140) ft. The TV Channels listed are those for which a site lies in the modified forward scattering regions as defined in the previous sections.

The following additional information may help to give a mental picture of each site.

Site A is E of the WT beside a gravel road that runs south and then east from Rainbow Trail (SR 1318). The immediate vicinity is quite hilly and wooded, and the WT cannot be seen from the site, though it is visible at a home 150 ft to the east. The gravel road ends about 900 ft further east, and field strength measurements were made at several places along the road.

Site B is NW of the WT beside a gravel road about 600 ft north of its intersection with the service road to the WT. The heavy woods obscure the WT both here and at a home about 300 ft to the east.

Table 2-2: Site Information

Site	Distance from WT (ft)	Direction from WT (° from N)	Approximate height below WT axis (ft)	TV Channels (forward)
A	3200	108°	1200	5,11
B	1900	294°	500	8,9
C	2600	316°	600	3,9
D	3000	36°	1100	7
E	3100	237°	1100	12
F	5200	186°	1300	none
G	6500	27°	1300	7
H	7400	338°	1200	3,9
I	8900	115°	1400	5,11
J	13,000	154°	1400	none

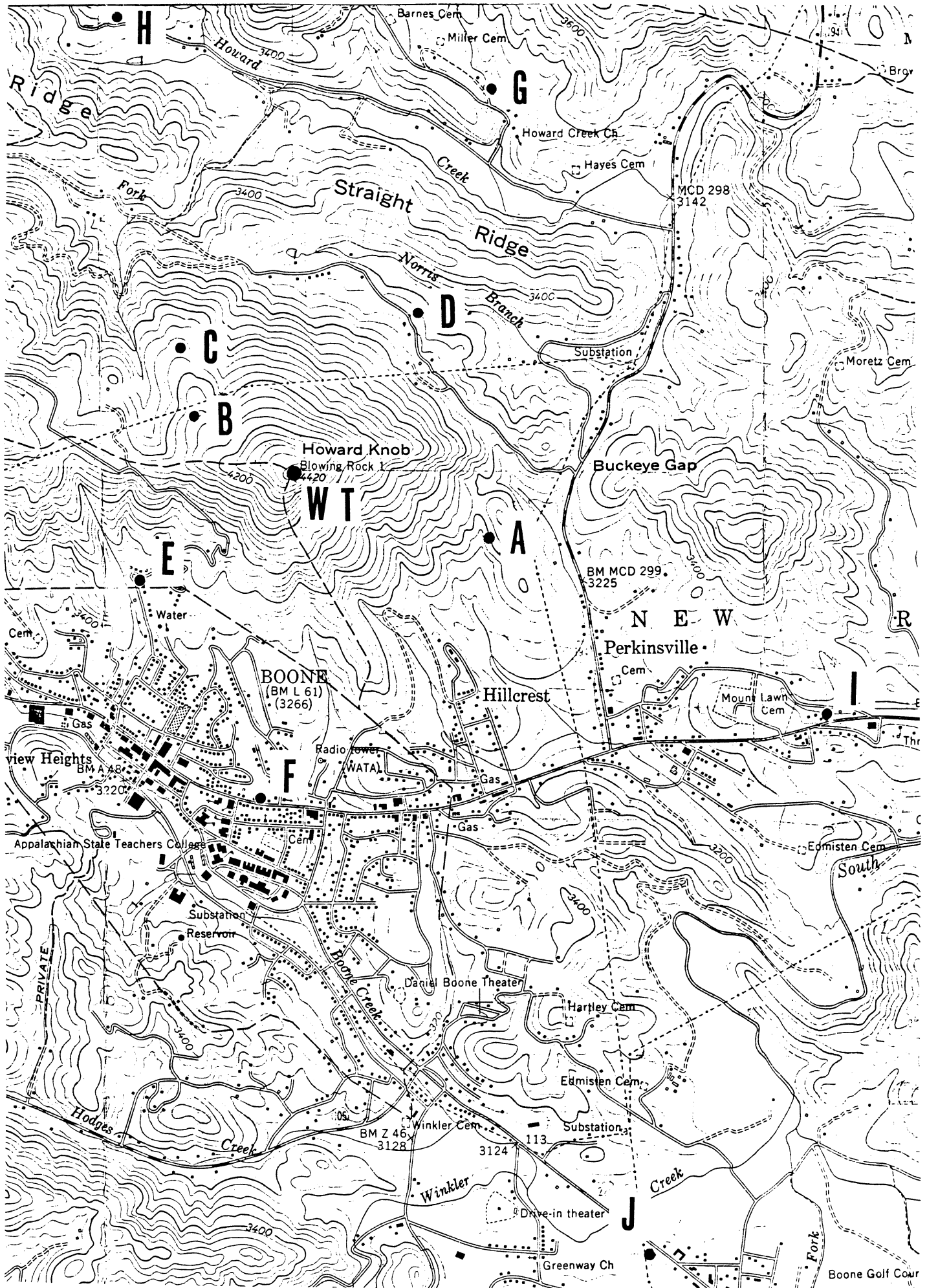


Fig. 2-8: Topographical map of the Boone area showing the test sites.

Site C is further north on the same gravel road as B, adjacent to a home. The area is more open and the WT is visible.

Site D is in an open field next to the Appalachian State University water treatment plant on Rainbow Trail (SR 1318). There is an unobstructed view SW to the WT.

Site E is at a sharp bend on Jonaluska Road outside a home on the outskirts of Boone. It is SW of the WT and affords a clear view of the machine. We understand that most homes in this area are on cablevision.

Site F is due S of the WT adjacent to the main street (US 321,421) of Boone, close to the city center. The antenna was set up in a parking lot next to the office of a local dentist. It is a generally clear area with a good view of the WT.

Site G is NE of the WT on J. R. Norris Road (SR 1320) about 1500 ft from its intersection with Howard Creek Road (SR 1306), adjacent to a residence. It is in a valley whose heavy woods obscure the WT, but we are informed that the WT is visible when the trees are bare.

Site H is in a parking area next to a home on Howard Creek Road (SR 1306). It is NW of the WT and has a steep hill to the west and north of the site that effectively blocks any TV reception from these directions. Although there are some trees in the area, these do not block the view of the WT.

Site I is on the lawn of a residence on SR 1329 SE of the WT. The house is one of many permanent and mobiles homes in

the area. Most are on cablevision, though some (including this one) are not. The terrain here rises gradually to the north and south, but there are few trees, and the WT is visible.

Site J is SE of the WT next to the BREMCO main office and to the electrical substation there, and in a residential area. The site is just off heavily travelled US 221-321, but the traffic did not affect the measurements. The nearest hills of any size are to the south, and there is a clear view of the WT.

For a given TV Channel, each site is typical of a number of homes at a similar distance from the WT and in the same scattering region (backward or modified forward) for that particular transmission. The resulting categorization of homes out to 1.5 miles from the WT is given in Table 2-3. The numbers in each annular sector were obtained by actual count using the large scale maps from which Fig. 2-2 was derived. The letters in parentheses identify sites, and as regards the interference phenomena, B is typical of 29 homes for Channel 3 but only 2 for Channel 9.

Table 2-3: Categorization of Homes

TV Channel	No. of homes at indicated distances (miles) from WT			
	0-0.25	0.25-0.5	0.5-1.0	1.0-1.5
3 backward	0	29 (B)	99 (A,D,E)	184 (G,H)
forward	0	1 (C)	26	26
5 backward	0	28 (B,C)	116 (D,E)	206 (G)
forward	0	2	9 (A)	4 (H)
7 backward	0	26 (B,C)	95 (A,E)	145 (H)
forward	0	4	30 (D)	65 (G)
8 backward	0	25 (C)	119 (A,D,E)	193 (G,H)
forward	0	5 (B)	6	17
9 backward	0	28	105 (A,D,E)	188 (G)
forward	0	2 (B,C)	20	22 (H)
11 backward	0	30 (B,C)	113 (D,E)	205 (G,H)
forward	0	0	12 (A)	5
12 backward	0	22 (B,C)	105 (A,D)	159 (G,H)
forward	0	8	20 (E)	51

CHAPTER 3. TEST EQUIPMENT AND PROCEDURES

The stated objectives of the measurements at Boone were to

(i) determine the TV interference (TVI) caused by the operating WT at selected sites in the vicinity of the machine;

(ii) relate the measured data to the ambient signal levels and establish site-specific TVI criteria for the Boone area;

(iii) determine the ability of a high performance receiving antenna to reduce the interference to a level judged acceptable, and establish guidelines for the antenna characteristics necessary to achieve reduced and/or no TVI at the affected homes; and

(iv) develop techniques that could be used by local TV technical personnel to conduct interference measurements.

The sites that were selected were described in the previous chapter. Each is typical of a number of homes in that particular area, and the classification of homes according to the type of TVI they could experience is set forth in Table 2-3. It is presumed that the interference observed at each site would also be found at the other homes in the same category, and that any solution to the problem that was developed for that site would also be applicable to these.

The mechanism for achieving the objectives was a series of detailed measurements carried out at each of the sites. In the following sections we describe the experimental equipment and procedures used to perform the tests, discuss the type of data that was collected, and

cite those parameters of the test components that are needed to analyze and interpret the data.

3.1 Equipment

The equipment used to perform the measurements was similar to that for our previous TVI tests [9]. A schematic block diagram of the system is shown in Fig. 3-1 where only those components pertinent to the data collection have been included. With any given TV transmission a portion of the signal is scattered by the WT and this, together with the desired (direct) signal, was picked up by an antenna and fed to a spectrum analyzer and a TV receiver. The receiving antenna, to be described later, was a commercially available directional antenna located about 20 ft above ground.

The vertical output of the spectrum analyzer was connected to a chart recorder which provided a record on paper tape for later evaluation. The combination of the spectrum analyzer and the recorder was used to measure the ambient levels of the video and audio signals without the WT in operation, and to record the total signal received as a function of time, including any modulation produced by scattering off the operating WT. The general quality of the ambient TV reception and the existence of any WT-produced video distortion were observed on the TV screen, and the video recorder was employed whenever it was felt desirable to record the program. At all of the test sites except C the equipment was powered from the commercially available 60 Hz supply. When, at the last minute, it was found that no such supply was possible at C, power was obtained from an automobile battery via an inverter.

All the test instruments fitted comfortably inside a station wagon. The receiving antenna and its associated tower and rotor

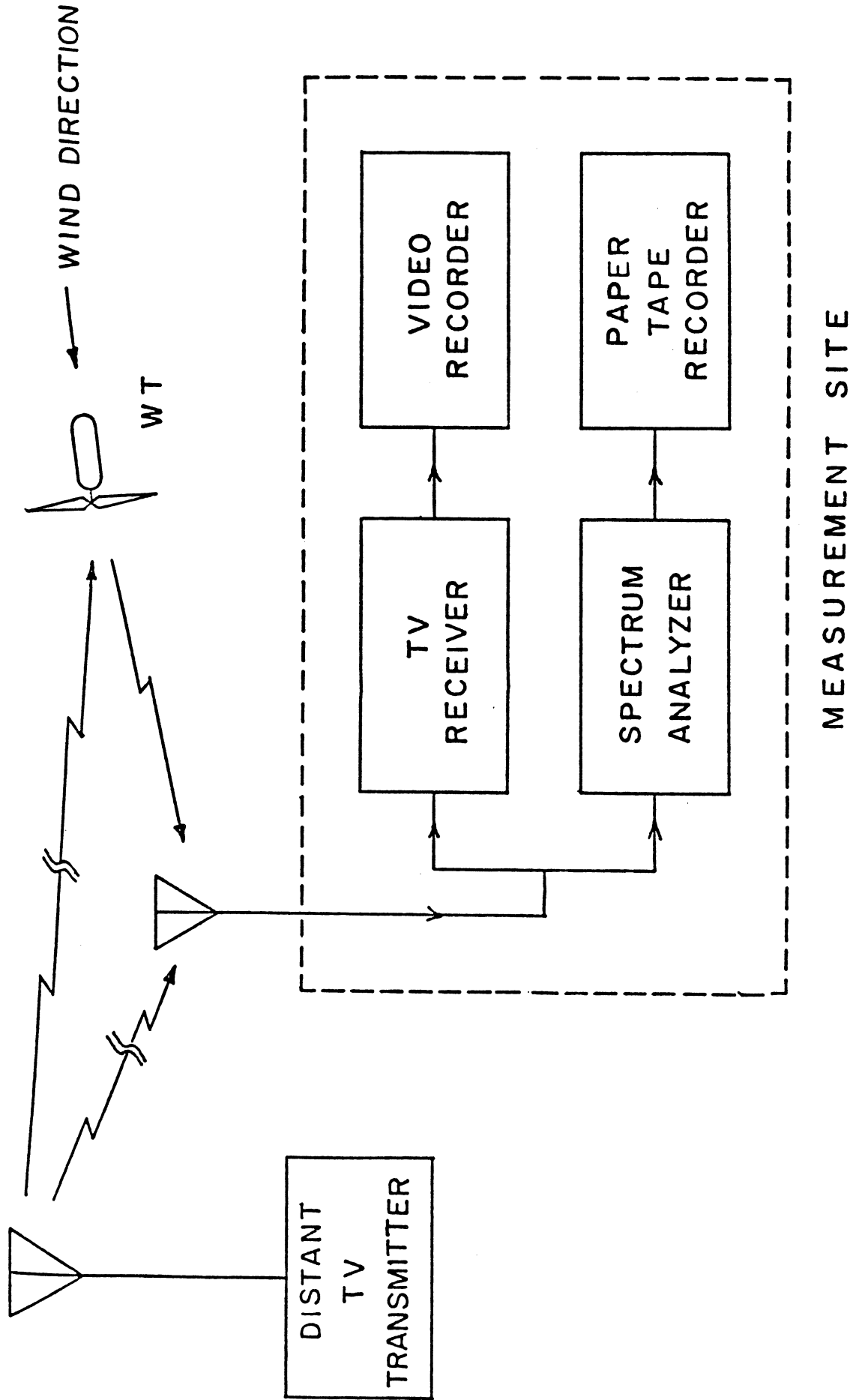


Fig. 3-1: Schematic block diagram of the measurement system.

assemblies were installed on the wagon in a demountable fashion as follows. A 4-ft section of a triangular tubular aluminum tower was mounted vertically on a metal plate attached to the right rear bumper of the station wagon. Hinged to the top of this was a further 8-ft section of the same type of tower containing a 5-ft telescopic section on which the antenna rotor assembly was mounted. The rotor was attached to (and turned) a 7-ft length of 1 1/2-inch diameter aluminum pipe, and the antenna was clamped to the pipe about 1 ft from its top. With the upper portion of the tower vertical and locked in position with a bolt, the antenna height above ground could be varied from about 20 to 25 ft by adjusting the telescopic portion. When moving from one site to another, it was a simple matter to lower the tower onto the roof of the car (protected by wooden beams) and to position the antenna down the side. For long distance transportation, e.g., the journeys from Ann Arbor to Boone and back, the antenna elements were also folded and secured.

When equipped in this manner, the station wagon served as a mobile laboratory and was used as such throughout the entire test program. Figure 3-2 is a photograph of the antenna system when in use, and Fig. 3-3 shows the system lowered for movement between sites. For future reference, the following is a list of the equipment included in the mobile laboratory:

1. Spectrum analyzer (Hewlett-Packard model 8558/182T)
2. Paper chart recorder (Hewlett-Packard model 7132A)
3. Video recorder (Sony model V02610)
4. Television receivers (2) (1976 Zenith model 17GC45)



Fig. 3-2: View of the tower erected.

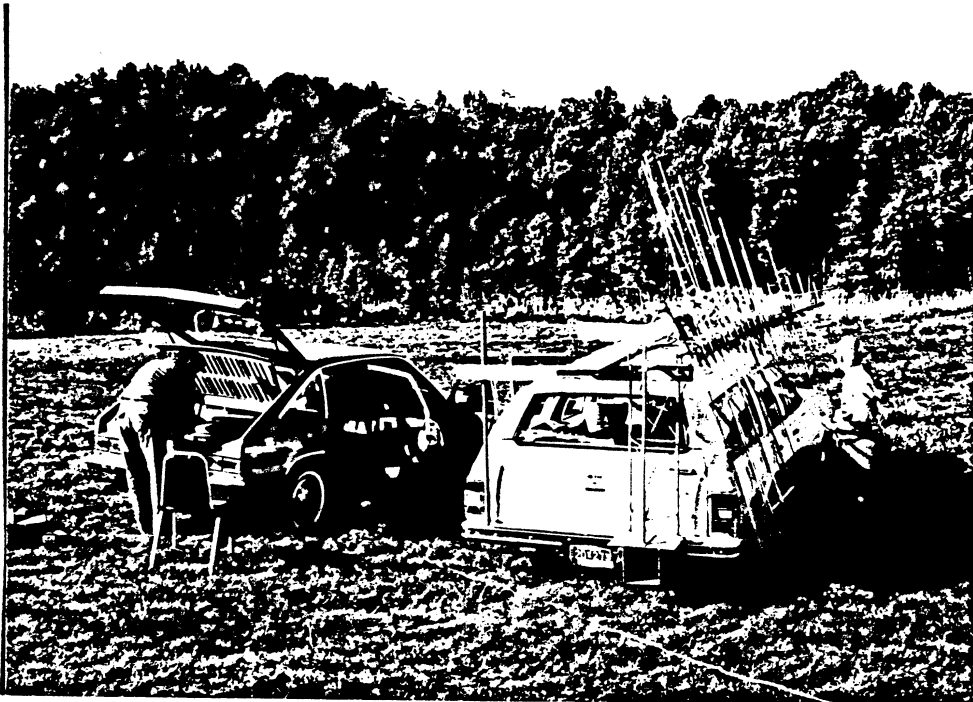


Fig. 3-3: Antenna and tower stowed for transportation.

5. Antenna and tower (minimum height 15 ft)
6. Antenna rotor
7. Walkie-talkies (2)
8. Portable power supply (optional)
9. Line conditioner (optional)
10. Station wagon or van

We have found it convenient to have two TV receivers, with one displaying the received program, whilst the other was used in conjunction with the video recorder; however, the second is not essential. The walkie-talkies are necessary to communicate between the test site and the WT, and to avoid extraneous interference, the one at the test site should not be used for transmission when video recording is in progress. Two people are sufficient to operate the equipment and perform the tests, and in a pinch it would be possible to get by with one person only. This is apart, of course, from the personnel needed to control the WT.

In addition to the above, a different system was supplied by SERI and was used to measure the ambient TV signal levels at some of the test sites. The system was coupled to the same antenna as before and had, as its heart, a programmable computer controlling a spectrum analyzer and a printer (see Fig. 3-4). For a given orientation of the antenna, the signal was sampled at incremental frequencies spanning the band of frequencies of the TV Channel of interest, and the results were plotted as a function of frequency. The peak signals exceeding a predetermined level were also printed out, along with the frequencies at which they occurred, and from this the received video and audio carrier signal strengths could be found. The process was repeated for different

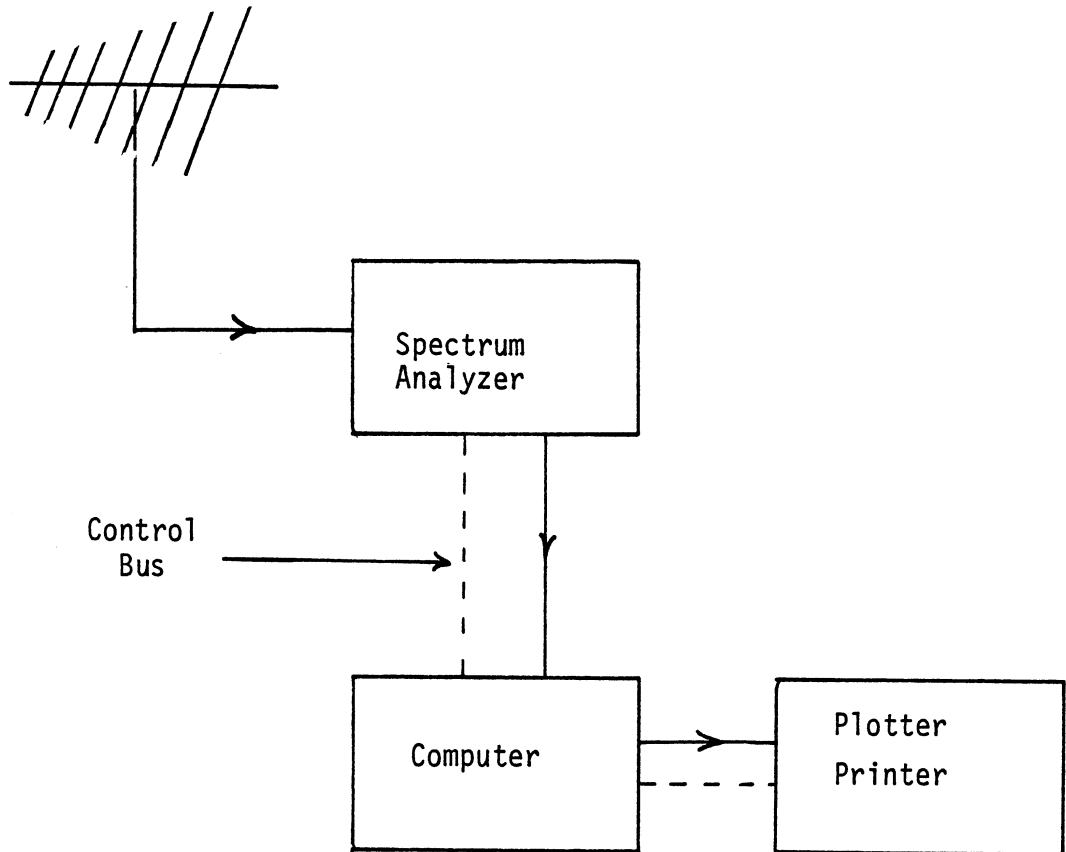


Fig. 3-4. Block diagram of field strength measurement setup using the computer-controlled equipment supplied by SERI.

orientations of the antenna in a horizontal plane, leading to a determination of the maximum available signal strength for each TV Channel.

The system could be left in an unattended mode and would update printed information every 15 minutes. It provided more detailed information than was needed for this program, but we also noticed that due to the frequency stepping the peak audio carrier signal strengths were often missed on some channels. It was used to supplement our other measurement procedures, but at the fifth site a malfunction developed which could not be rectified, and the system remained inoperable for the rest of the program.

3.2 Antennas

The antenna used by a homeowner could have a major impact on the amount of interference observed, and one of the objectives of the program was to determine how a high performance antenna affects the interference. The selection and calibration of the antenna to be used in the measurements was therefore an important aspect of the project.

During the months prior to the actual measurements, a number of antennas were accumulated. They were:

(i) Channel Master (model unknown): This was purchased by the Radiation Laboratory at the beginning of our WT interference studies. It was designed for VHF/UHF reception in an urban area and is a modified log periodic antenna with 5 VHF and 10 UHF elements, and 9 UHF directors.

(ii) Archer (model VU-160): This is a VHF/UHF fringe area antenna marketed by Radio Shack and was purchased by the Radiation Laboratory

on the recommendation of NASA (Lewis) personnel. It is also a modified log periodic antenna, with 8 VHF and 1 UHF elements, plus 13 UHF directors.

(iii) Winegard (model CH8200): Some residents of the Boone area have found this to be a very effective antenna, and at the suggestion of one home owner who has experienced no problem with WT interference, the antenna was purchased by BREMCO and supplied to us. It is a modified log periodic designed to cover the VHF and UHF bands, and is recommended for fringe area reception. It has 11 VHF and 6 UHF elements, 12 UHF directors, and a corner reflector associated with the UHF section. However, the elements are cut in a rather unusual manner to produce almost a resonant log periodic antenna.

(iv) Blonder Tongue Broadband (model 0719): According to the manufacturer's specifications, the Blonder Tongue line of (fringe area) antennas have very good front-to-back ratios, and on the recommendation of the Radiation Laboratory, this antenna and the following two were purchased by BREMCO for trial use at selected homes in the Boone area. It is a modified log periodic antenna with 10 VHF elements, 6 UHF elements and 10 UHF directors. The VHF elements are cut to resonate in the lower portion of the band and there are no elements for the upper portion.

(v) Blonder Tongue Channel 3 (model Y-310): This is a Yagi-Uda array with one active element, one reflector element and 8 directors. The active element has a gamma matching section to transform from a balanced to an unbalanced feed so that a 75 ohm coax may be used with the antenna.

(vi) Blonder Tongue Channel 8 (model Y-810): The basic features of the design are similar to those of the Channel 3 version.

The Channel Master, Archer and Blonder Tongue Broadband antennas all have a balanced feed and should be used with a 300 ohm twin lead transmission line. Their impedances are nominally 150 ohm, providing a 3:1 standing wave ratio. The Winegard, on the other hand, is equipped with a balun, and can be used with either a conventional (300 ohm) twin lead or a 75 ohm coax, for a standing wave ratio of 3:1.

The azimuthal and elevation plane patterns of all six antennas were measured at the average of the audio and video carrier frequencies for each of the TV Channels 2 through 13. The frequencies that were used are given in Table 3-2, and a block diagram of the system is shown in

Table 3-2: Antenna Measurement Frequencies

Channel	Frequency (MHZ)	Channel	Frequency (MHZ)
2	57	8	183
3	63	9	189
4	69	10	195
5	79	11	201
6	85	12	207
7	177	13	212

Fig. 3-5. At each frequency the output level of the signal source was adjusted to produce 0.3 mW power to the transmitting antenna, and this was monitored throughout the test. The frequency was

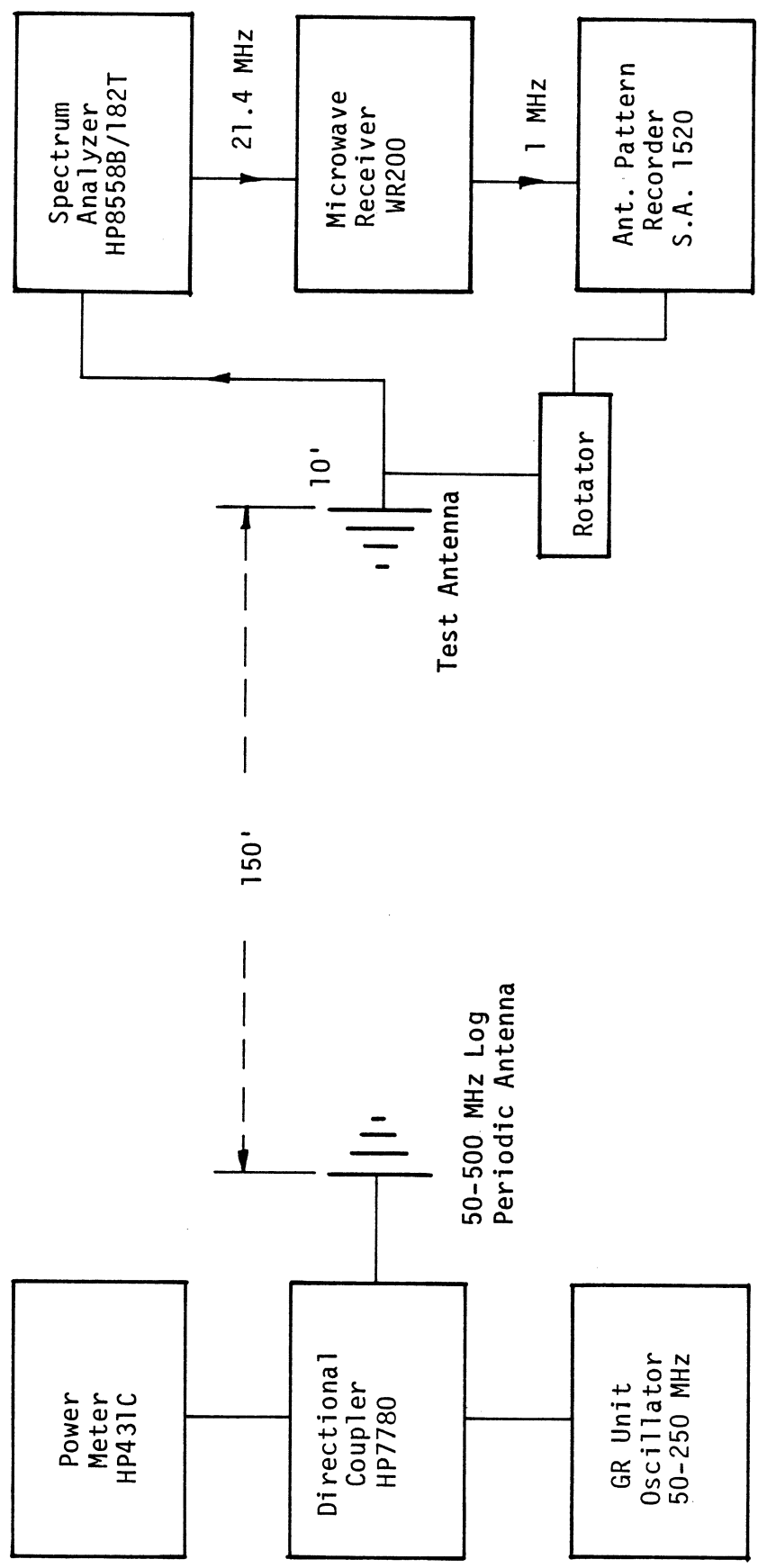


Fig. 3-5: Block diagram of the antenna measurement system.

also monitored by the spectrum analyzer at the output of the receiving (test) antenna, and the frequency and sensitivity of the spectrum analyzer were calibrated periodically throughout the data collection process. The use of a spectrum analyzer made possible the filtering out of any TV interference present in the outdoor environment where the measurements were made. The output from the receiver was fed to a pattern recorder along with positional information from the pedestal on which the test antenna was mounted, to produce 360° patterns. Patterns were also recorded for a standard dipole from which the gain of each test antenna relative to an isotropic source could be obtained by the substitution method.

The resulting gains are plotted in Fig. 3-6. Overall, the Winegard antenna is superior, with a gain which is relatively constant and averages 9.5 dB over the entire VHF band. The front-to-back ratios are shown in Fig. 3-7, and we observe that neither of the Blonder Tongue antennas for Channels 3 or 8 achieve the -25 dB values specified by the manufacturer. This could explain why the results of the trial installation of these antennas at selected sites in the Boone area (see Chapter 1) were not more encouraging. For most of the broadband antennas, the average front-to-back ratios are in the middle teens, but once again the Winegard antenna is the best, with a value of about -22 dB. As a result of these measurements, this antenna was selected for the on-site tests in Boone, and its azimuthal and elevation plane patterns at the frequencies corresponding to Channels 2 through 13 are shown in Figs. 3-8 to 3-19.

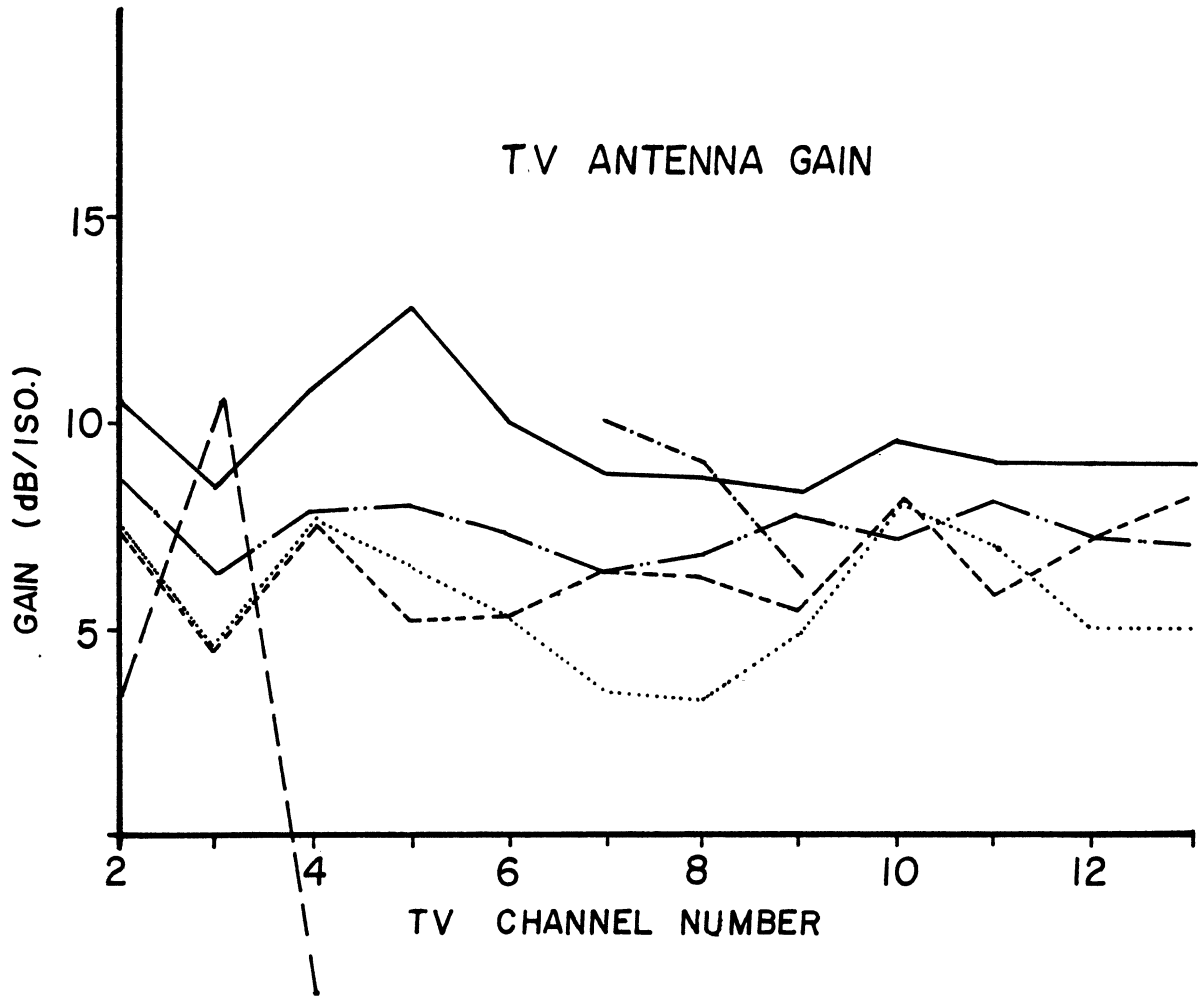


Fig. 3-6: Measured gains for the Channel Master (---), Archer (-.-.-), Winegard (—), Blonder Tongue Broadband (.....), Blonder Tongue Channel 3 (— —) and Blonder Tongue Channel 8 (-.-.-) antennas.

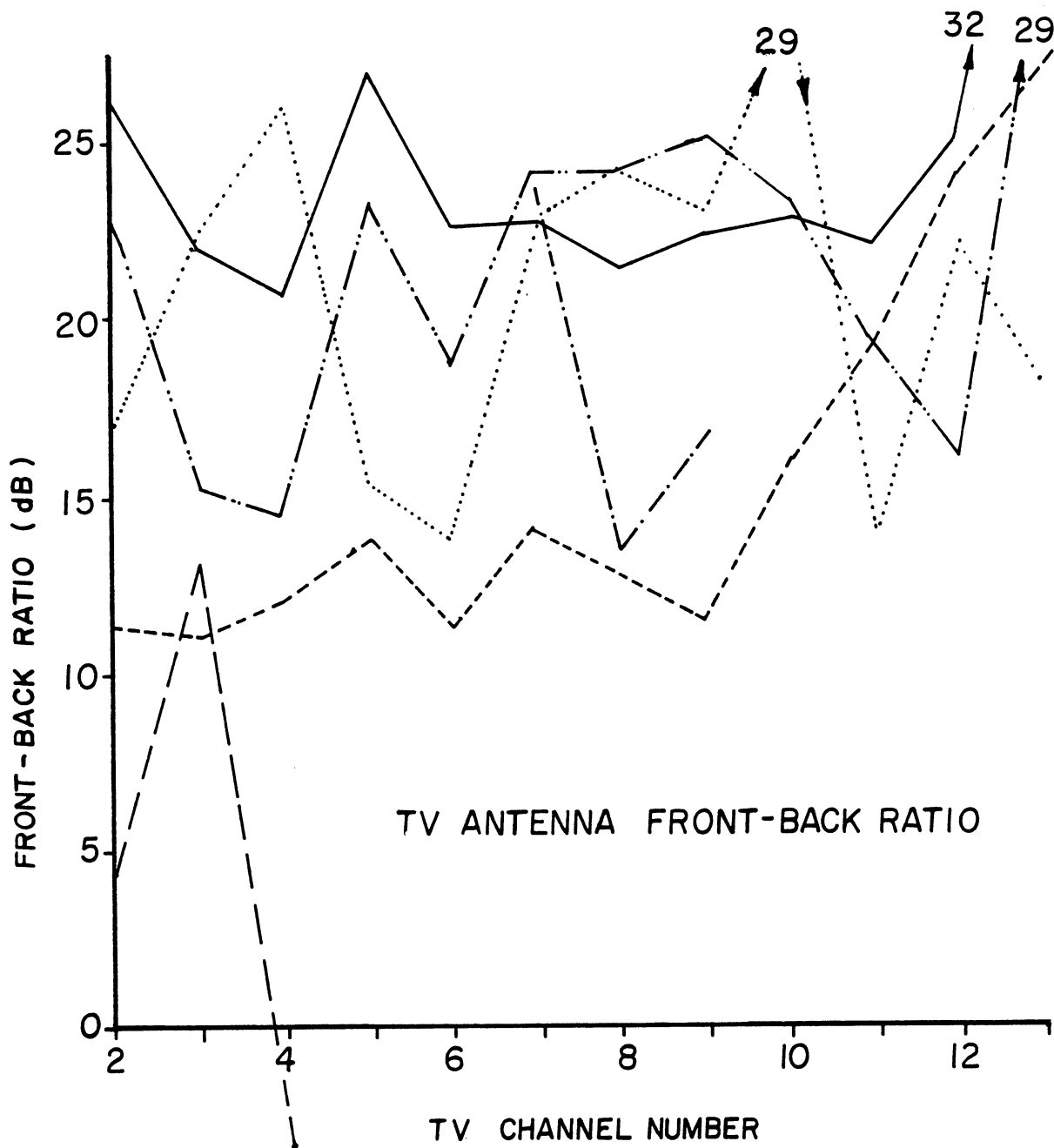


Fig. 3-7: Measured front-to-back ratios for the Channel Master (-----), Archer (-·-·-), Winegard (————), Blonder Tongue Broadband (·····), Blonder Tongue Channel 3 (———) and Blonder Tongue Channel 8 (-·-·-) antennas.

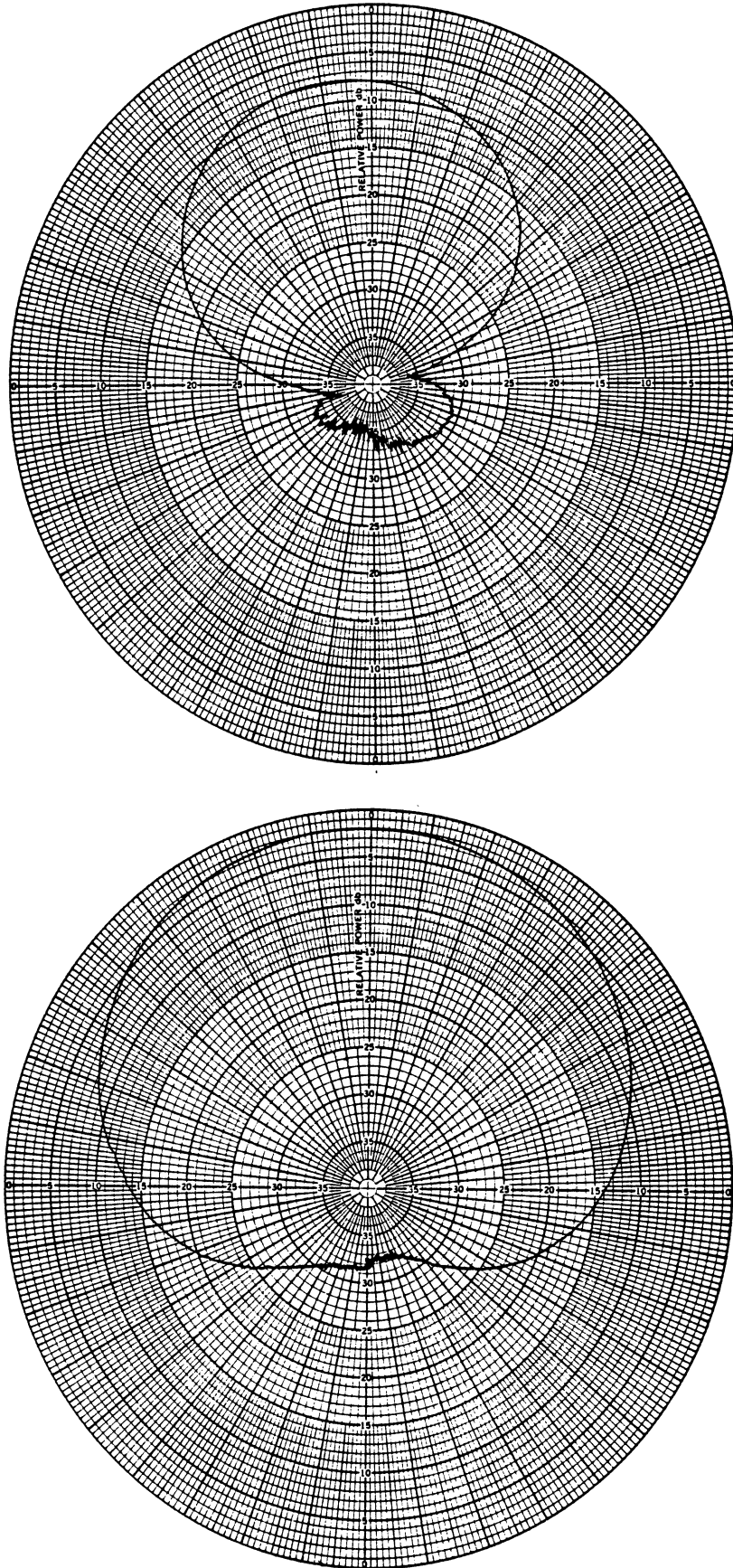


Fig. 3-8: Azimuthal (top) and elevation (bottom) plane patterns for the Winegard antenna at 57 MHz (Channel 2).

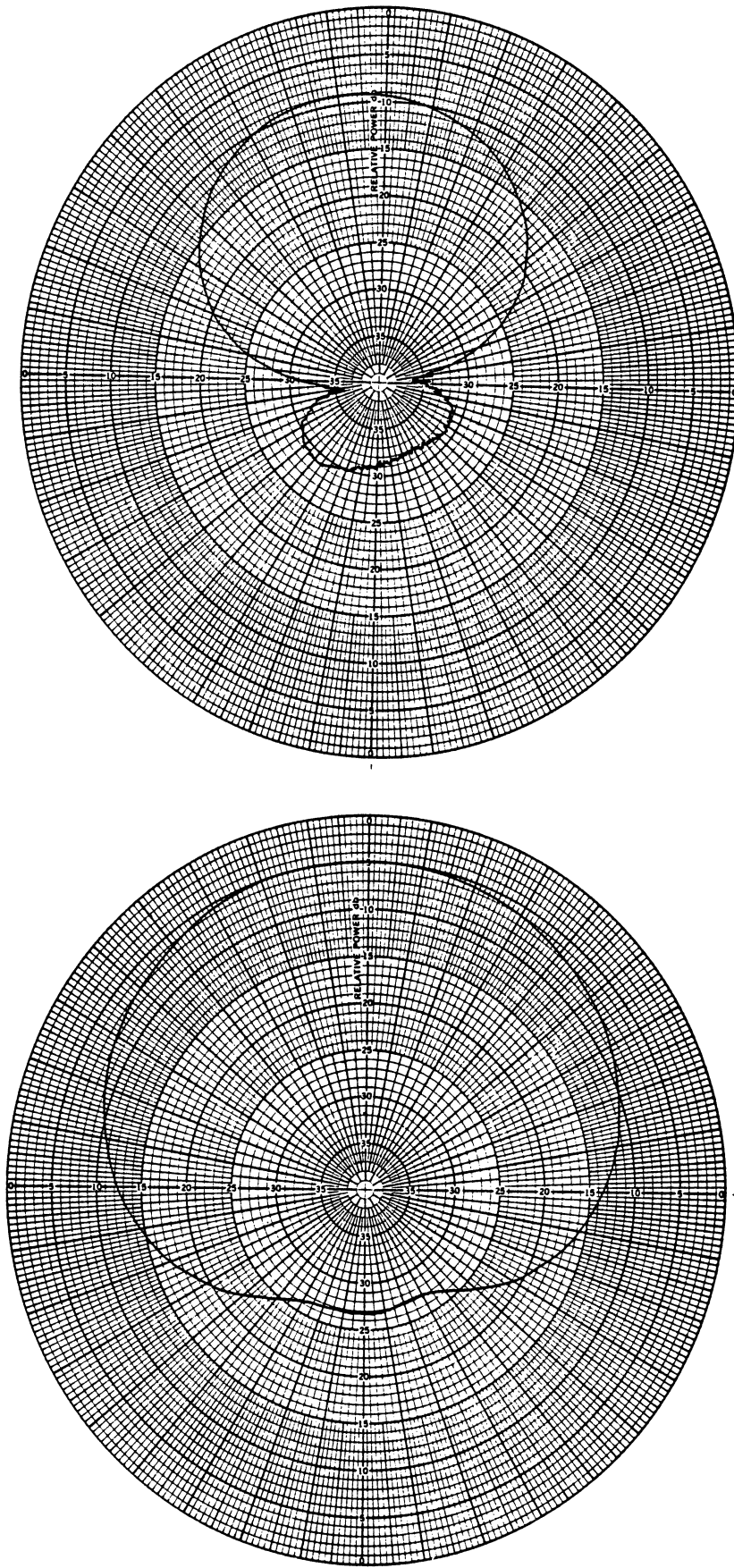


Fig. 3-9: Azimuthal (top) and elevation (bottom) plane patterns for the Winegard antenna at 63 MHz (Channel 3).

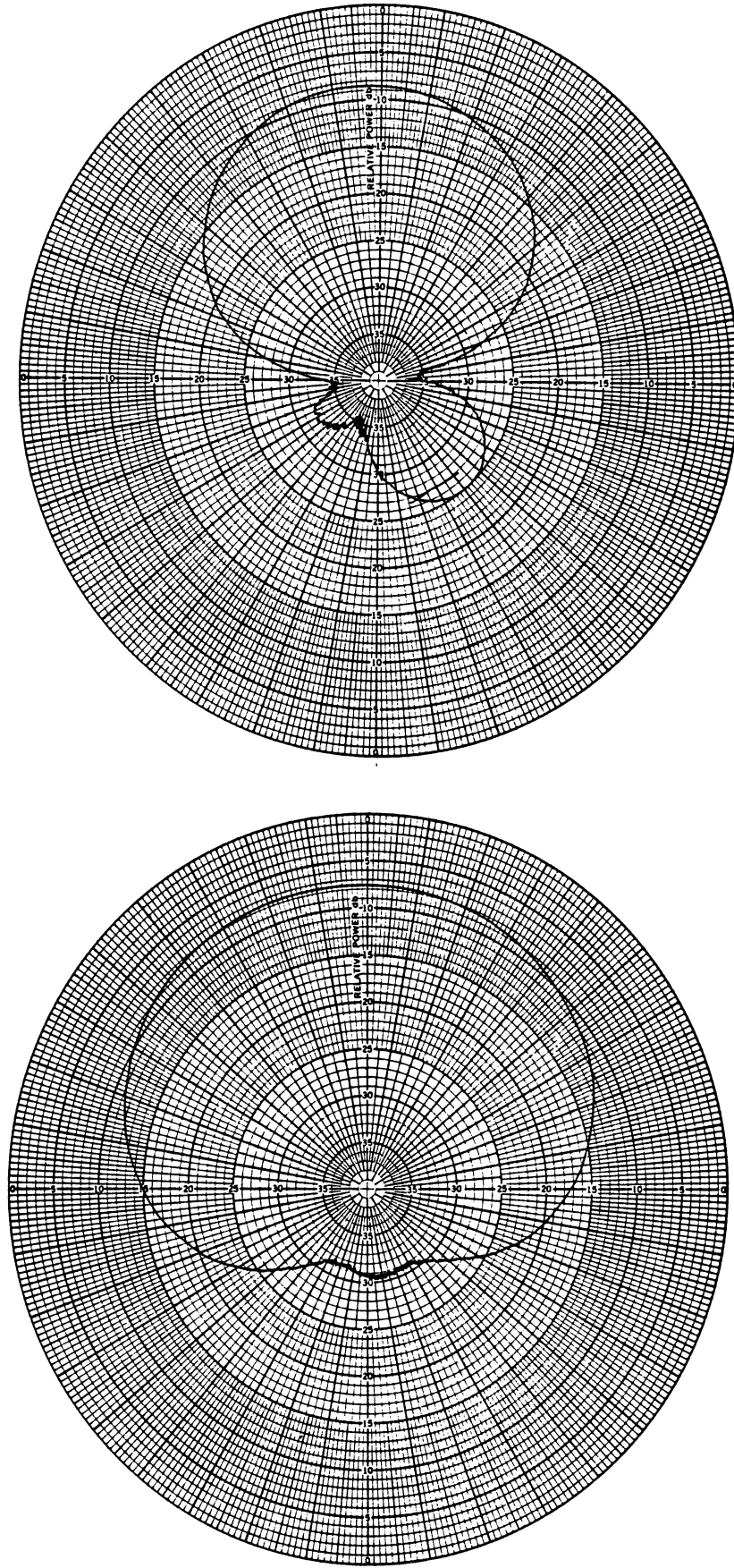


Fig. 3-10: Azimuthal (top) and elevation (bottom) plane patterns for the Winegard antenna at 69 MHz (Channel 4).

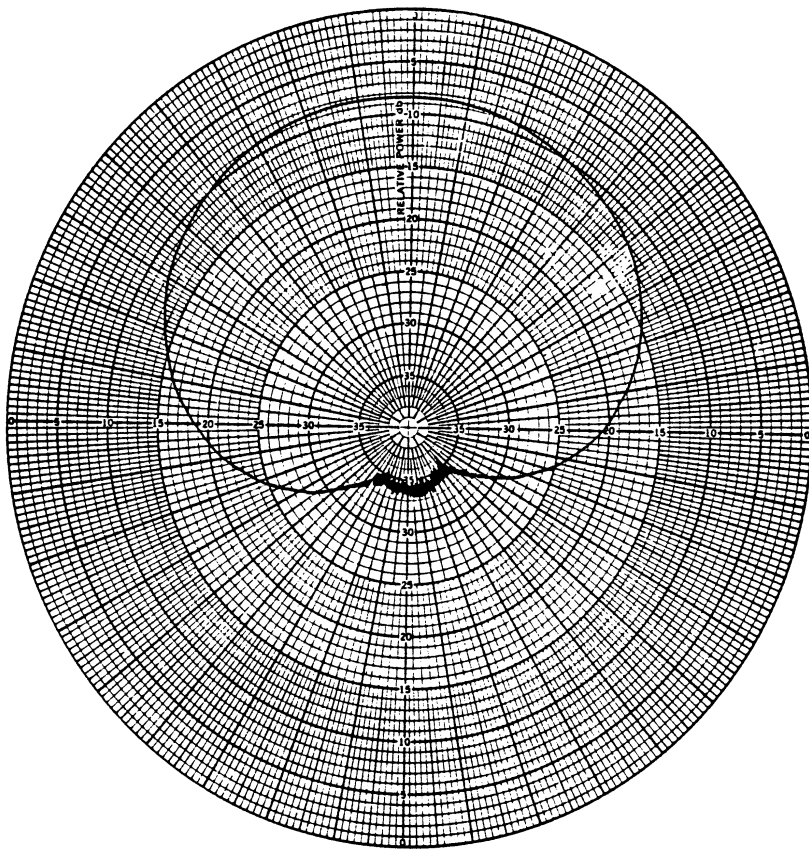
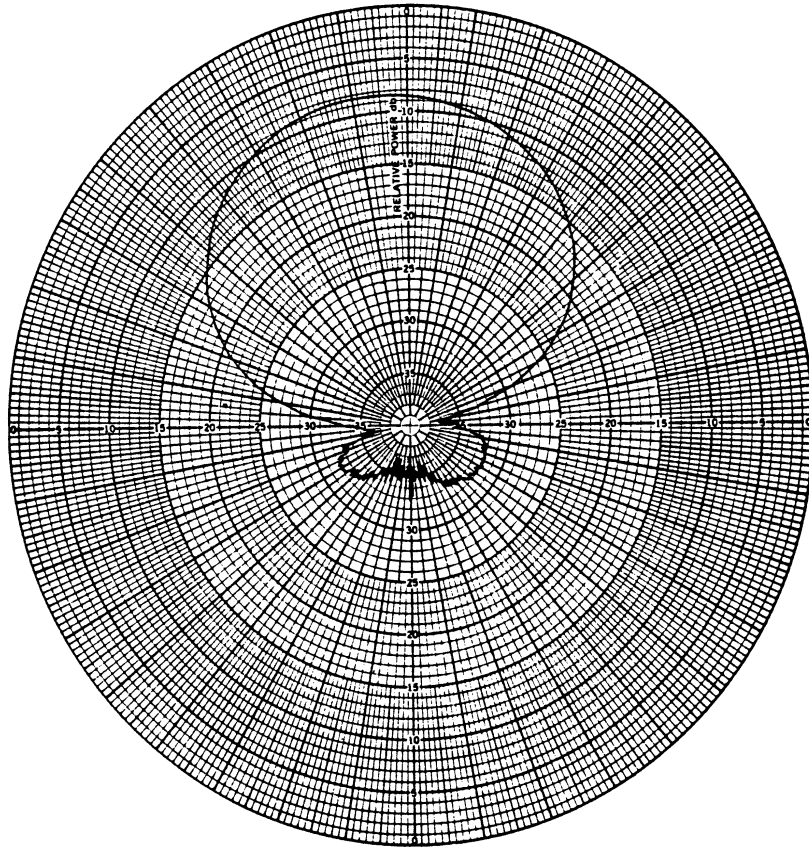


Fig. 3-11: Azimuthal (top) and elevation (bottom) plane patterns for the Winegard antenna at 79 MHz (Channel 5).

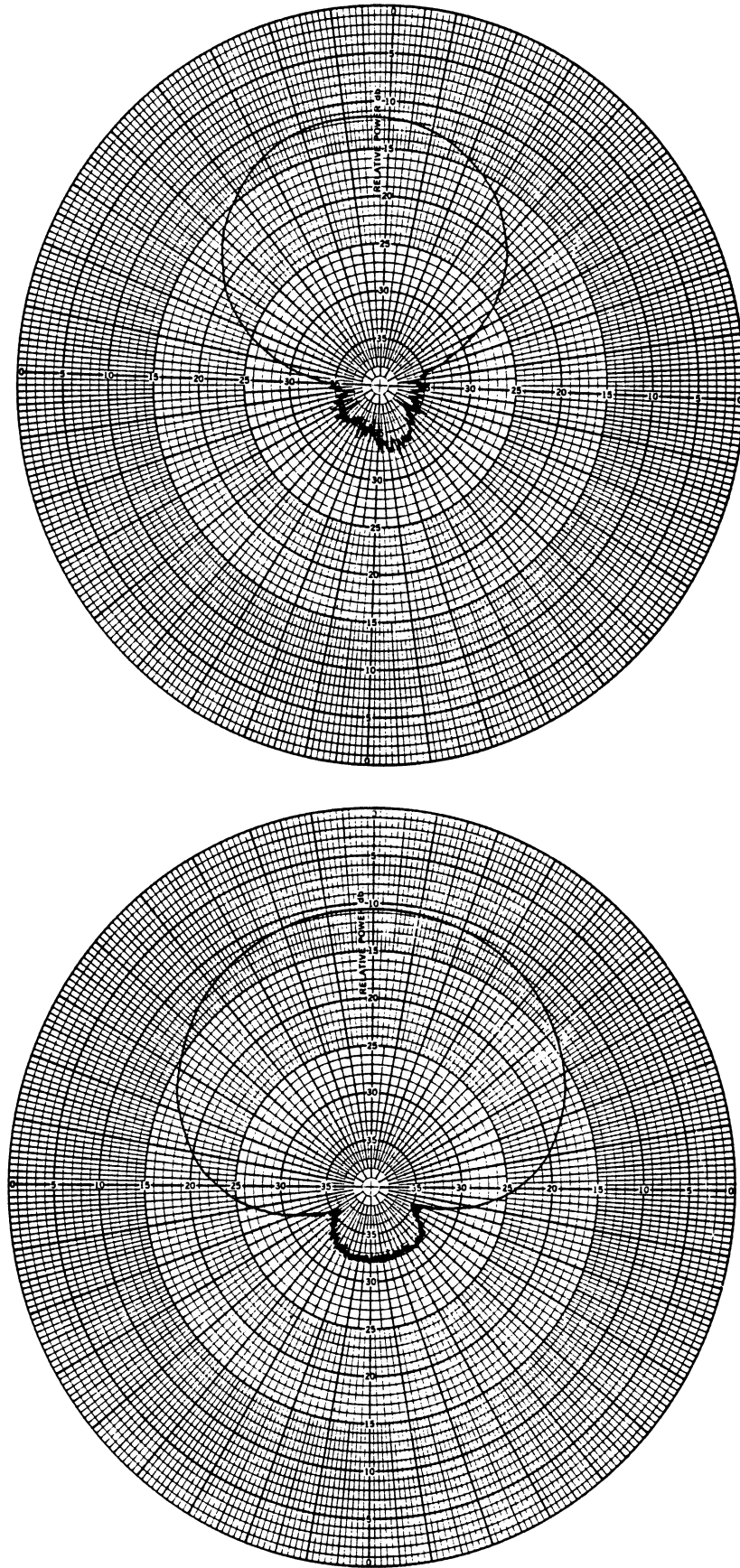


Fig. 3-12: Azimuthal (top) and elevation (bottom) plane patterns for the Winegard antenna at 85 MHz (Channel 6).

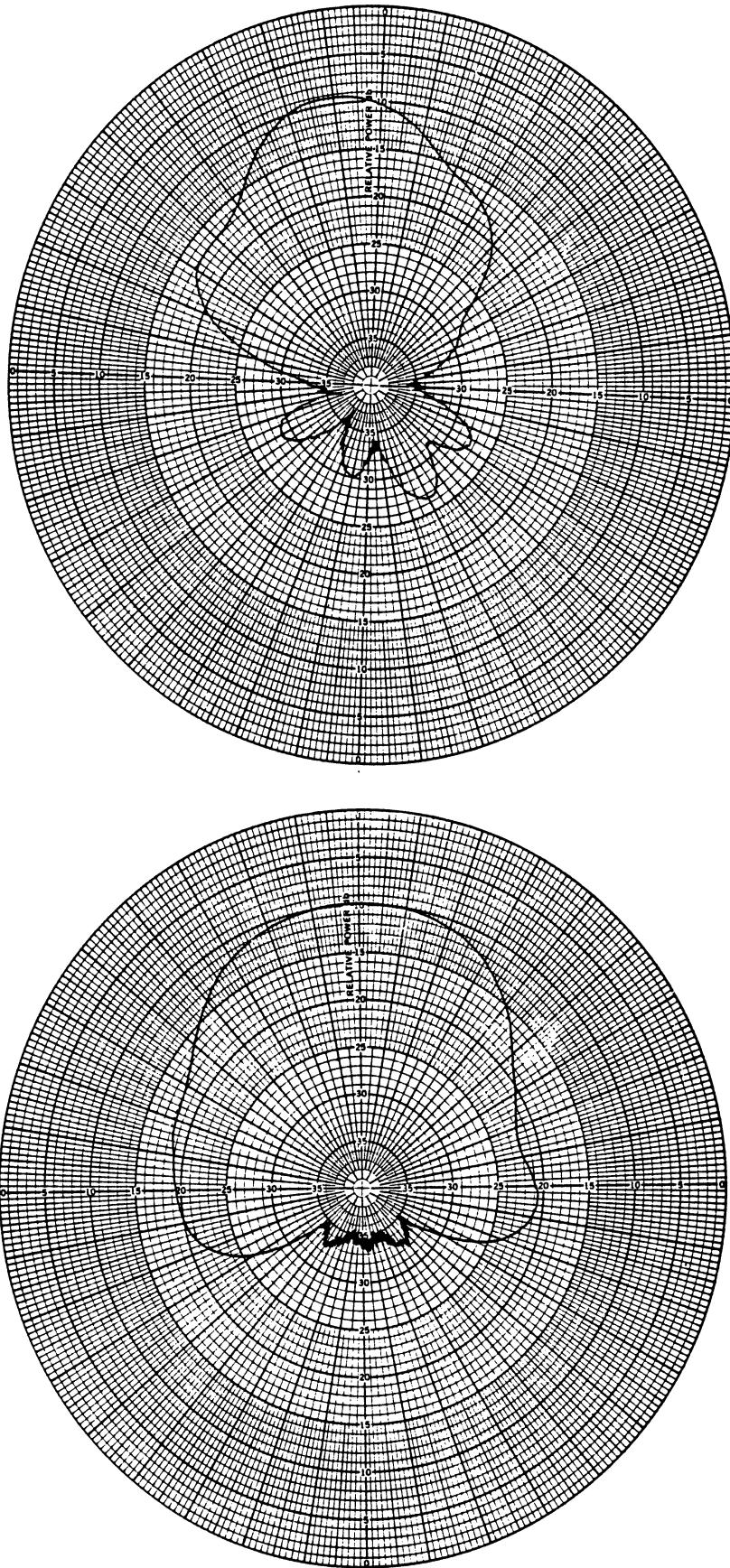


Fig. 3-13: Azimuthal (top) and elevation (bottom) plane patterns for the Winegard antenna at 177 MHz (Channel 7).

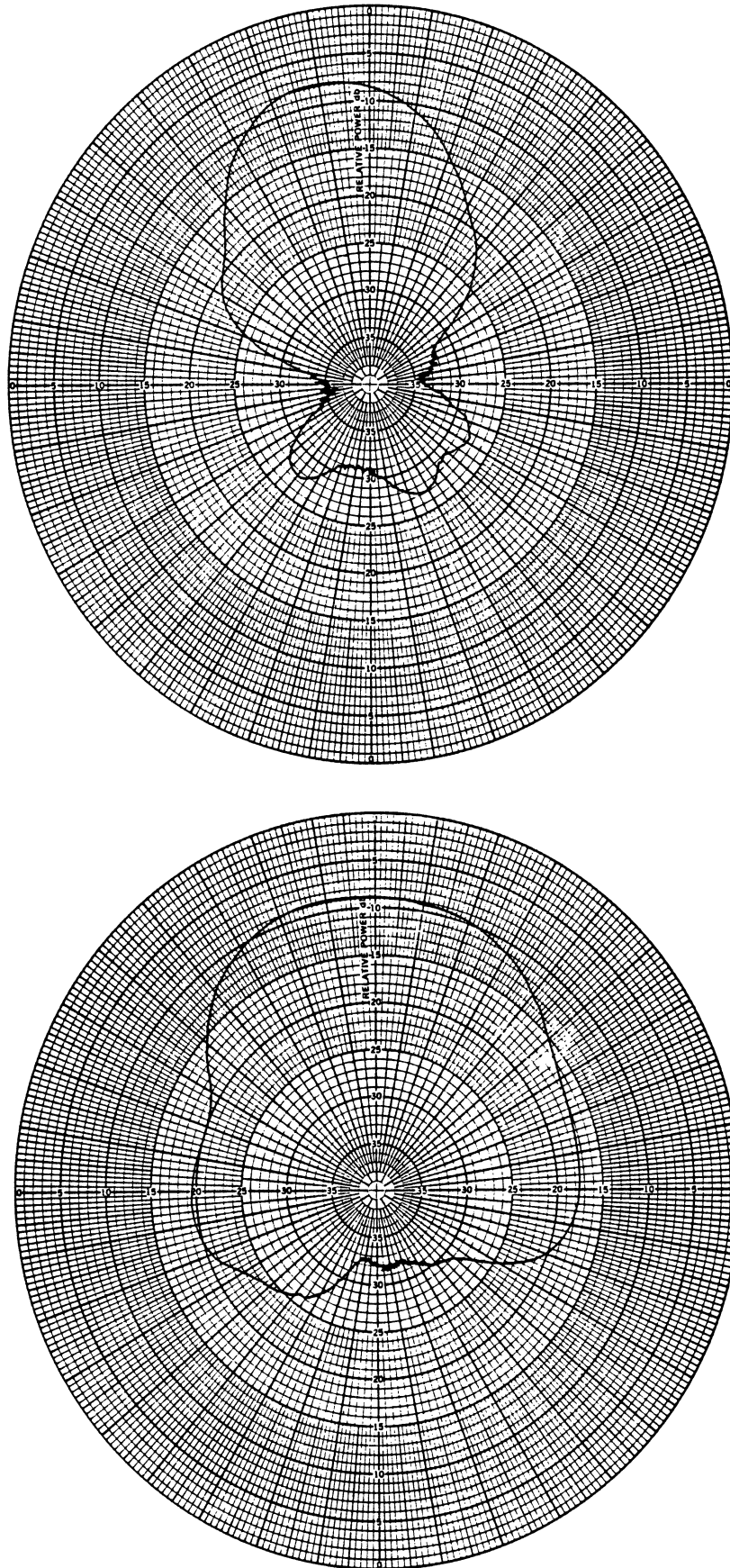


Fig. 3-14: Azimuthal (top) and elevation (bottom) plane patterns for the Winegard antenna at 183 MHz (Channel 8).

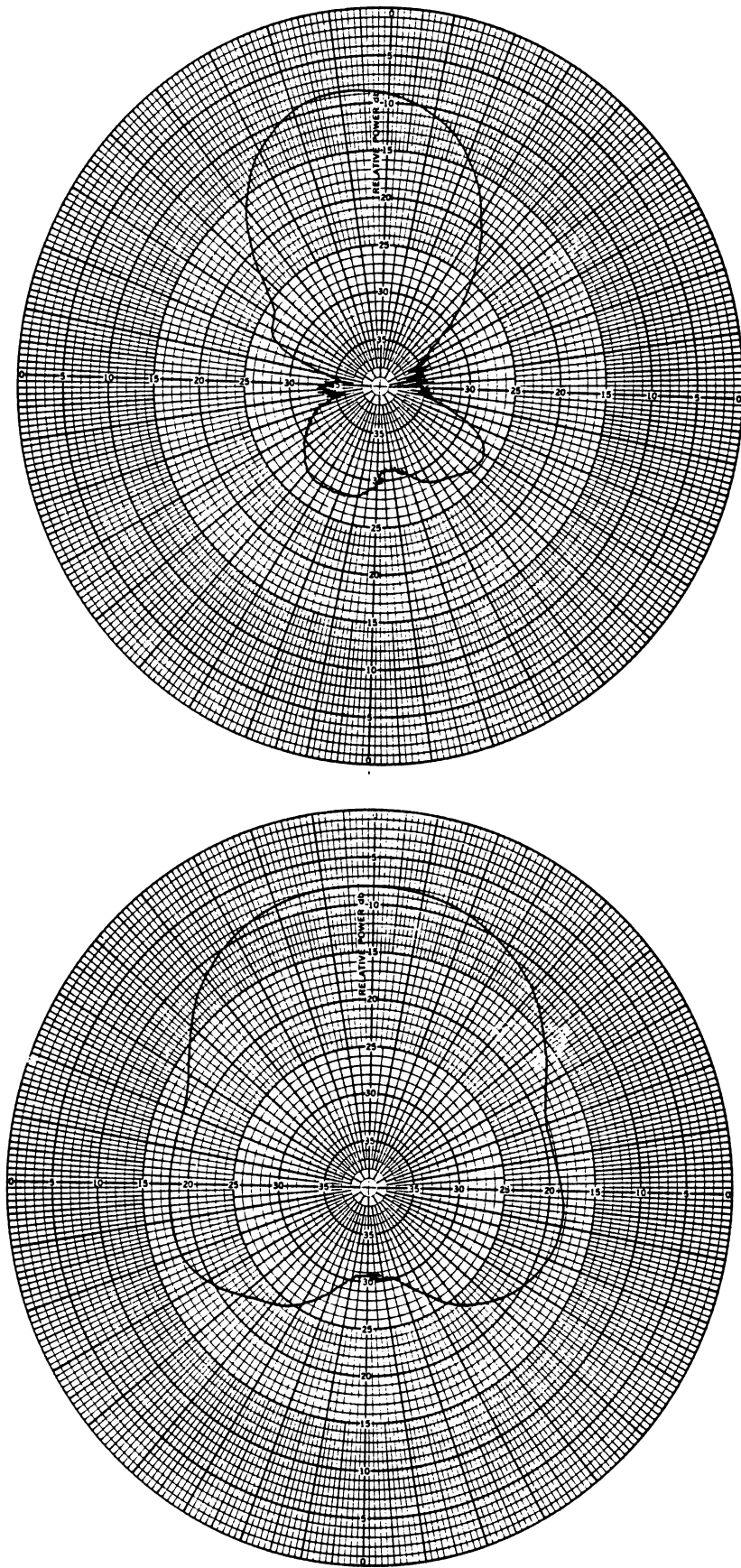


Fig. 3-15: Azimuthal (top) and elevation (bottom) plane patterns for the Winegard antenna at 189 MHz (Channel 9).

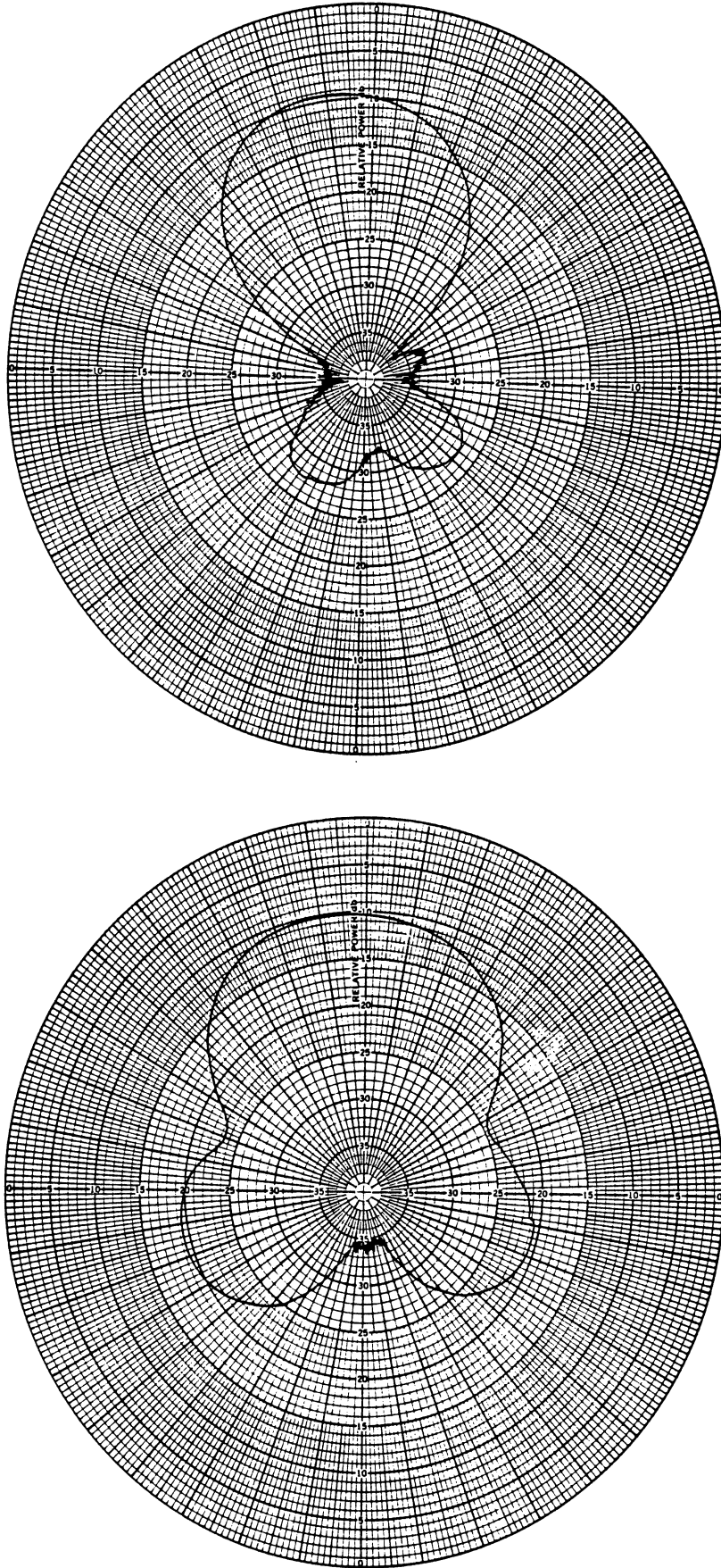


Fig. 3-16: Azimuthal (top) and elevation (bottom) plane patterns for the Winegard antenna at 194 MHz (Channel 10).

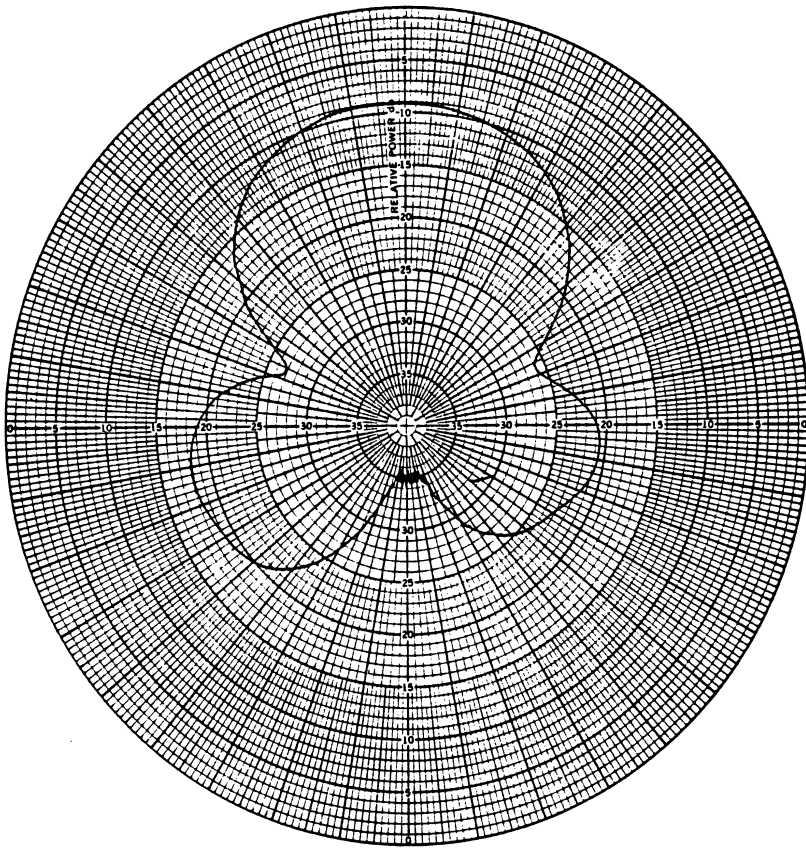
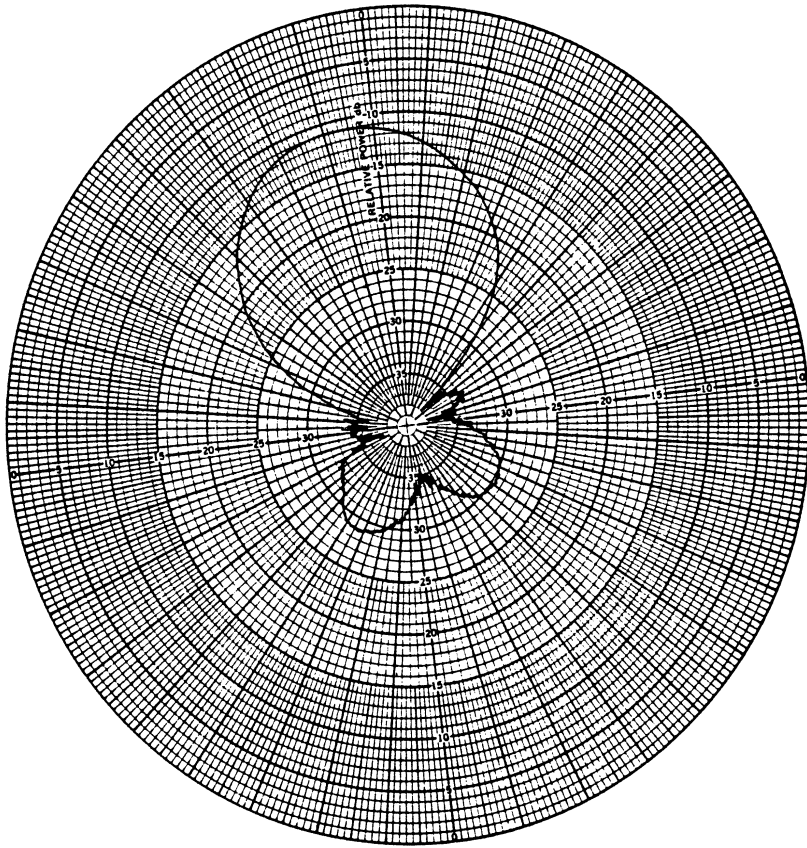


Fig. 3-17: Azimuthal (top) and elevation (bottom) plane patterns for the Winegard antenna at 201 MHz (Channel 11).

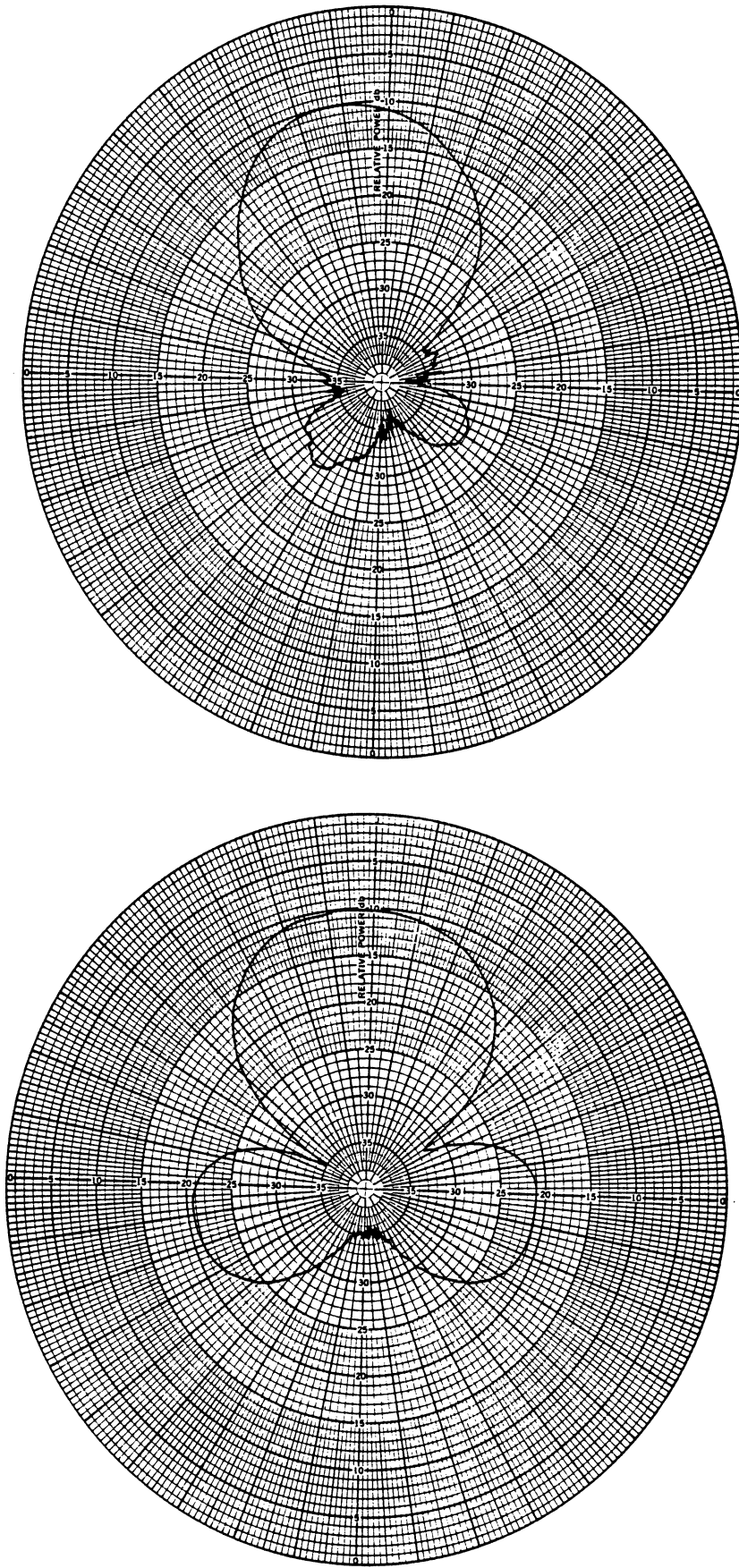


Fig. 3-18: Azimuthal (top) and elevation (bottom) plane patterns for the Winegard antenna at 207 MHz (Channel 12).

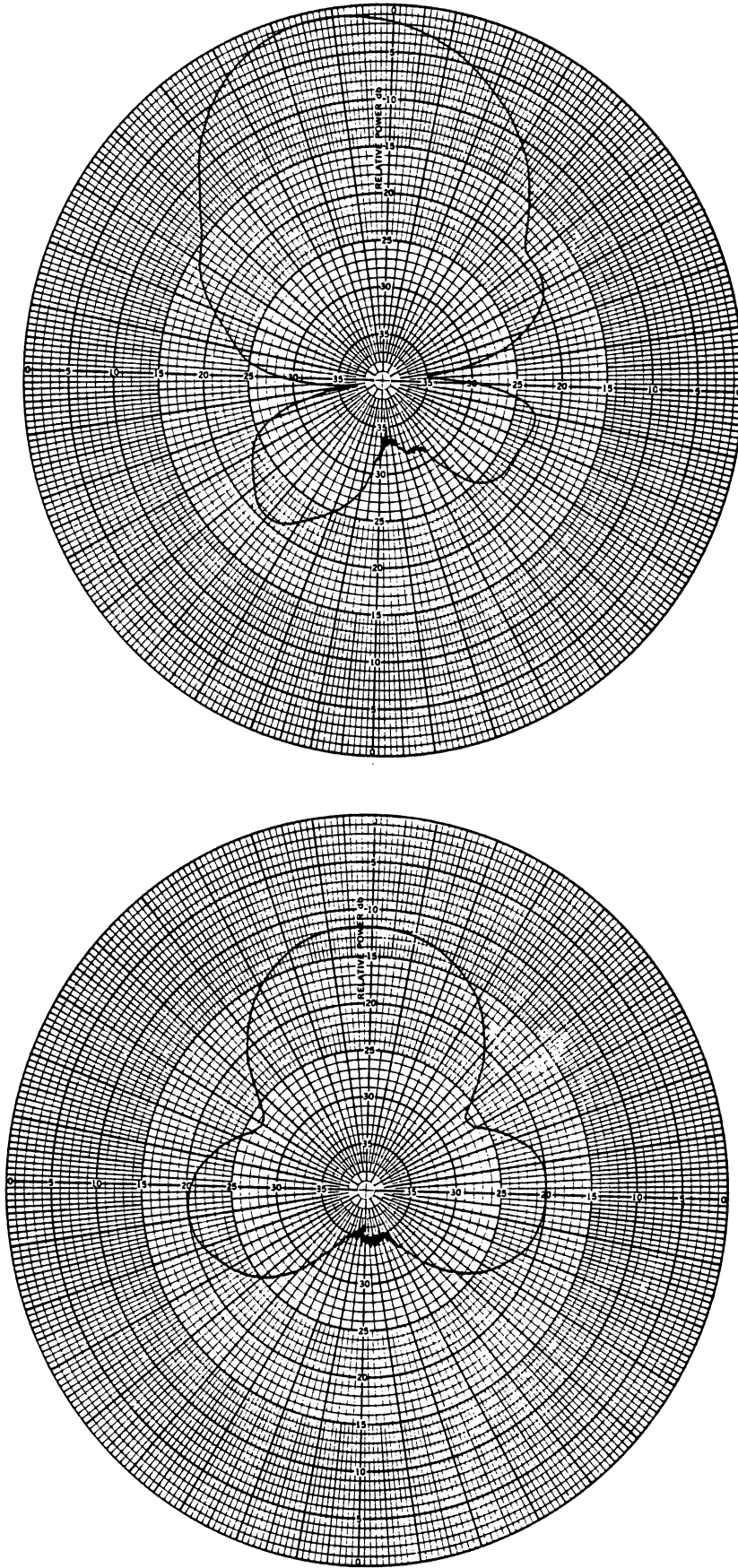


Fig. 3-19: Azimuthal (top) and elevation (bottom) plane patterns for the Winegard antenna at 213 MHz (Channel 13).

Some on-site measurements were also made using the Channel Master antenna whose azimuthal and elevation plane patterns at 8 VHF TV Channel frequencies are given in Figs. 3-20 through 3-27.

3.3 Types of Measurement

At each test site, some or all of the following types of measurements were performed for every TV Channel of interest,

(i) Received signal strength: With the WT stationary, the strength of the received signal was measured by rotating the mainbeam of the receiving antenna until the output was a maximum. The direction for which this maximum occurred was noted and compared with the theoretical (smooth earth) prediction (see Table 2-1). By tuning the spectrum analyzer through the TV Channel band of frequencies, a chart recording the output versus frequency was obtained from which the video and audio signal strengths in dBm (dB above one mW) could be found.

(ii) Antenna response: As the antenna was rotated, the output of the spectrum analyzer tuned to the audio carrier frequency was recorded as a function of time, with and without the WT blades rotating. These measurements served to determine (a) the horizontal plane pattern of the antenna in the actual test environment, (b) the effect of the WT on the received signal, and (c) the amount of signal modulation produced by the blade rotation.

(iii) Blade scattering: With the WT blades locked in a desired position and their pitch set for maximum power, the WT was yawed in azimuth through 360°. By measuring the TV signal received with

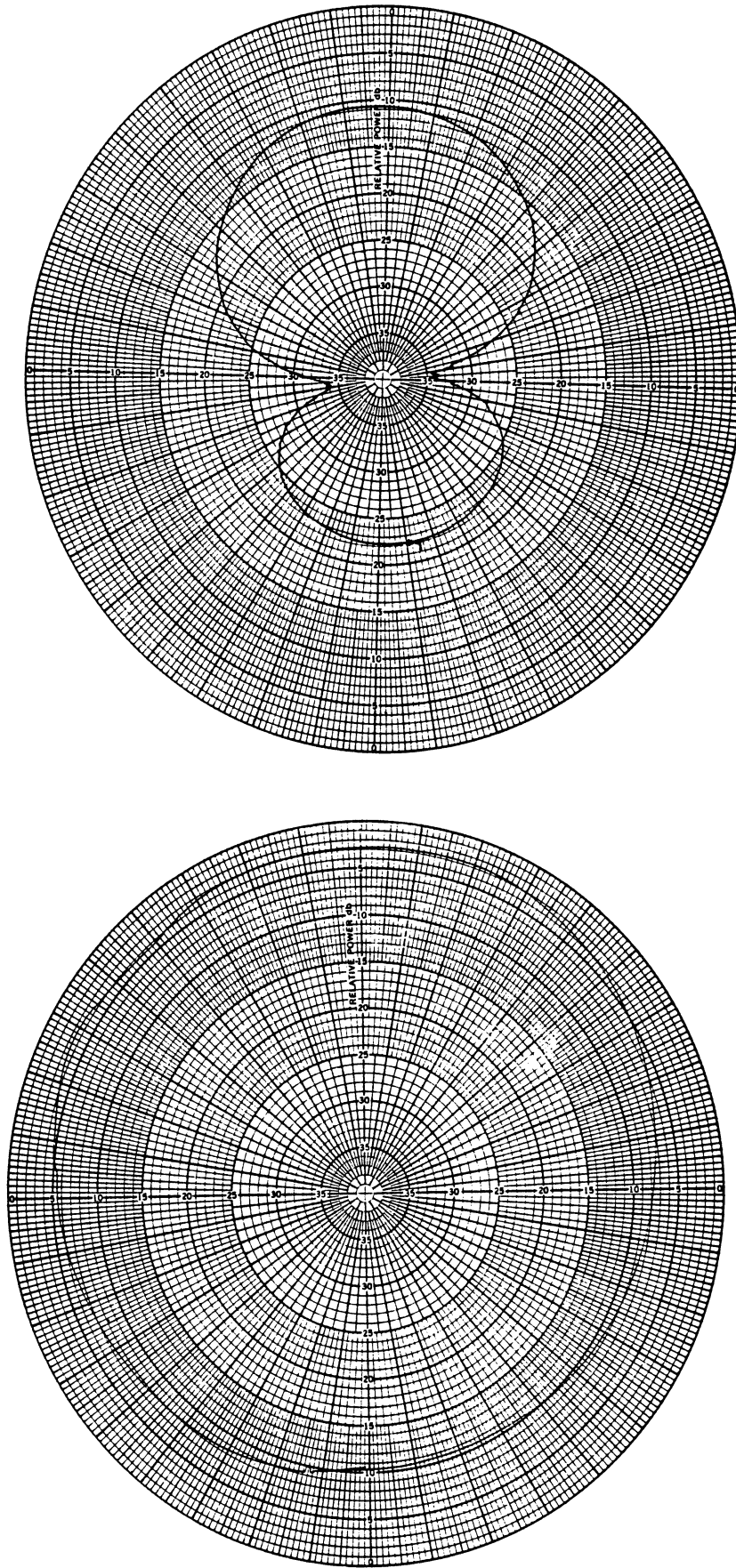


Fig. 3-20: Azimuthal (top) and elevation (bottom) plane patterns for the Channel Master antenna at 57 MHz (Channel 2).

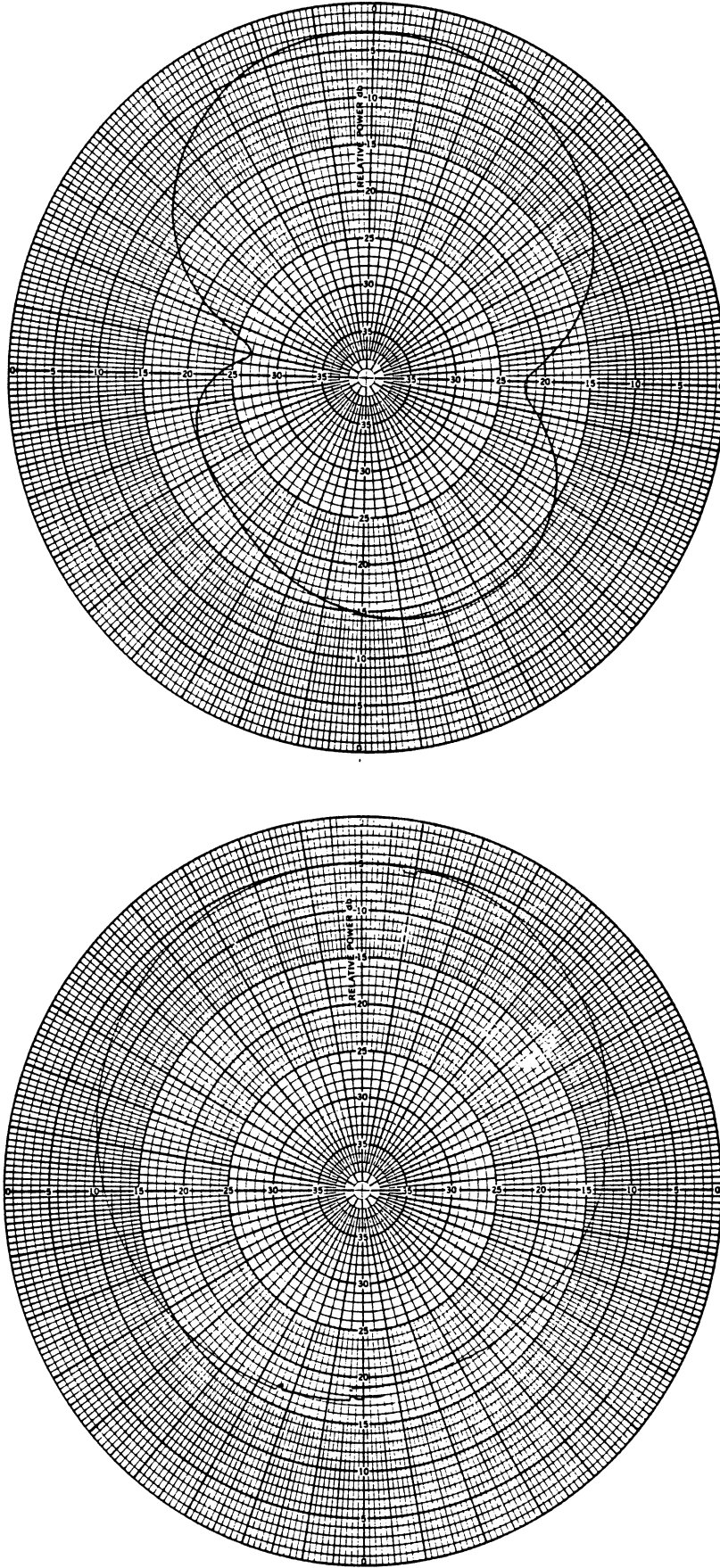


Fig. 3-21: Azimuthal (top) and elevation (bottom) plane patterns for the Channel Master antenna at 63 MHz (Channel 3).

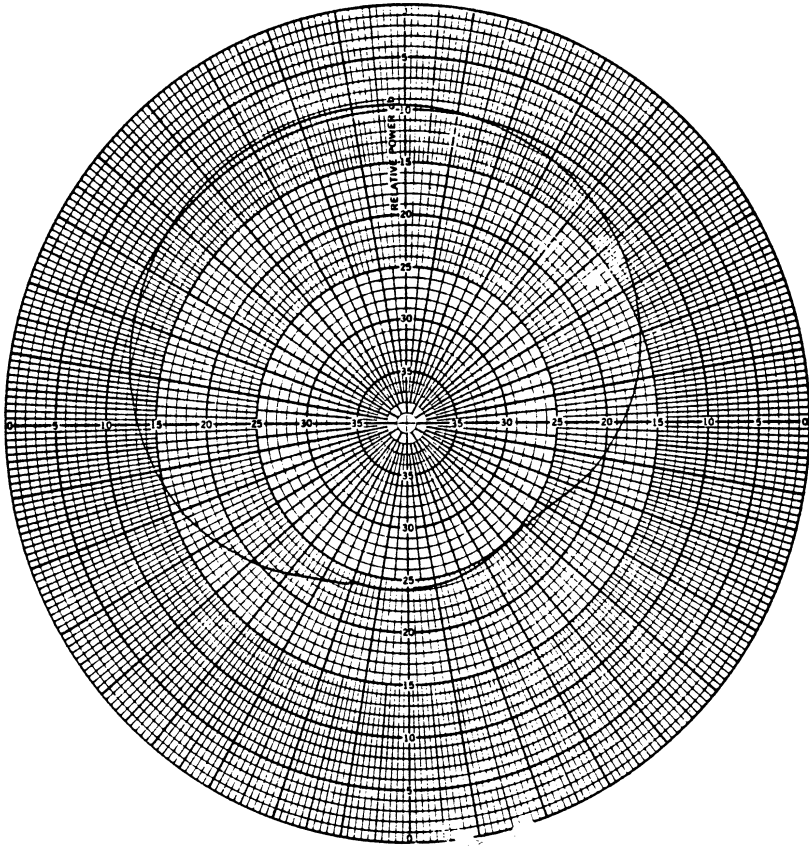
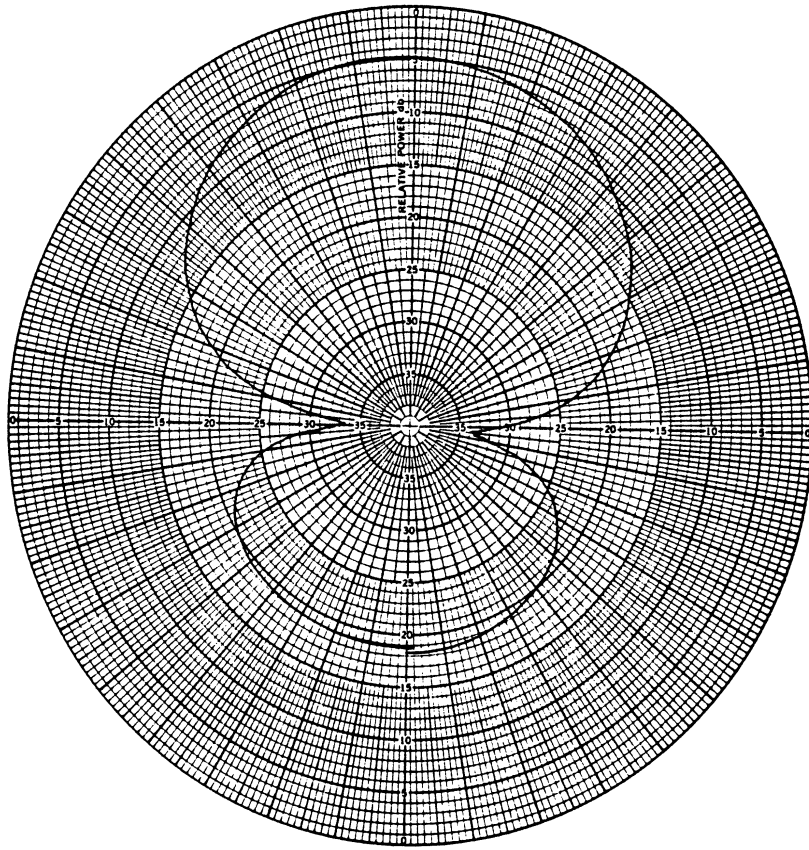


Fig. 3-22: Azimuthal (top) and elevation (bottom) plane patterns for the Channel Master antenna at 79 MHz (Channel 5).

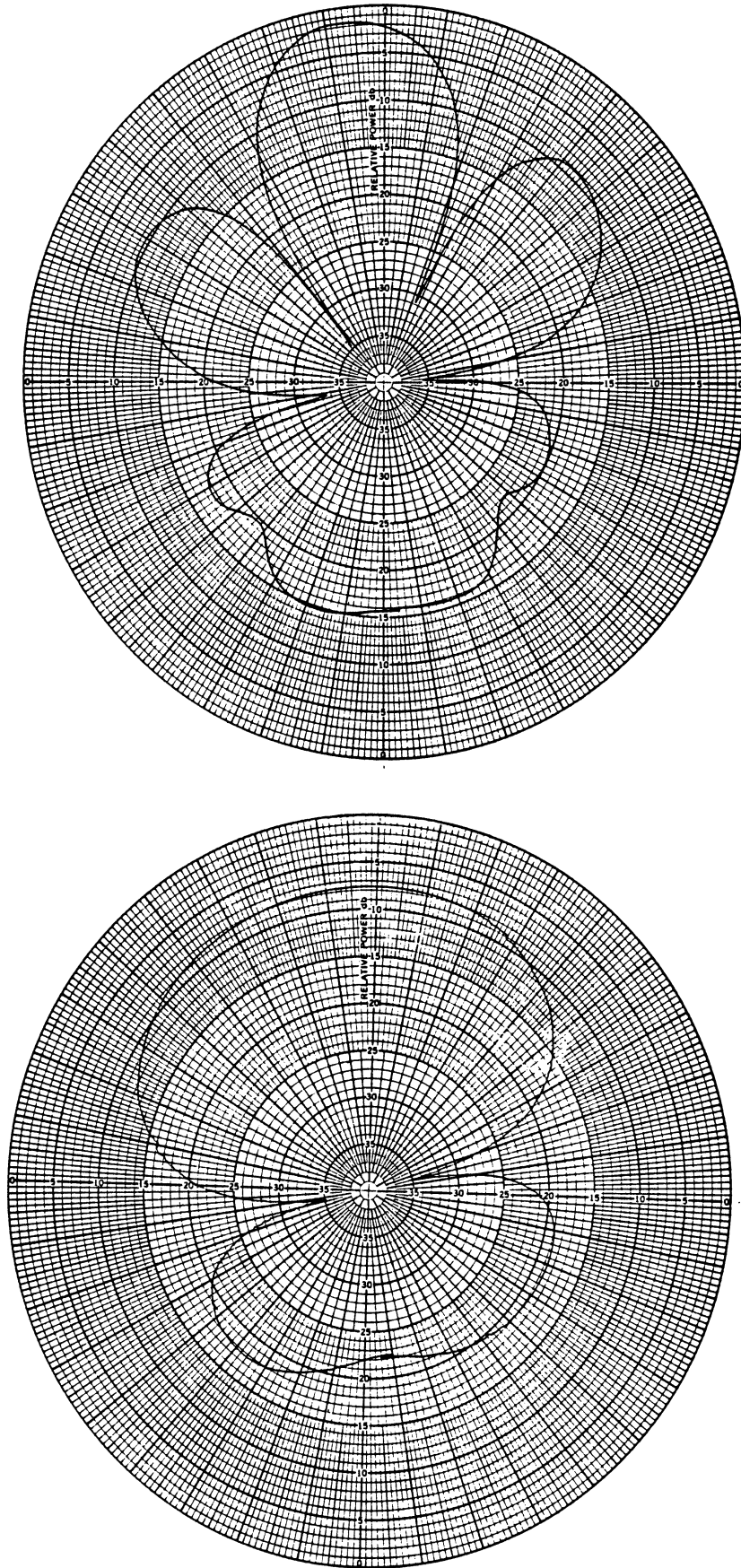


Fig. 3-23: Azimuthal (top) and elevation (bottom) plane patterns for the Channel Master antenna at 177 MHz (Channel 7).

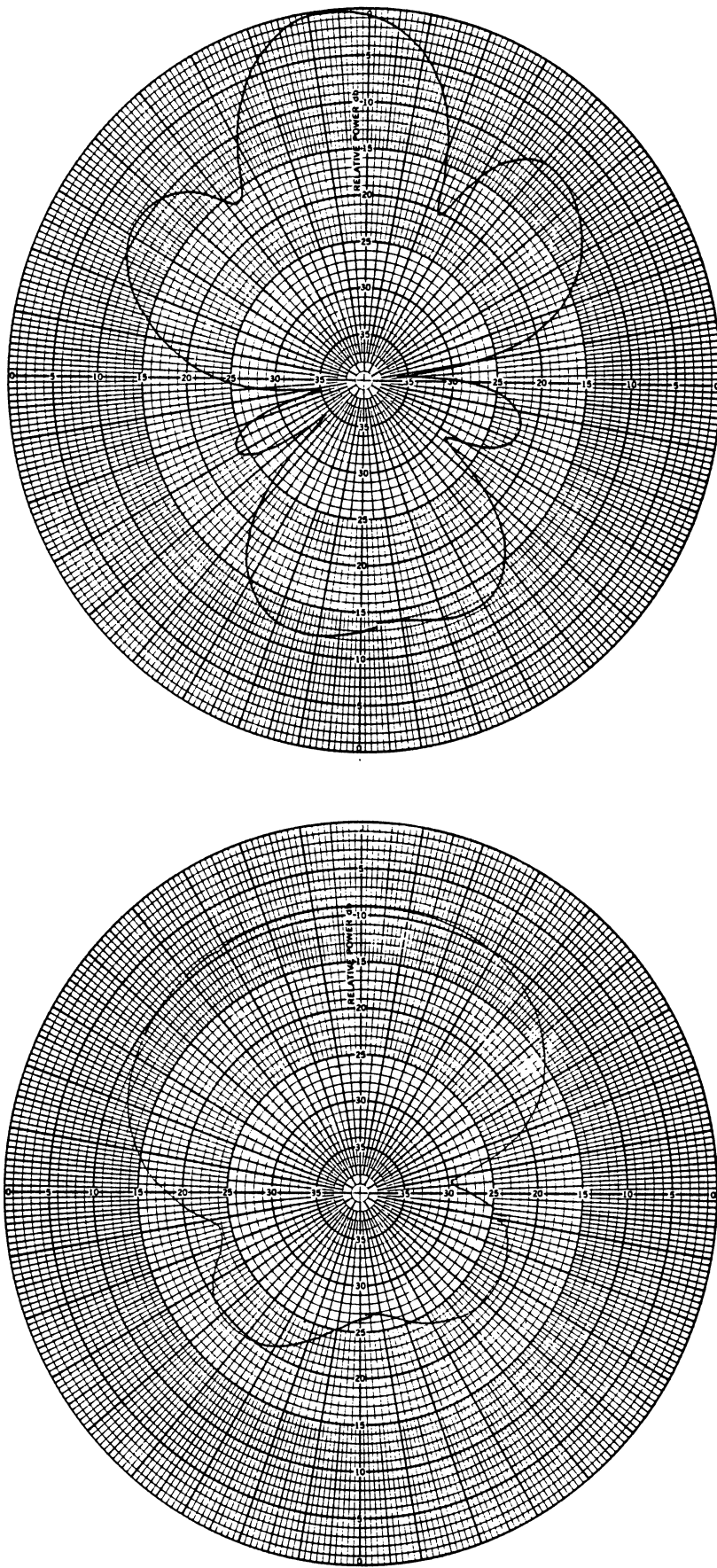


Fig. 3-24: Azimuthal (top) and elevation (bottom) plane patterns for the Channel Master antenna at 183 MHz (Channel 8).

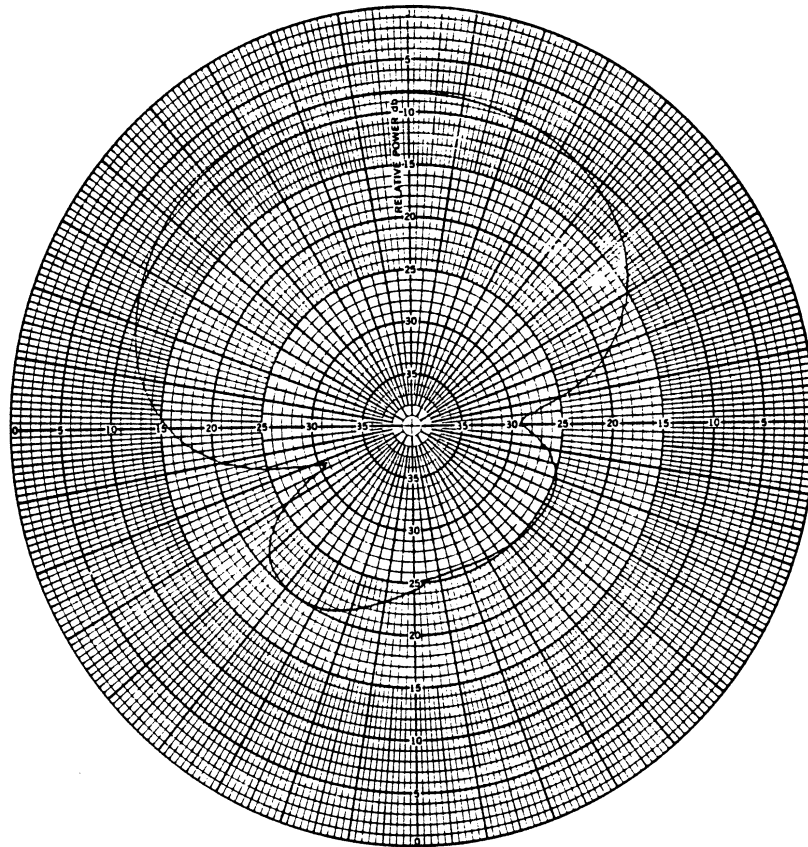
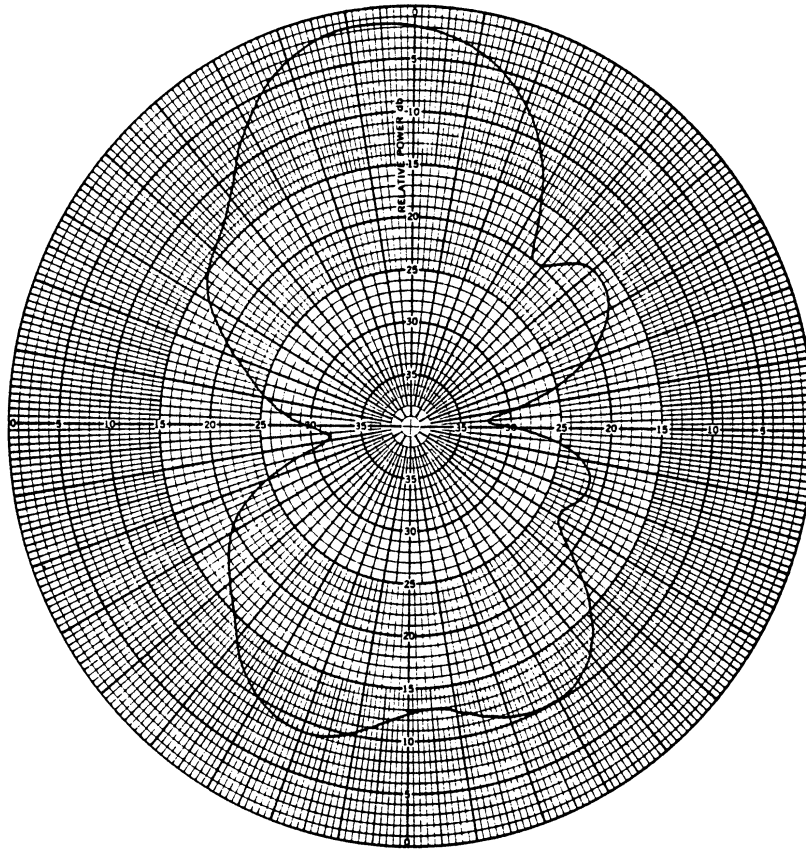


Fig. 3-25: Azimuthal (top) and elevation (bottom) plane patterns for the Channel Master antenna at 189 MHz (Channel 9).

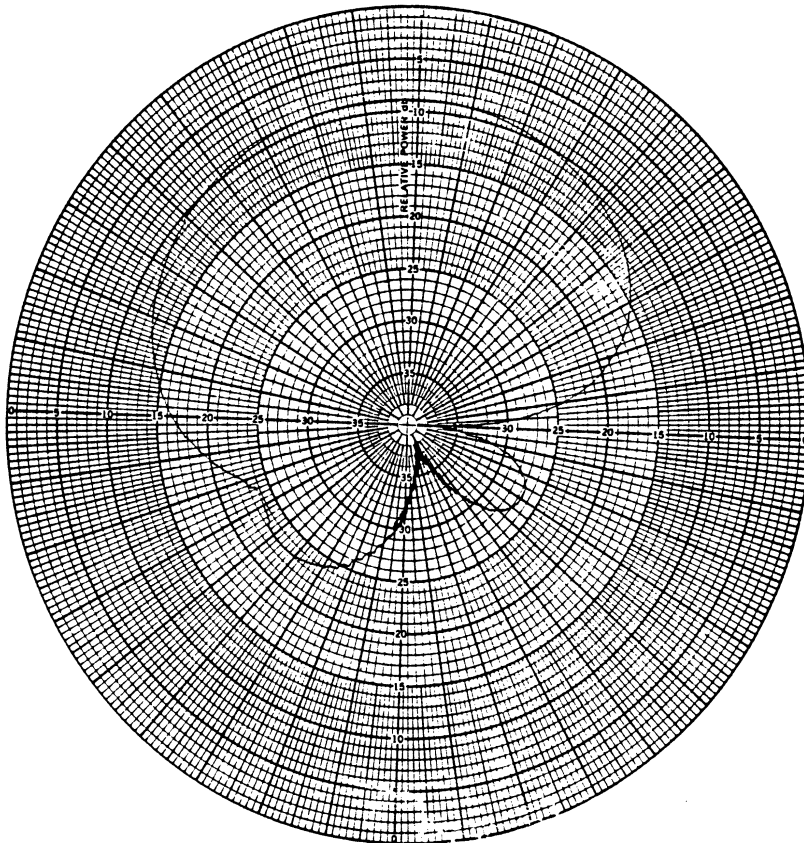
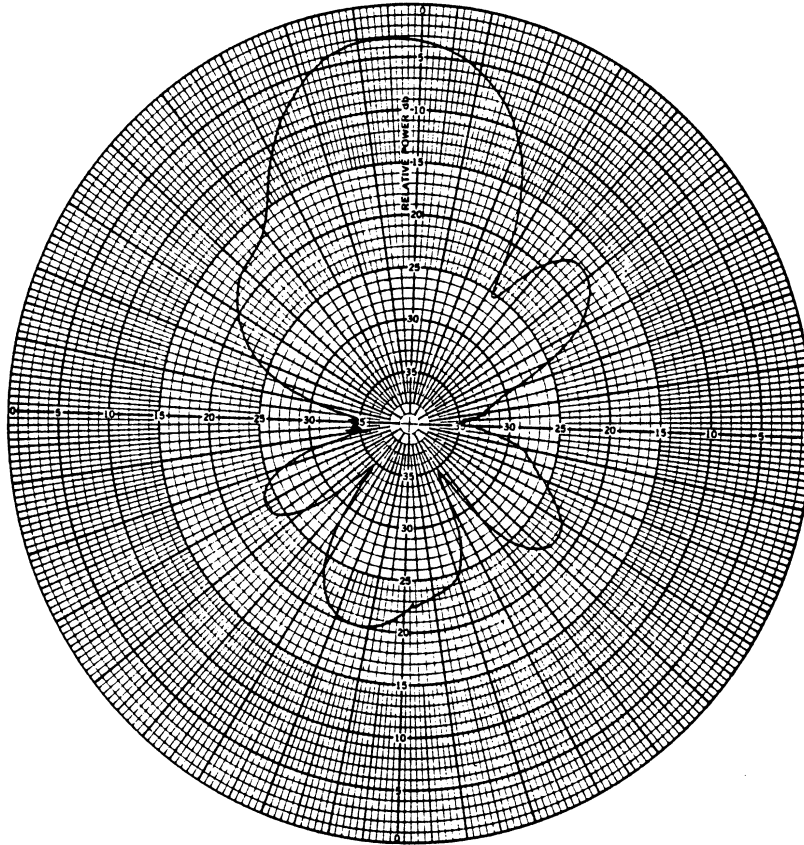


Fig. 3-26: Azimuthal (top) and elevation (bottom) plane patterns for the Channel Master antenna at 201 MHz (Channel 11).

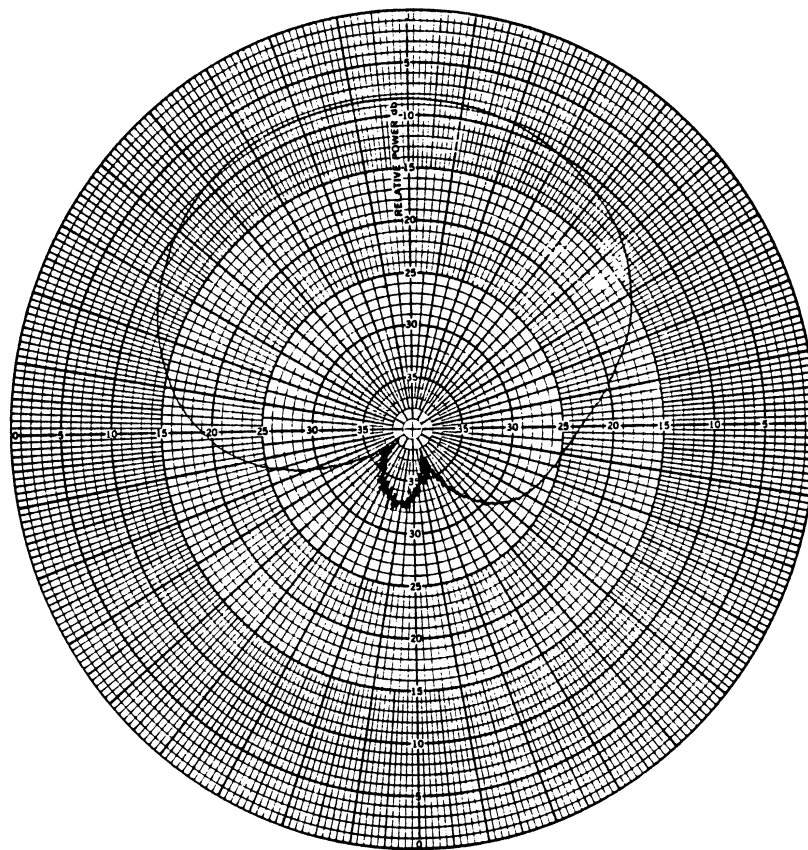
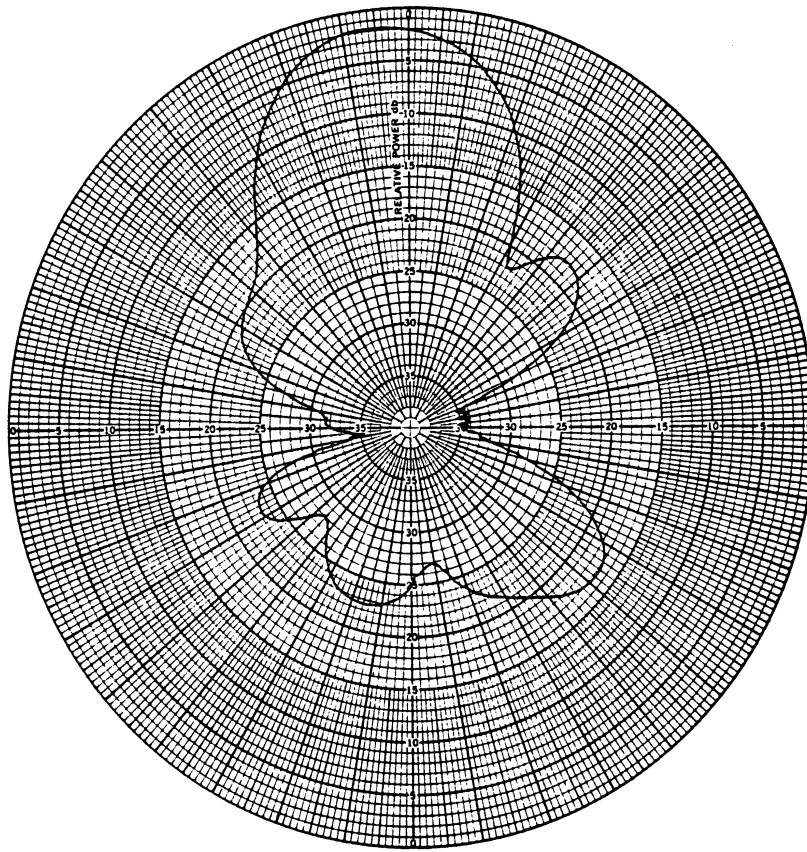


Fig. 3-27: Azimuthal (top) and elevation (bottom) plane patterns for the Channel Master antenna at 207 MHz (Channel 12).

the antenna pointed at the TV transmitter and then at the WT, the maximum blade-scattered signal could be determined. These static tests were performed when the wind was insufficient to operate the machine, and served to supplement the information obtained from the dynamic tests. Conversely, the static tests were not carried out when the wind was strong enough to rotate the blades.

(iv) TV interference: These dynamic tests required the WT blades to be rotating. The antenna beam was positioned to receive the maximum signal (this was generally when the beam was directed at the TV transmitter) and the spectrum analyzer was tuned to the audio carrier frequency. Its output was then recorded as a function of time, and the received picture on the TV screen was observed for any video distortion. In a few instances the measurements were repeated with the antenna beam pointed at the WT to simulate the worst possible situation of a mis-positioned antenna. The result was usually a high level of interference.

(v) Video recording: This was done whenever it was felt desirable to preserve the video effects.

To the extent possible and appropriate, the above measurements were made on all TV Channels of interest at all of the sites A through J. In addition, field strength measurements were made at the WT site (base of the tower and on top of the nacelle) and at points along the gravel road near site A to check on the local variations of the field. The antenna used was the Winegard, but at site A some dynamic measurements were also made with the Channel Master antenna and a half-wave dipole to bring out the effect of lower performance antennas

on the observed backward region interference. A detailed description of the complete test plan followed during the measurements is given in Appendix B.

3.4 Measured Antenna Response

The free space patterns of the test antennas were presented in §3.2 above, but these do not necessarily reflect the actual performance in the test environment. At each site and for each TV Channel, a knowledge of the response $F(B,T)$ of the antenna in the direction of the WT blade phase center B relative to the response in the direction of the distant TV transmitter T is needed to analyze the test results (see Chapters 5 and 6) and this may differ from the value deduced from the free space patterns. Prior to a static or dynamic test, we therefore measured the horizontal plane (azimuthal) pattern of the antenna by recording the output of the spectrum analyzer (tuned to the audio carrier) as the antenna was rotated with the WT stationary (see §3.3(ii)). To illustrate the results obtained, some of the patterns recorded at site A are presented here.

Figures 3-28 through 3-31 show the patterns of the Winegard antenna on Channels 3, 5, 7 and 8, with the directions of the transmitter and the WT marked. For Channel 3 the pattern is similar to the free space one in Fig. 3-9, but the value of $F(B,T)$ is now only 12.5 dB, compared with 16 dB in free space. The Channel 7 pattern also compares favorably with the free space one, but on Channel 5 there is a significant side lobe which does not appear in the free space pattern. The Channel 8 pattern is unusual in that there is a very strong reflected signal present. This is as much as 2 dB above the main beam level and may be due to reflection from Howard Knob.

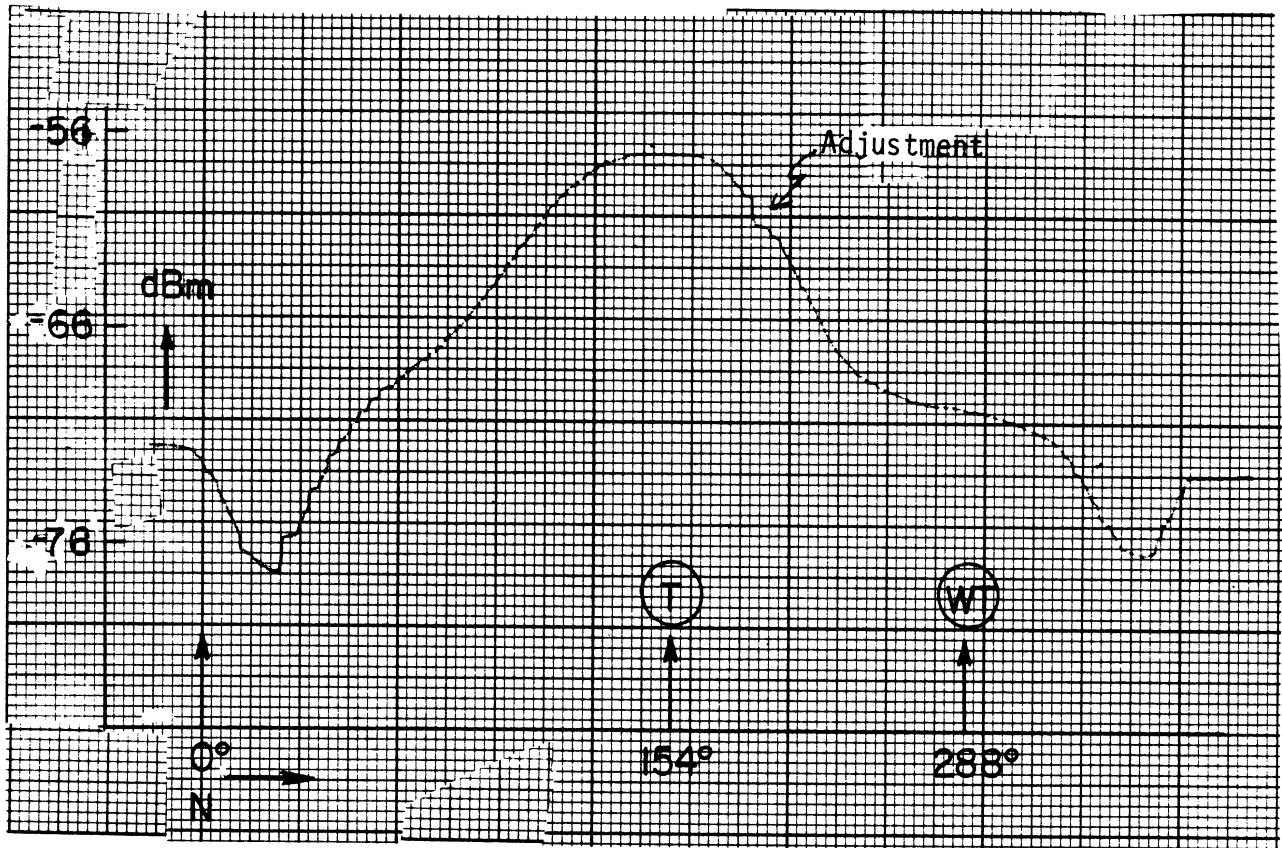


Fig. 3.28 Static response of the Winegard antenna on Channel 3 obtained at site A.

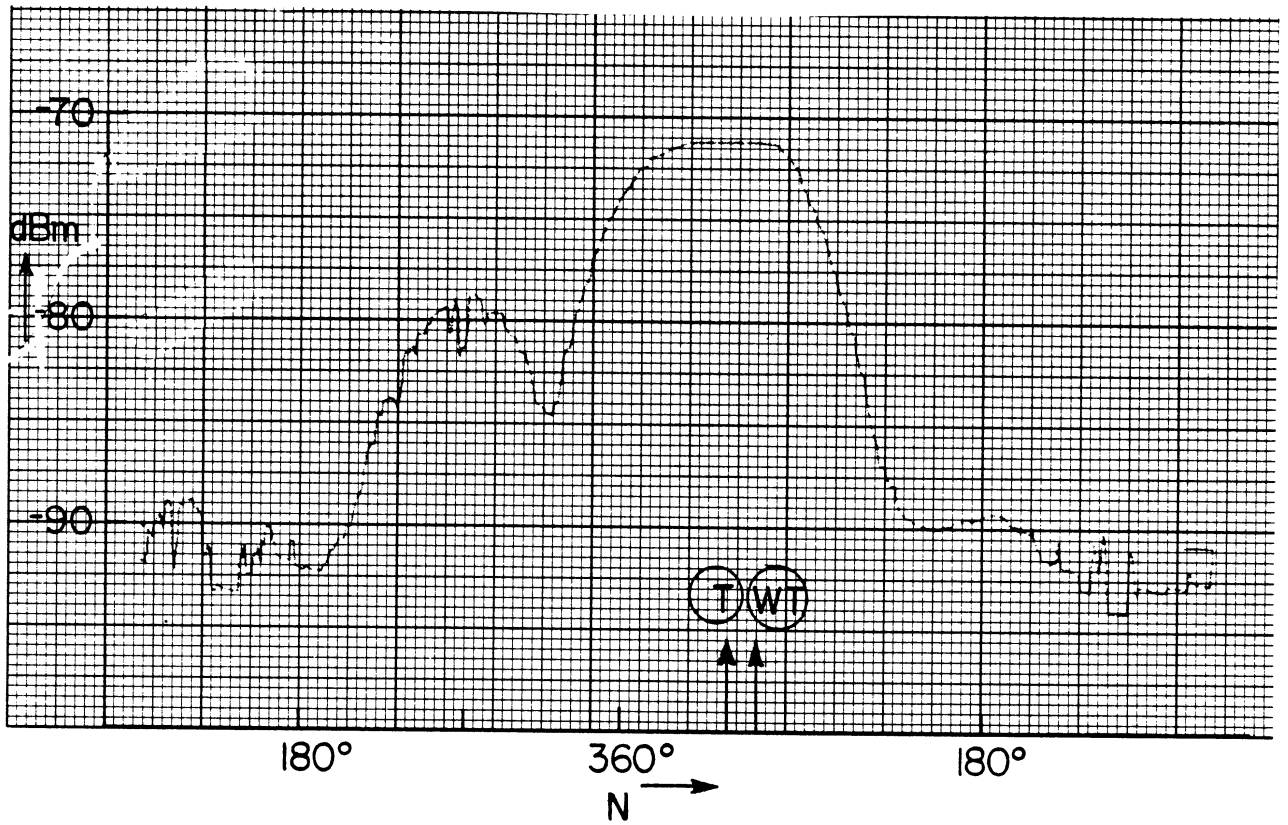


Fig. 3.29 Static response of the Winegard antenna on Channel 5 obtained at site A.

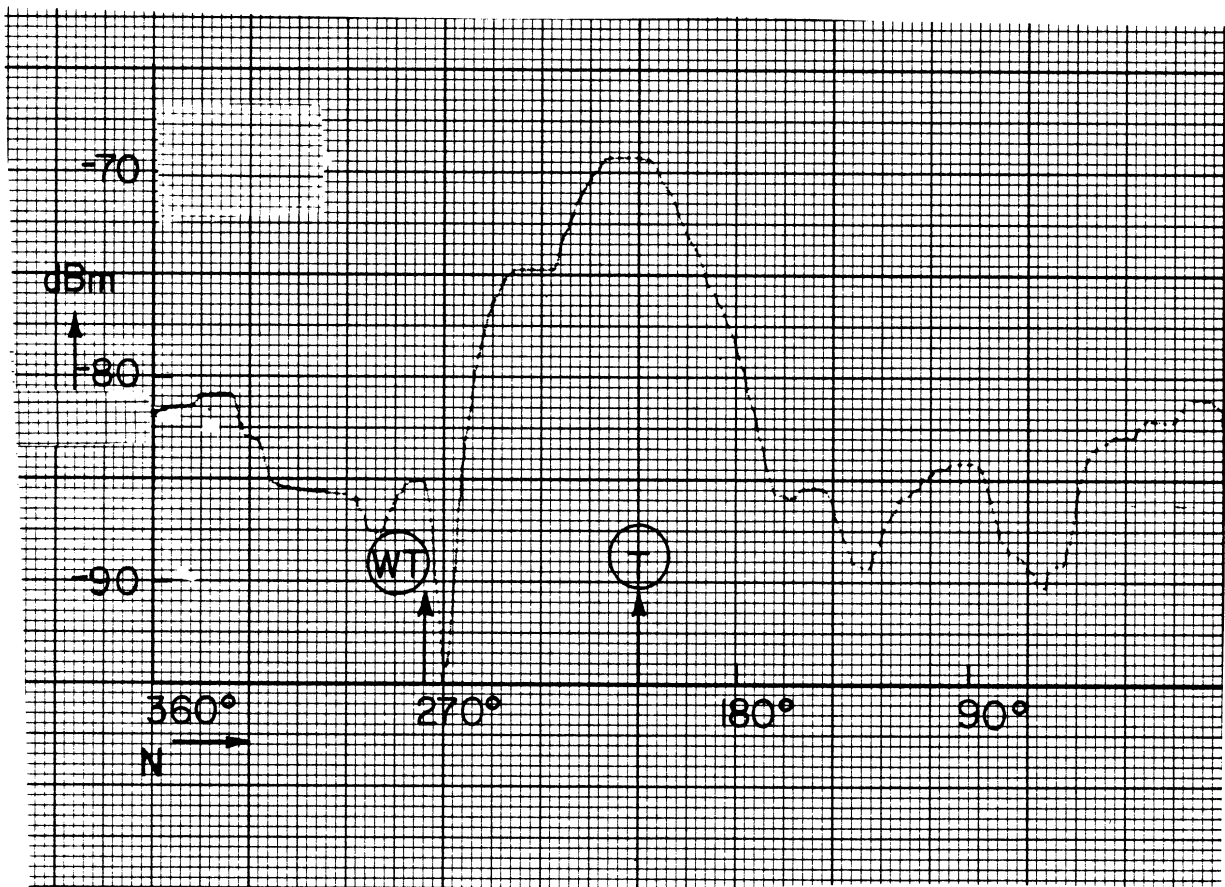


Fig. 3.30 Static response of the Winegard antenna on Channel 7 obtained at site A.

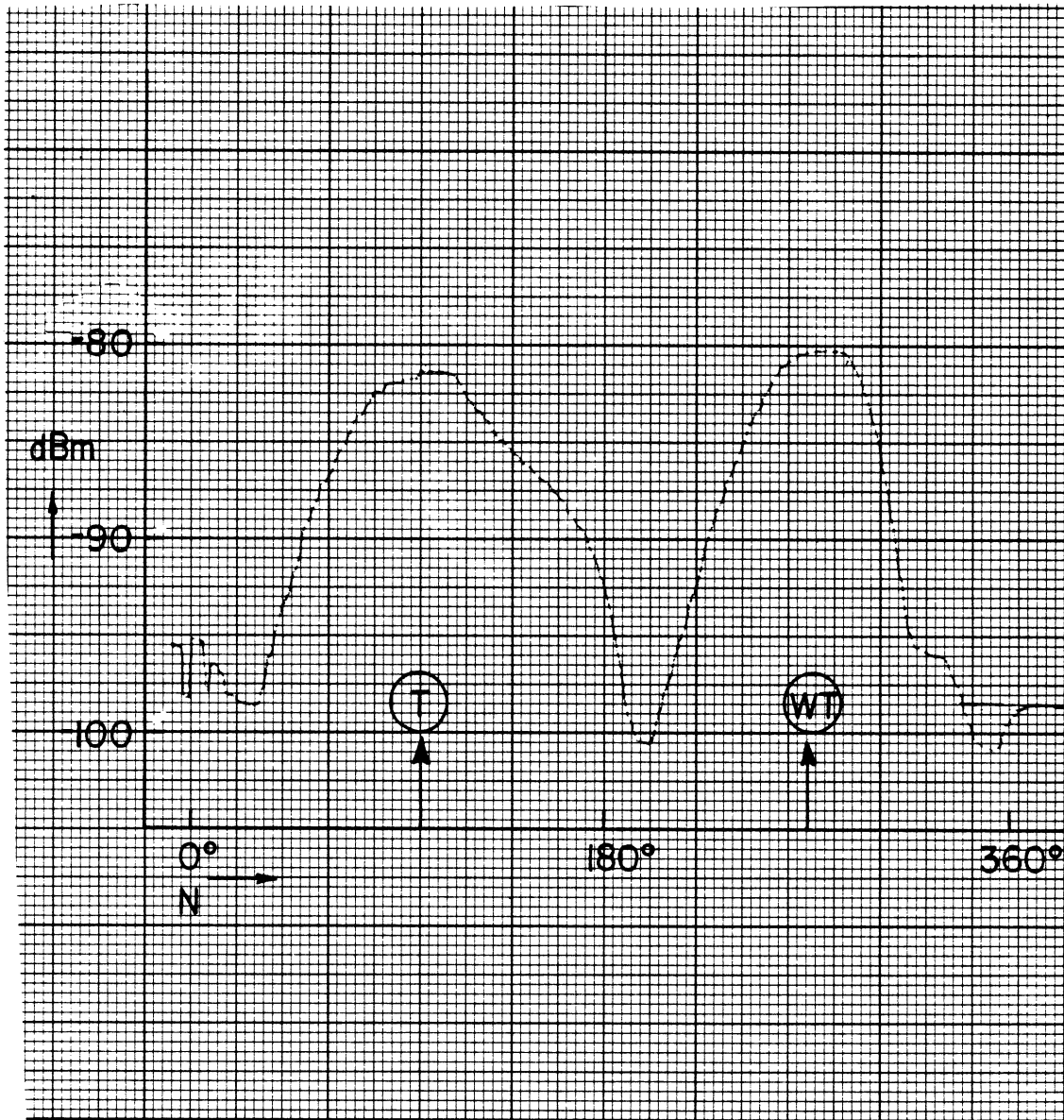


Fig. 3.31 Static response of the Winegard antenna on Channel 8 obtained at site A.

A typical pattern for the Channel Master antenna is that shown in Fig. 3-32 for Channel 3, also at site A. The measured front-to-back ratio is about 15 dB, which is slightly above the free space value.

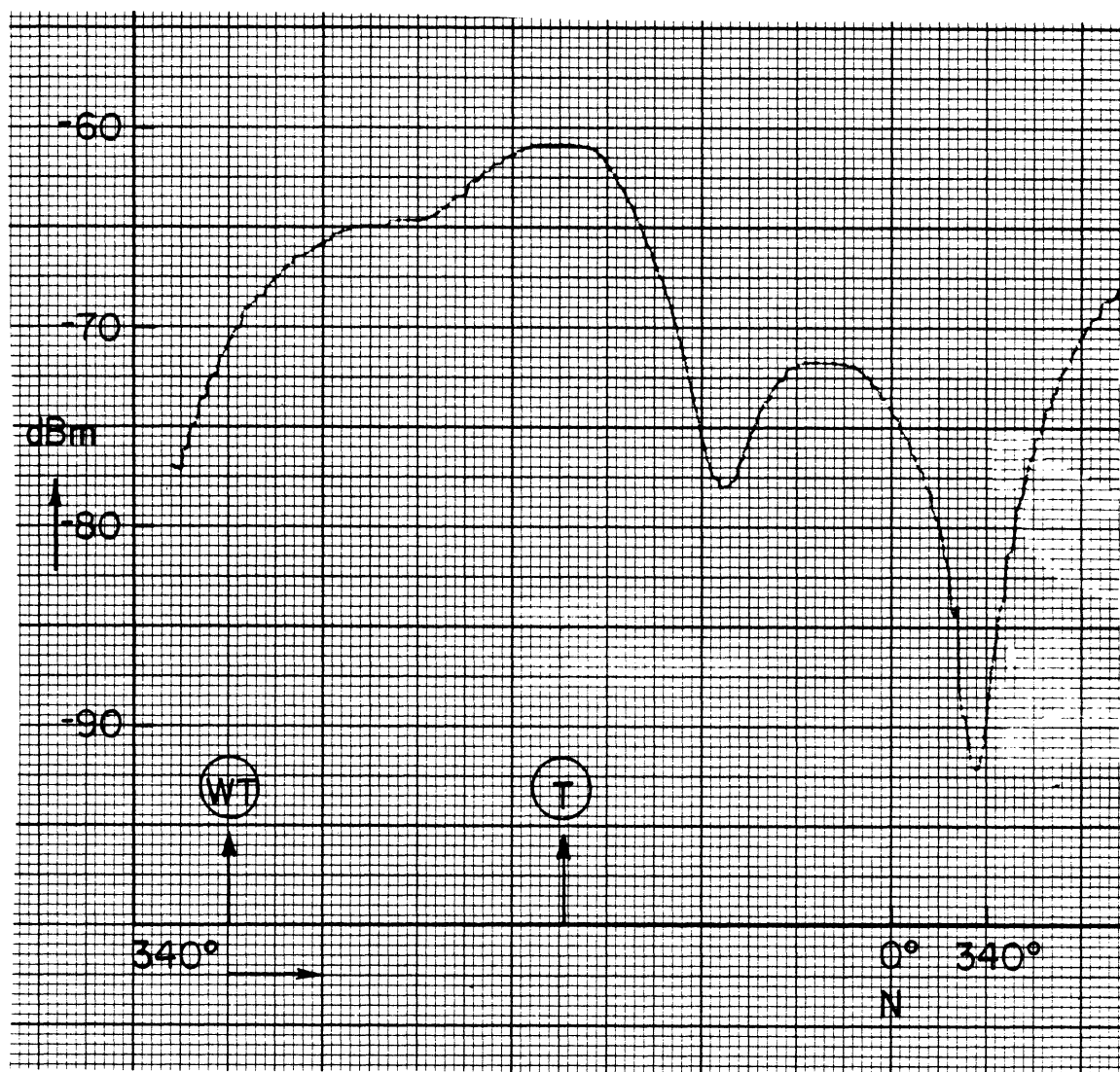


Fig. 3.32 Static response of the Channel Master antenna on Channel 3 obtained at site A.

CHAPTER 4. MEASURED AMBIENT FIELD STRENGTHS

The quality of TV reception at any place depends on the signal to noise ratio of the receiver, the receiving antenna used, and (obviously) the TV signal strength. To determine the quality that is possible in the Boone area, the ambient field strengths were measured at all of the test sites on all of the available TV Channels. Since most homes are located in the valleys 1000 (or more) ft below the top of the surrounding hills, it was expected that the TV signals would be weak due to shadowing. This proved to be the case, and according to the industry specification of the signals needed for Grades A and B of service (see §2.2), the reception of most Channels at almost all homes would be classified as poor.

There was also a second reason for the measurements. The severity of WT interference with TV reception depends on the ratio of the WT-scattered signal to the ambient signal at the site in question, and the WT-scattered signal is, in turn, proportional to the ambient field strength at the WT. To predict the level of TVI for comparison with our measured interference data, it is therefore necessary to know the ambient field strengths at the WT as well as at the test sites.

In the following sections we discuss the measurements that were made at the WT, at the ten sites A through J described in §2.4, and also along the road near site A, and summarize the results obtained.

4.1 Data Reduction

The measurements were made with the WT stationary using the Winegard antenna. Except for the tests on top of the WT nacelle, the antenna was located about 20 ft above ground. At each site and for all of the desired TV Channels, the received video and audio powers, P_v and P_a respectively, were obtained from the recordings of the spectrum analyzer output in the manner described in §3.3. In addition, the quality of reception was examined using the TV receiver.

It is convenient to begin by illustrating the type of raw data obtained. With the spectrum analyzer tuned to the audio frequency of a particular TV Channel, the output P_a was recorded as the antenna was rotated through 360°. This was done to measure the horizontal plane pattern of the antenna in the actual test environment, and to determine the direction from which the TV signal was received for comparison with the theoretical direction. The recording for Channel 3 at the base of the WT (the actual site was about 50 ft from the base of the tower in the SE direction) is shown in Fig. 4-1. As it should at this site, the antenna response is in good agreement with the azimuthal pattern in Fig. 3-9. With the antenna oriented to receive the maximum signal, the spectrum analyzer was then tuned through the TV Channel band of frequencies and the output recorded. Figure 4-2 shows the result for Channel 3 at the same site. As is true for all TV Channels, the audio power peak occurs at a frequency 4.5 MHz above the video power peak. The received video and audio carrier signal strengths P_v and P_a can be obtained directly in dBm (dB above one milliwatt), and from Fig. 4-2 we have $P_v = -22$ dBm, $P_a = -27$ dBm.

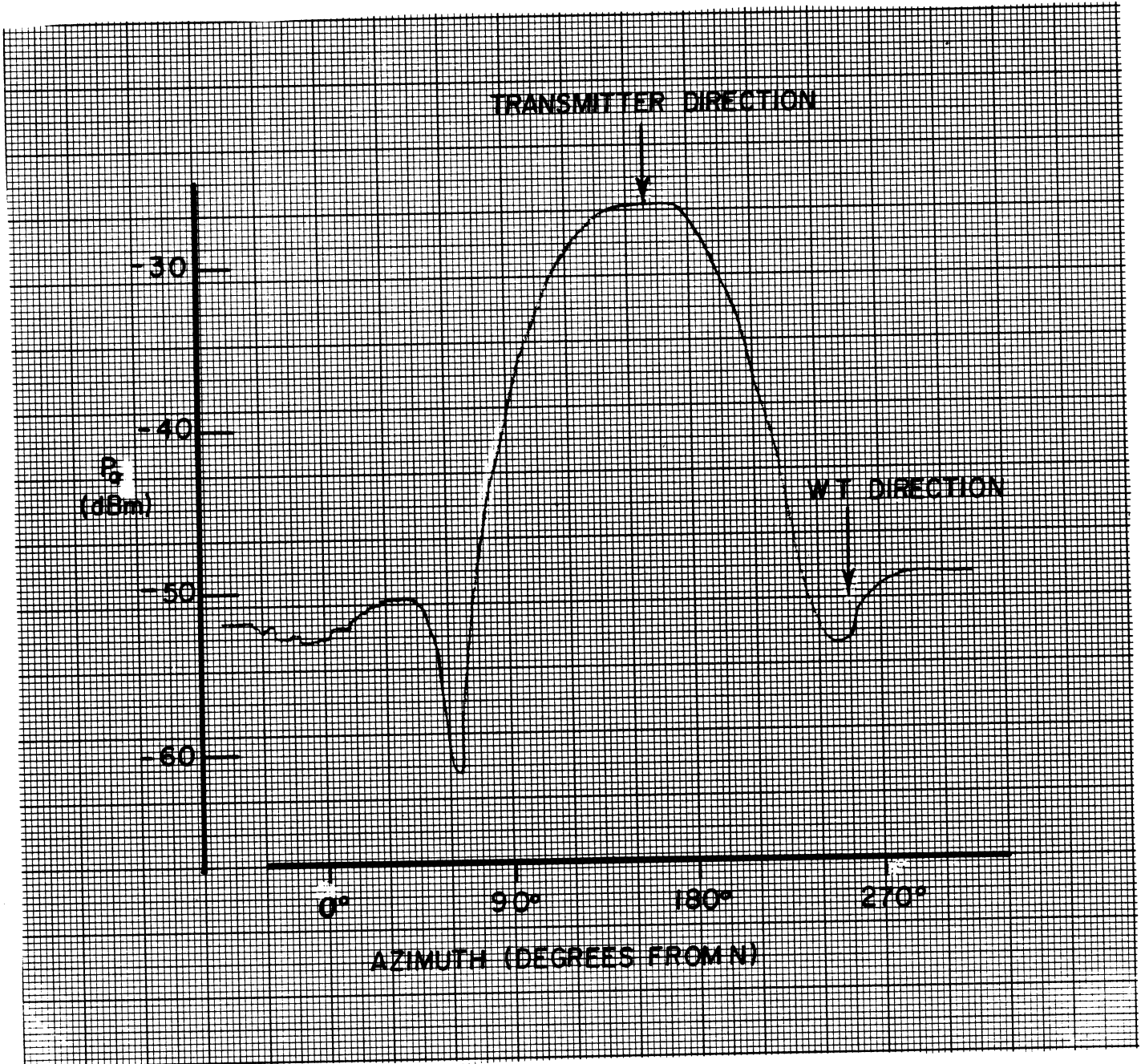


Fig. 4-1: Audio carrier signal strength on Channel 3 vs. antenna rotation angle at the base of the WT.

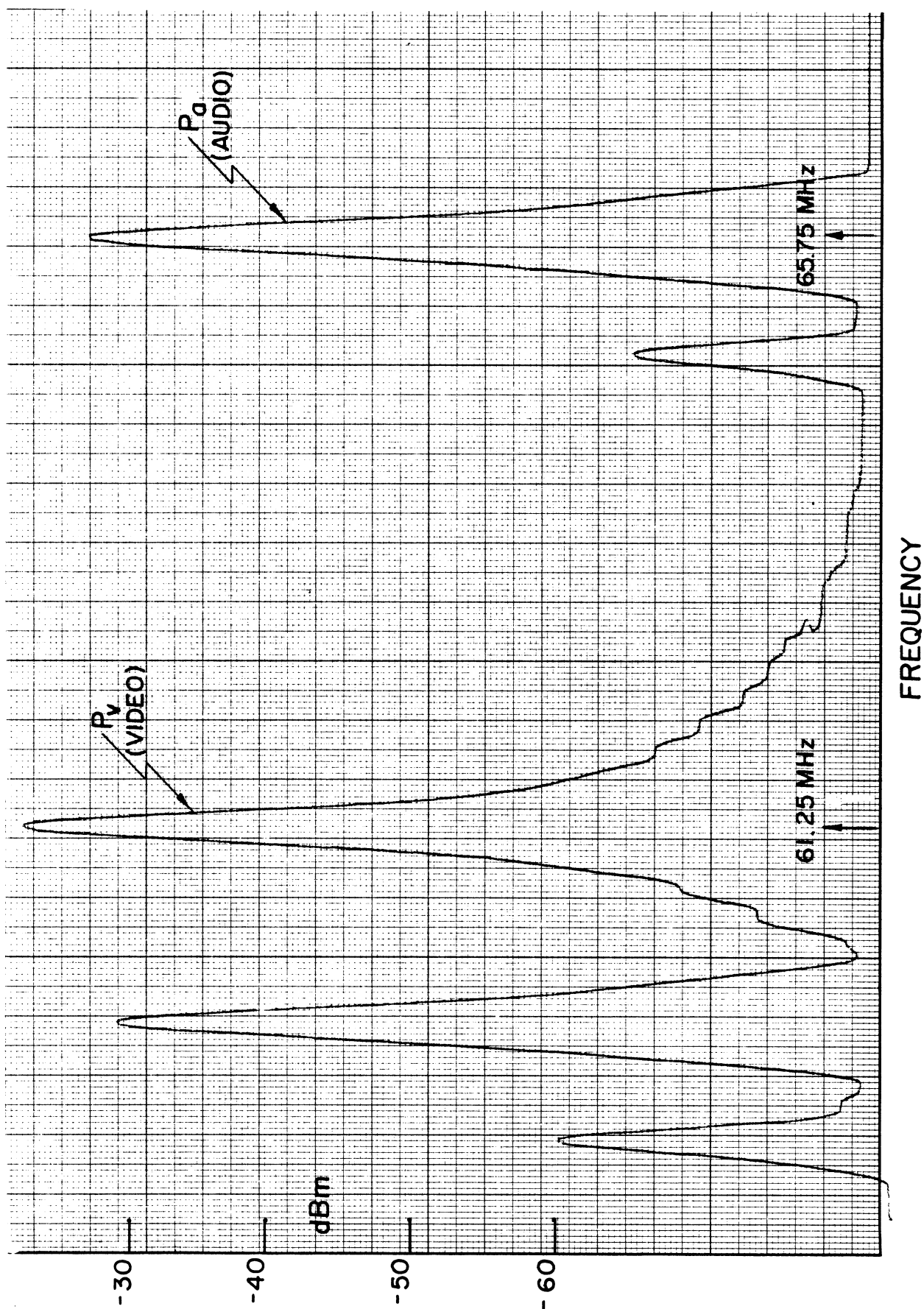


Fig. 4-2: Video and audio carrier signal strengths on Channel 3 at the base of the WT.

Recordings similar to these were made at all sites, and it will henceforth suffice to give only the key quantities determined from them. P_v and P_a are of particular interest. At the transmitter, the radiated audio signal power radiated [11], i.e., the radiated audio power is 7 to 10 dB below the video, but because of different losses suffered during propagation, the ratio of P_a to P_v may differ from this, and may vary from Channel to Channel and from site to site. It was observed that P_a was, in general, 0 to 10 dB below P_v , but in a few instances (discussed later) P_v was actually below P_a .

The received signal powers P_a and P_v are those at the spectrum analyzer (or receiver) and depend on the antenna gain and the antenna-receiver coupling losses. To judge the grade of TV service and to facilitate the analysis described later, it is desirable to remove the effects of the antenna gain and system losses, and to express the ambient signals at a site in terms of the electric field strengths E_v and E_a . The ambient strength E_v of the video carrier signal can be obtained from the measured P_v using (1), where G is the gain obtained from Fig. 3-6 and any system losses are assumed negligible. The corresponding audio carrier signal strength can also be obtained from (1) by replacing P_v and λ_v by P_a and λ_a . The two formula imply

$$E_a = \frac{\lambda_v}{\lambda_a} 10^{\frac{1}{20}(P_a - P_v)} E_v \quad (2)$$

where P_a and P_v are measured in dBm, and this provides a convenient method for computing E_a from E_v .

TV service grades are specified in terms of E_v (in mV/m), but as noted in §2.2, the quality of reception available can also be judged from the received video carrier signal power P_v . If $P_v \geq -49$ dBm, good reception is possible, but as P_v decreases below -49 dBm, the reception will become increasingly poor (snowy), and for $P_v < -63$ dBm the reception will be extremely poor/unacceptable. During our measurements of P_v , the simultaneous observations of the picture quality obtained with the Zenith receiver were generally consistent with these criteria.

For measurements of WT interference, the spectrum analyzer is tuned to the TV Channel audio carrier frequency. Since the relevant ambient signal strength is then P_a , it is convenient to express the criteria for quality of reception in terms of this parameter. From our measurements and observations with the present receiver for Channels 2 through 12, it has been found that the quality of reception is approximately related to P_a as follows:

$$\begin{array}{rcl} & P_a \geq -56 \text{ dBm} & \text{good reception} \\ -56 \text{ dBm} > & P_a \geq -70 \text{ dBm} & \text{poor (snowy) reception} \\ & P_a < -70 \text{ dBm} & \text{extremely poor} \\ & & \text{(unacceptable) reception} \end{array} \quad (3)$$

These imply that, on average, $P_a/P_v = -7\text{dB}$.

4.2 Signal Strengths at the WT

Signal strengths were measured near the base of the WT tower and on top of the nacelle, approximately 150 ft above ground. For the latter measurements, the Winegard antenna was mounted on a 6 ft metallic pole placed vertically on the roof of the nacelle at the end furthest from the blades. The blades were locked in a vertical position, and the antenna was positioned with its elements horizontal and its main beam directed away from the blades. The antenna was connected to the spectrum analyzer using a 250-ft length of coaxial cable, and the 6 dB (approx.) attenuation that this introduced has been taken into account in quoting the field strengths that were measured. The desired results were obtained by yawing the WT in azimuth to receive the maximum signal on each Channel.

The video and audio signal strengths P_v and P_a at the top and base of the WT are listed in Table 4-1, along with the directions to the transmitters and the antenna beam pointing directions for which the maximum signals were obtained. We observe that (i) there were no significant differences between the directions of the transmitters and those of the maximum signals (ii) the signal strengths at the top and base of the WT were comparable, and (iii) the signals received on all Channels were quite strong. In every case the quality of reception was considered good. To appreciate these results, it should be remembered that the WT site is 1.35 km above sea level, and an antenna at this height above a smooth spherical earth would be within the illuminated regions of all of the transmitters. The

Table 4-1

Received Signal Strengths at the WT Site

TV Channel Number	Direction of Trans. (Deg. from N)	Antenna Beam Angle (Deg. from N)	Top of the WT		Base of the WT	
			P _v (-dBm)	P _a (-dBm)	P _v (-dBm)	P _a (-dBm)
2a	278	280	33	38	33	39
2b	103	108	29	33	31	34
3	154	155	22	27	22	27
5	302	305	28	33	30	35
7	205	208	30	38	31	40
8	105	103	34	40	35	41
9	141	140	38	45	35	42
11	299	295	33	40	35	42
12	82	85	37	43	38	44

increase in height on going to the top of the WT represents only a small percent change, and should not be expected to produce any noticeable height-gain effect.

Some UHF TV Channels not shown in Table 4-1 were also available at the WT site. A Channel 19 signal was received having $P_v = -40$ dBm and $P_a = -45$ dBm, and a Channel 36 signal with $P_v = -54$ dBm and $P_a = -58$ dBm. The video reception was very good on Channel 19, but only fair on 36. Since we did not explore further the UHF frequencies, other Channels may be available, and our previous tests [12] on nearby Rich Mountain showed that Channels 42 and 58 were present there.

From the data in Table 4-1 the ambient field strengths E_v and E_a on top of the WT were obtained in the manner described in §4.1, and these are shown in Table 4-2. As expected, the field strengths on all Channels are sufficient for Grade A service, and with the WT stationary, an antenna of only modest performance should be adequate to provide good reception.

4.3 Signal Strengths at Sites A-J

The video and audio carrier signal strengths at the test sites are given in Tables 4-3 and 4-4 respectively. Where no value is shown, the signal was either not available or too weak to be measured. In general, the antenna beam pointing direction for which the maximum signal was received was within 5 to 8 degrees of the actual direction of the transmitter. In the cases of Channel 8 at Site A and Channel 12 at Site C, maximum signals were received for two

Table 4-2

Field Strengths on Top of the WT

TV Channel Number	E_v (mV/m)	E_a (mV/m)
2a	2.80	0.98
2b	4.21	2.95
3	13.65	7.65
5	5.80	3.42
7	14.33	6.16
8	9.52	4.38
9	6.44	2.96
11	11.40	5.24
12	7.49	3.82

Table 4-3
Received Video Carrier Signal Strengths at Sites A - J

		P _v (-dBm)										
Site	TV Channels											
	2a	2b	3	5	7	8	9	11	12			
A	-	-	45	66	57	66 67	-	-	-	-	-	
B	-	-	59	42	59	78	83	60	-	-	-	
C	-	-	70	43	68	50	80	70	50 55	-	-	
D	63	61	63	58	72	72	69	77	-	-	-	
E	-	76	58	79	-	-	-	-	-	-	-	
F	72	64	67	-	76	78	-	-	-	70	-	
G	-	68	67	68	-	73	-	-	-	-	-	
H	-	65	64	75	-	77	80	-	-	-	-	
I	-	63	75	71	-	68	-	75	-	-	-	
J	66	54	78	46	71	66	-	60	-	72	-	

Table 4-4
 Received Audio Carrier Signal Strengths at Sites A - J

		P _a (-dBm)										
Site	TV Channels											
	2a	2b	3	5	7	8	9	11	12			
A	-	-	53	71	68	69 66	-	-	-	-	-	
B	-	-	64	46	67	84	85	62	-	-	-	
C	-	-	75	48	76	56	84	72	50 54	-	-	
D	69	63	67	60	76	74	70	75	-	-	-	
E	-	76	64	82	-	-	-	-	-	-	-	
F	77	69	71	-	81	80	-	-	74	-	-	
G	-	71	72	77	-	76	-	-	-	-	-	
H	-	68	66	80	-	80	80	-	-	-	-	
I	-	64	80	75	-	72	-	88	-	-	-	
J	71	62	82	52	78	72	-	68	75	-	-	

different directions of the antenna, and it is believed that the extraneous signals were produced by scattering off the WT nacelle or from the sides of the hill on which the WT is located. The upper values in the two tables refer to the signals received from the expected directions, and the lower values to the scattered signals. Both scattered signals had video peaks which were only comparable to or less than the audio peaks, and the resulting TV reception was poorer than with the direct signals.

According to our previous criteria for quality of reception, the data in Tables 4-3 and 4-4 show that even with a high performance antenna like the Winegard, good reception is possible only at a few sites and, even then, only on a few Channels. Thus, good reception was obtained on Channel 3 at site A, and on Channel 5 at sites B, C and J, and fair reception on Channel 26 at site J. In all other instances, the reception ranged from poor to unacceptable.

The corresponding video and audio field strengths are given in Tables 4-5 and 4-6 respectively. The fields are generally weak, and judged by these values, the service provided on all Channels is Grade B or worse.

4.4 Signal Strengths along the Road near Site A

The audio carrier signal strengths of a few TV Channels were measured at places 150 ft (= 46 m) apart along the gravel road extending east from Site A. Because of trees overhanging the road, it was necessary to partially dismantle the antenna to move from one location to the next, and since there were no power lines

Table 4-5
Video Carrier Field Strengths at Sites A - J

Site	E_v (mV/m)											
	TV Channels											
	2a	2b	3	5	7	8	9	11	12			
A	-	-	0.944	0.073	0.639	0.239 0.213	-	-	-	-	-	-
B	-	-	0.187	1.15	0.507	0.060	0.036	0.516	-	-	-	-
C	-	-	0.053	1.03	0.179	1.51	0.518	0.161	1.67 0.94	-	-	-
D	0.874	0.112	0.126	0.181	0.113	0.127	0.182	0.077	-	-	-	-
E	-	0.020	0.223	0.017	-	-	-	-	-	-	-	-
F	0.031	0.078	0.075	-	0.071	0.060	-	-	0.176	-	-	-
G	-	0.048	0.075	0.061	-	0.107	-	-	-	-	-	-
H	-	0.072	0.034	0.026	-	0.068	0.054	-	-	-	-	-
I	-	0.090	0.032	0.041	-	0.190	-	0.091	-	-	-	-
J	0.062	0.245	0.022	0.725	0.126	0.240	-	0.515	0.139	-	-	-

Table 4-6
Audio Carrier Field Strengths at Sites A - J

		E _a (mV/m)										
		TV Channels										
Site	2a	2b	3	5	7	8	9	11	12			
A	-	-	0.406	0.043	0.185	0.172 0.243	-	-	-	-	-	
B	-	-	0.110	0.077	0.208	0.025	0.030	0.212	-	-	-	
C	-	-	0.031	0.610	0.073	0.770	0.337	0.130	1.67 1.07	-	-	
D	0.437	0.090	0.079	0.015	0.072	0.085	0.167	0.062	-	-	-	
E	-	0.022	0.096	0.012	-	-	-	-	-	-	-	
F	0.020	0.047	0.057	-	0.041	0.051	-	-	0.106	-	-	
G	-	0.037	0.047	0.021	-	0.078	-	-	-	-	-	
H	-	0.050	0.030	0.015	-	0.049	0.056	-	-	-	-	
I	-	0.081	0.018	0.027	-	0.122	-	0.021	-	-	-	
J	0.037	0.105	0.015	0.400	0.058	0.122	-	0.211	0.093	-	-	

in the vicinity, the equipment was powered from the automobile battery using an inverter.

The measured values of P_a at four locations (including Site A) are listed in Table 4-7. The Site A values differ slightly from those in Table 4-4, but represent a second set of measurements made two days later. The terrain was similar at each location, and the similarity of the data in Table 4-7 suggests that the field strengths measured at Site A are typical of the immediate vicinity.

Table 4-7

Received Audio Carrier Signal Strengths at Distance d from Site A

TV Channel Number	P_a (-dBm)			
	Site A	d = 46m	d = 92m	d = 138m
3	54	55	54	55
5	70	72	72	72
7	69	68	70	73
8	70	73	72	71

4.5 Conclusions

It is evident from the above results that:

(i) In the city of Boone and its surrounding area, the field strengths of all of the available TV Channels are weak. The only exceptions are those few sites with higher elevations where the hills do not produce shadowing. The quality of TV reception in the area is generally poor to unacceptable even with the WT stationary,

and a high performance antenna such as the Winegard could not suffice to make it good.

(ii) At distances up to about 150 m from site A, the signals received on Channels 3 and 5 were within 2 dB of those at the site itself, and within 4 dB on Channels 7 and 8. On this basis it is concluded that each site is typical of its immediate environs.

(iii) At the WT site the field strengths are quite strong and are not significantly different at the top and base of the WT. Even a poor antenna could provide good reception. The fact that the fields here are so much stronger than at the surrounding homes has an important bearing on the TV interference produced by the WT.

CHAPTER 5. BLADE SCATTERING (STATIC TESTS)

The interference produced by the rotating blades of a WT is directly proportional to the scattering from a single blade. From our previous laboratory (model) and full scale scattering measurements of MOD-0 and MOD-0A blades [6], and the fact that the MOD-1 metal blade is similar in general form (though not in size), it was theoretically determined that the equivalent scattering area of a MOD-1 blade is $A_e = 40\text{m}^2$, with $L_1 = 25\text{ m}$ and $L_2 = 1.6\text{ m}$. The present program provided the opportunity to check these values experimentally by static measurements of the blade scattering at a few of the test sites. In the following sections we discuss the test results and describe how the equivalent scattering cross section can be obtained from the measured data.

5.1 Procedure

As mentioned in Section 3.3, the blades of the WT were maintained at 0° pitch and locked in a vertical position ($\theta_s = 0$) throughout these tests. Using a local TV transmitter as the RF source, and with the receiving antenna directed at the WT (or the transmitter), the received signal was recorded in dBm as a function of time as the machine was yawed in azimuth. Simultaneously, information about the yaw voltage was received from the WT operating personnel via walkie-talkie and was inserted on the signal record. Using the calibration curve in Fig. A-3,

the voltage was later converted into WT nacelle pointing direction to produce, in effect, a plot of the scattered signal versus WT orientation.

5.2 Results

Data were obtained at sites A, B and C, but because of the similarity of sites B and C, we present only the results of tests at site C on Channels 5 and 11 and at site A on Channel 3. For these Channels the sites are almost precisely in the backscattering (specular) direction, and the maximum scattered signals were observed when the WT nacelle was pointing almost directly towards the site.

Figures 5-1 and 5-2 show the received signals vs nacelle direction at site C for Channels 5 and 11 respectively. The directions are measured clockwise from N and the directions of the TV transmitters are also indicated. Data of this type provide a wealth of information. In addition to the blade scattering, we have also identified contributions from various parts of the nacelle assembly. The blade front and back returns indicated in the figures were from the upper and lower blades respectively. In general the lower blade return is smaller, and this may be due to shadowing produced by the WT tower. We also note the significant contributions from the nacelle housing whose metallic sides act as efficient scatterers.

The results obtained at site A on Channel 3 are shown in Fig. 5-3, and we again observe the scattering from the nacelle.

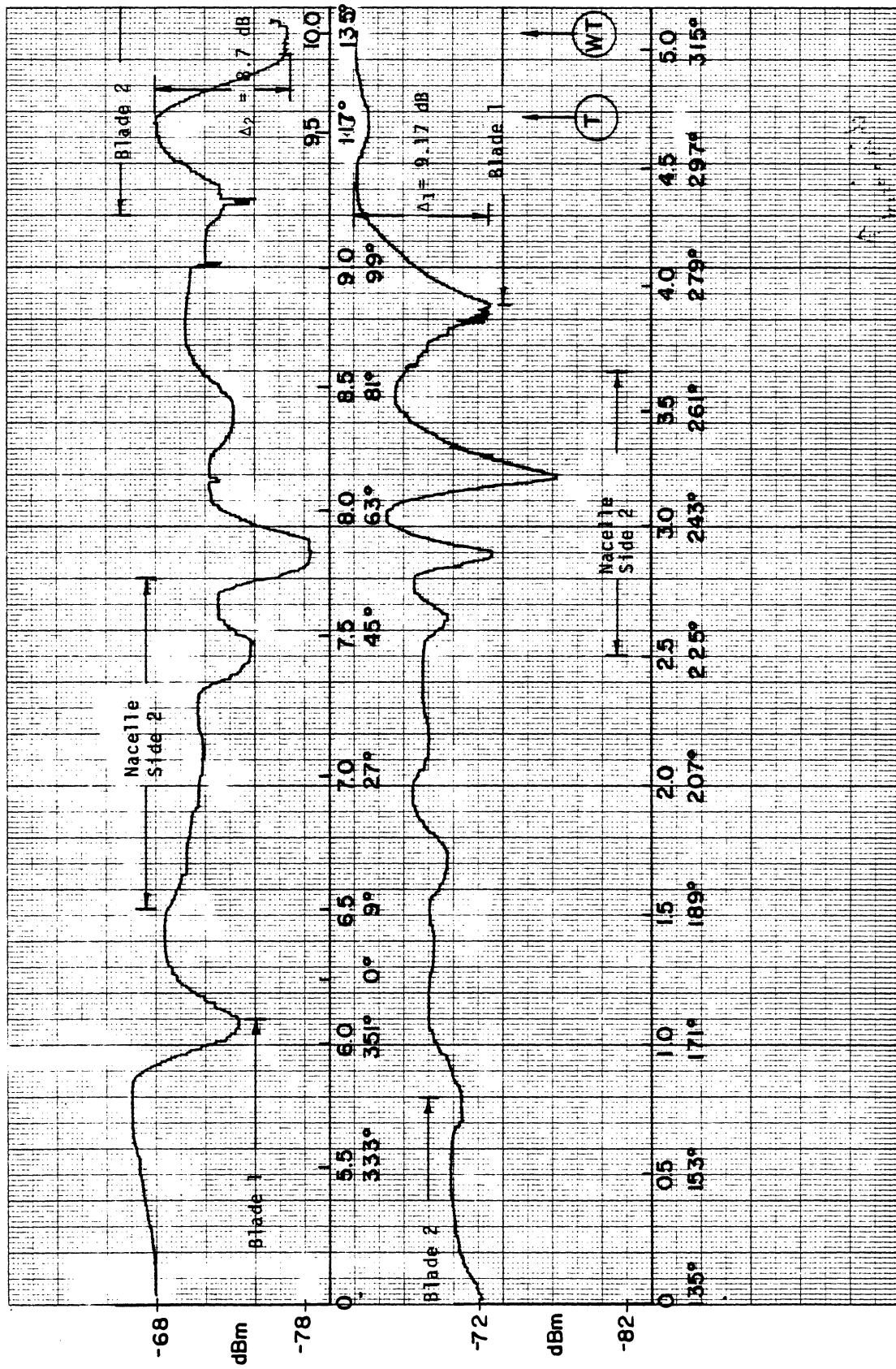


Fig. 5-1 P_a (in dBm) versus nacelle voltage (or angle) on Channel 5 obtained at site C.

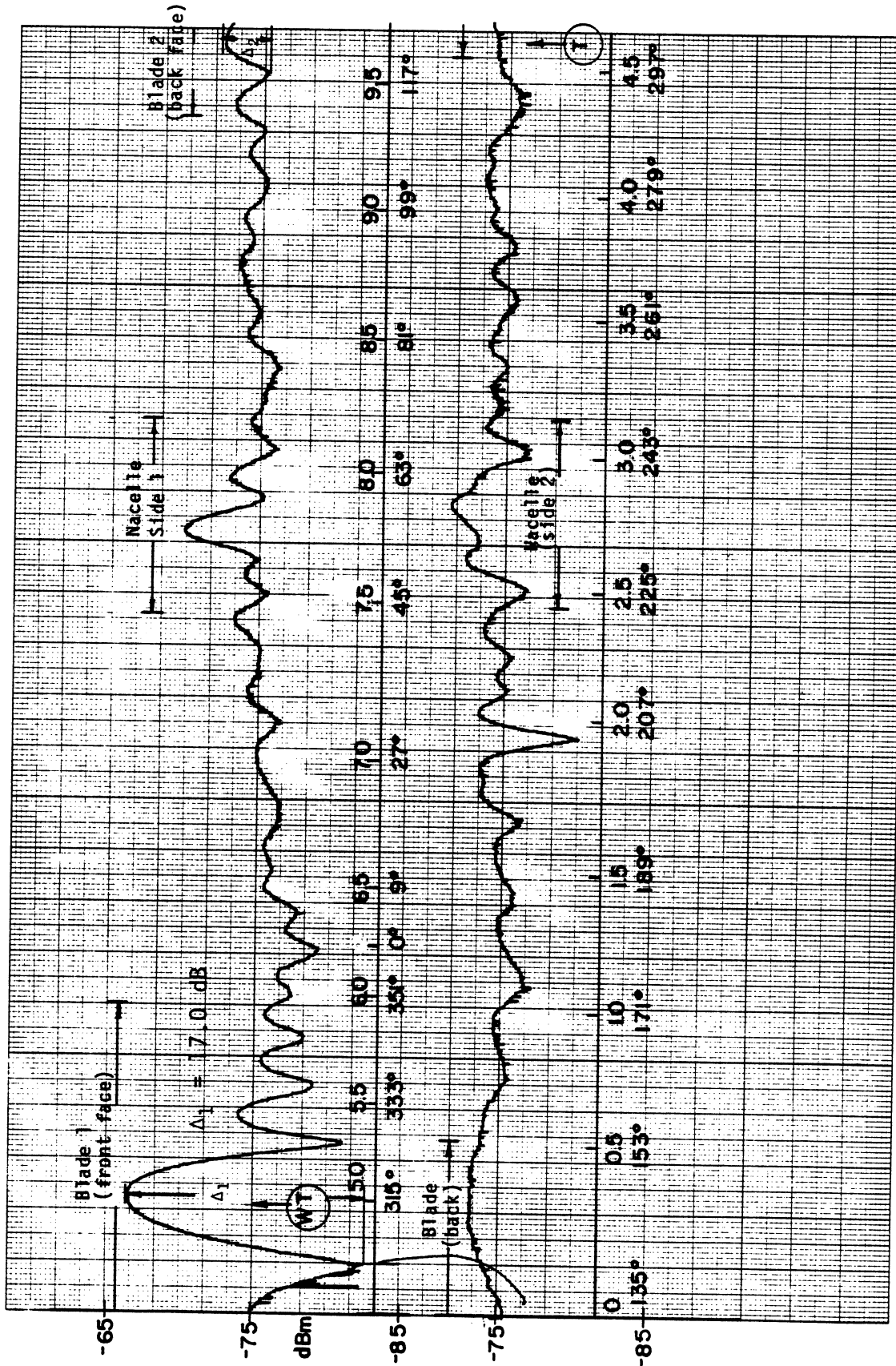


Fig. 5-2 P_a (in dBm) versus nacelle voltage (or angle) on Channel 11 obtained at site C.

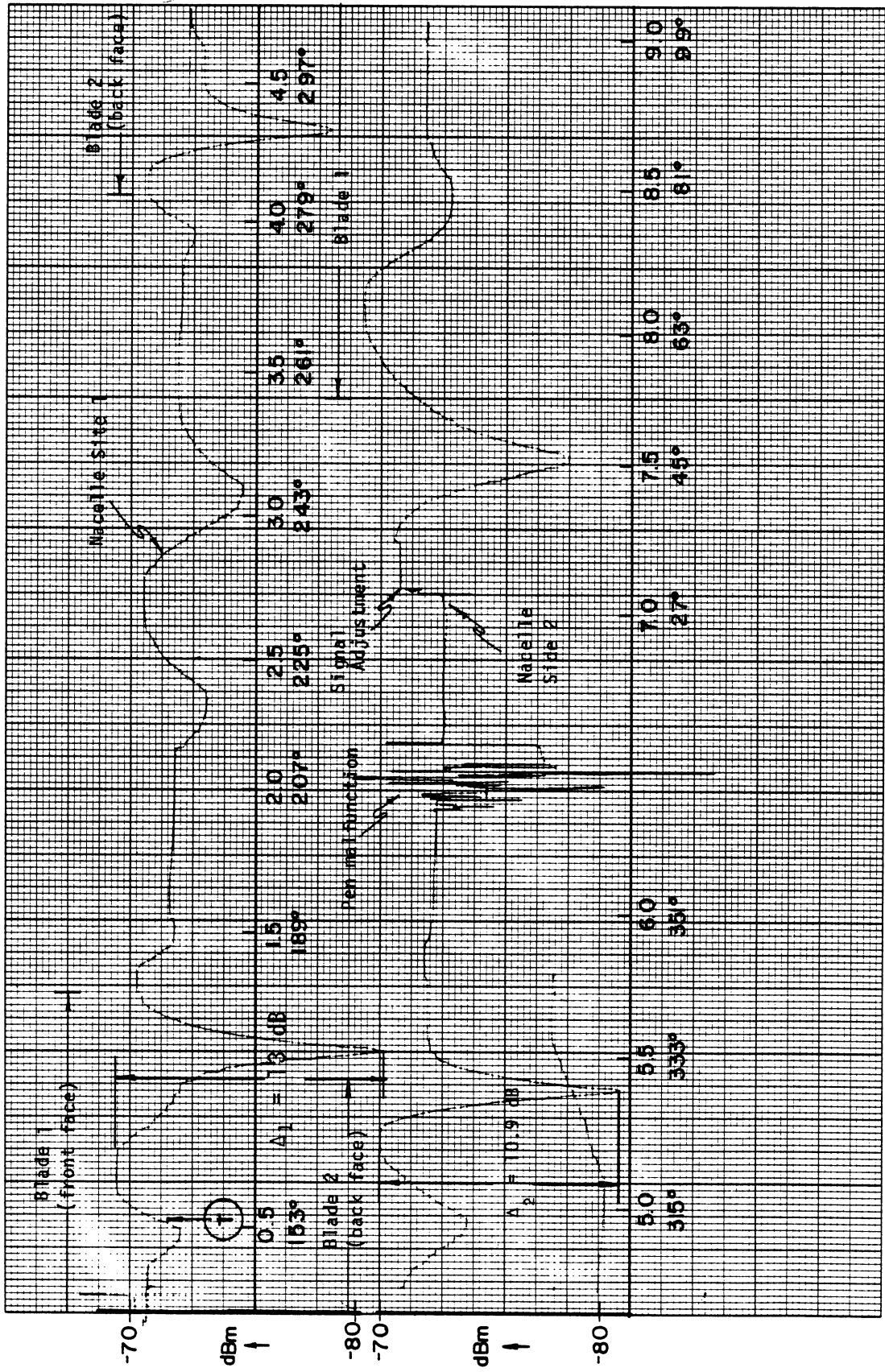


Fig. 5-3 P_a (in dBm) versus nacelle voltage (or angle) on Channel 3 obtained at site A.

5.3 Data Analysis

The equivalent scattering area of the MOD-1 blade can be obtained from the above data by applying the theory outline in §A.2. The symbols used are defined in that section, and we show the detailed calculations for one case only.

(i) Site C, Channel 5

Known parameters:

$$\lambda(\text{audio carrier wavelength}) = 3.67 \text{ m,}$$

$$h_t = 183 \text{ m, } h_a = 6 \text{ m, } D = 792 \text{ m,}$$

$$L_1 = 25 \text{ m, } L_2 = 1.6 \text{ m, } \alpha_c = 9^\circ,$$

site location 316°

transmitter location 302° .

Measured parameters:

$$E_B/E_R = 15 \text{ dB (see Tables 4-1 and 4-4),}$$

$F(\text{BT}) = 20 \text{ dB}$, as obtained by pointing the antenna at the TV transmitter and then at the WT,

$\Delta_1 = 9.17 \text{ dB}$ (= total deviation of the received signal caused by scattering from the upper blade),
obtained from Fig. 5-1; implying (see Fig. A-5)

$$m_1 = 0.495,$$

$\Delta_2 = 8.67 \text{ dB}$ (= total deviation of the received signal caused by scattering from the lower blade),
obtained from Fig. 5-1; implying (see Fig. A-5).

$$m_2 = 0.495,$$

Calculations:

$$r = (h_t^2 + h_a^2)^{1/2} = 813 \text{ m,}$$

$$\alpha = \tan^{-1}\{(h_t - h_a)/D\} = 12.6^\circ,$$

$$\phi_0 = -1/2(-316 + 302) = 7^\circ, \cos \phi_0 = 0.9926,$$

$$\sin \equiv \sin \{2\pi h_t h_a / (\lambda r)\} = 0.7375,$$

$$\cos \alpha_c = 0.9877,$$

$$\text{sinc}_1 \equiv \text{sinc}[L_1 / \lambda \{\sin \alpha_c - \sin(\alpha - \alpha_c)\}] = 0.4533,$$

$$\text{sinc}_2 \equiv \text{sinc}[L_2 / \lambda \{\cos \alpha_c - \cos(\alpha - \alpha_c) \sin \phi_0\}] \approx 1$$

$$(E_B/E_R)F(BR) = 35 \text{ dB} = 56.2.$$

Using eq. (A.6), the equivalent scattering areas of the front face of the upper blade and the back face of the lower blade are, respectively,

$$A_1 = \frac{0.95 \times 3.67 \times 813}{2 \times 0.9877 \times 0.9926 \times 0.4533 \times 0.7375 \times 56.2} = 40.1 \text{ m}^2$$

$$A_2 = 40.1 \times \frac{0.455}{0.495} = 36.7 \text{ m}^2 .$$

Ideally, $A_2 = A_1$, but in the present case A_2 is 8.5 percent less.

(ii) Site C, Channel 11

The known parameters are identical to those in case (i) above except $\lambda = 1.47 \text{ m}$:

$$E_B/E_R = 32 \text{ dB,}$$

$$F(B,T) = 12 \text{ dB,}$$

$$\Delta_1 = 17.0 \text{ dB; } m_1 = 0.76,$$

$$\Delta_2 = 3 \text{ dB; } m_2 = 0.17,$$

$$\begin{aligned}\phi_0 &= 8.5^\circ, \\ \sin &= -0.4887, \\ \text{sinc}_1 &= -0.1917, \\ \text{sinc}_2 &\approx 1.\end{aligned}$$

We obtain

$$A_1 = 31.4 \text{ m}^2, \quad A_2 = 7.0 \text{ m}^2 \text{ (79 percent less than } A_1 \text{)}.$$

(iii) Site A, Channel 3

$$\begin{aligned}\lambda &= 4.56 \text{ m}, \\ h_t &= 366 \text{ m}, \quad h_a = 6 \text{ m}, \quad D = 975 \text{ m}, \\ L_1 &= 25 \text{ m}, \quad L_2 = 1.6 \text{ m}, \quad \alpha_c = 9^\circ, \\ &\text{site location } 108^\circ, \\ &\text{transmitter location } 154^\circ, \\ E_B/E_R &= 33 \text{ dB}, \\ F(B,T) &= 12.5 \text{ dB}, \\ \Delta_1 &= 13.0 \text{ dB}; \quad m_1 = 0.64, \\ \Delta_2 &= 10.9 \text{ dB}; \quad m_2 = 0.56, \\ r &= 1041 \text{ m}, \quad \alpha = 20.3^\circ, \\ \phi_0 &= -23^\circ, \\ \sin &= 0.2334, \\ \text{sinc}_1 &= 0.8969, \\ \text{sinc}_2 &\approx 1.\end{aligned}$$

We obtain

$$A_1 = 36 \text{ m}^2, \quad A_2 = 31.5 \text{ m}^2 \text{ (12.5 percent less than } A_1 \text{)}.$$

The average of the values of A_1 in (i), (ii) and (iii) above is 35.8 m^2 , which is in remarkable agreement with the theoretical value.

5.4 Discussion

Based on the measurements carried out on two TV Channels at site C and a different Channel at site A, the following observations can be made:

(i) The measured values for the equivalent scattering area A_1 of the front face of the upper blade are very similar to one another, and the average is in excellent agreement with the theoretical value. The tests provide confidence in the validity of the theoretical estimate, and henceforth it will be assumed that the equivalent scattering area of the MOD-1 metal blade is $A = 40 \text{ m}^2$.

(ii) The measured values for the equivalent scattering area A_2 of the back face of the lower blade are more variable, and $A_2 < A_1$. Since the WT tower does shadow a vertically oriented lower blade to a degree which depends on the angle of incidence, the reduction and variability of the scattering are both attributable in part to this shadowing.

(iii) The excellent agreement in (i) above is also due to the fortuitous locations of sites A and C. At both sites the depression angles α are close to twice the coning angle for the blades, thereby ensuring that the maximum specularly scattered signal from the upper blade can be picked up. Although the rectangular plate model of a blade is adequate for most purposes, it is less accurate in predicting the scattering at angles well away from the specular direction, and since the sites were not as fortuitously placed for the lower blade, some of the variability in the deduced values of A_2 may be a consequence of this.

(iv) The metallic side walls of the nacelle housing produce significant amounts of scattering, and the combination of the scattered signals from the nacelle and from the rotating blades could increase the amount of TVI at some sites. The design of future nacelle housings should take this fact into account.

CHAPTER 6. TELEVISION INTERFERENCE MEASUREMENTS (DYNAMIC TESTS)

The nature and degree of television interference caused by the operating WT was determined by carrying out dynamic tests at the sites. As indicated in §3.3, the tests involved the measurement of P_a vs antenna beam pointing direction as the antenna was rotated in a horizontal plane, and P_a vs time for the antenna pointed at the TV transmitter and at the WT. The latter have been referred to as TVI tests, and while they were being performed, the quality of TV reception was simultaneously monitored using the TV receiver. Whenever it was felt desirable, the received picture was video recorded for later evaluation.

In the following sections we discuss the results of the dynamic tests conducted using the available TV Channels at all of the test sites and for various operating conditions of the WT. The most comprehensive tests were conducted at site A with three antennas having different gain and side-lobe (front-to-back) ratios. The results obtained at sites A and I are analyzed in some detail, and for the remaining sites the results are summarized.

6.1 Site A

The TV Channels 3,5,7 and 8 were all available at this site (see Tables 4-3 and 4-4), but Channel 3 was the only one whose signals were strong enough to provide good reception under normal conditions. The reception on the other Channels ranged from poor to unacceptable. As

can be seen from Table 2-2, site A is in the forward interference region of the WT for Channel 5, and in the backward interference region for the others.

6.1.1 Results Obtained with the Winegard Antenna. The antenna response under dynamic conditions obtained on Channel 3 is shown in Fig. 6-1, where the angles corresponding to the transmitter (T) and WT directions are indicated. The time scale is inserted on the abscissa so that the time behavior can also be examined.

A recording such as that in Fig. 6-1 generally indicates the type of TVI that may occur, and the severity of the interference for a given pointing direction of the antenna. The variable amplitude modulation pulses in Fig. 6-1 are typical of backward region interference, and the 1.3 sec spacing between the pulses is half the rotation period of the blades rotating at 23 rpm. When the antenna was pointed at or close to the transmitter, the modulation pulses produced very small ($\Delta \sim 0$) variations in the received signal, but in directions close to the WT, the pulses are quite strong. The total signal variation ($\Delta \geq 12$ dB) is then stronger than the 2.6 dB corresponding to the threshold level of interference. From Fig. 6-1 we conclude that no appreciable video distortion would occur with the Winegard antenna properly oriented to receive the Channel 3 signal, and the ambient level (~ -55 dBm) is such as to provide good reception. However, if the antenna were pointed at the WT instead, the average received signal would be 10 dB lower, causing poor reception, and the modulation pulses would produce severe video distortion.

For quantitative analyses of the interference, more detailed measurements of the modulation pulses are desirable. The appropriate

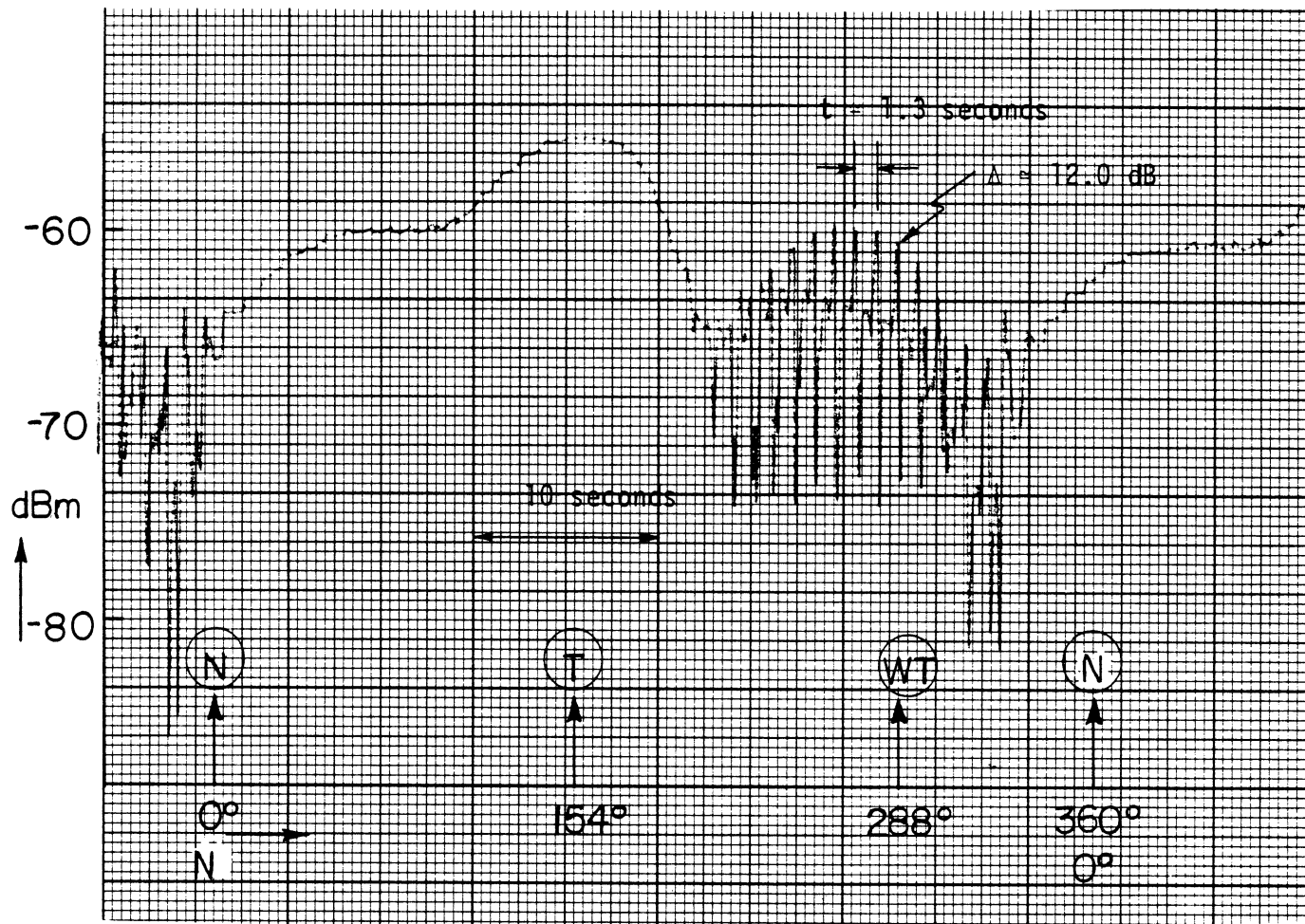


Fig. 6-1 Dynamic response of the Winegard antenna on Channel 3 at site A. (rpm = 23, $\phi_p = -15^\circ$, nacelle direction = 135° from N)

data are shown in Figs. 6-2a and b for the antenna pointed at the transmitter and the WT respectively. The difference in the average power levels P_a is about 12.5 dB, representing the antenna response in the direction T relative to that in the direction B when the antenna directed at T, i.e., the parameter $F(T,B)$ of Appendix A. As a result of the blade rotation, the total variation Δ in the received signals in the directions T and WT are 0.5 and 12.0 dB, respectively.

Figures 6-3 and 6-4a,b show the analogous results obtained a week later. The same effects are present, but because of the different state of the WT, the signal variations differ from those in Figs. 6-1 and 6-2a,b.

The received signal P_a vs time obtained on Channel 5 with the antenna directed at the WT operating at 10 rpm is shown in Fig. 6-5. Since the site is in the forward direction for this Channel, the antenna provided very little discrimination, i.e., $F(B,T) \approx F(T,B) \approx 1$. Because of the low ambient or average P_a (≈ -80 dBm), the quality of reception was extremely poor even with the WT stationary, and for this reason the antenna response was not measured. The total signal variation in Fig. 6-5 is 17.5 to 19.0 dB, and we observed forward region type of video distortion.

The antenna response on Channel 7 is shown in Fig. 6-6a. The behavior is characteristic of the backward interference region, but the modulation is insignificant even in the direction of the WT. P_a vs time for the antenna pointed at the transmitter is presented in Fig. 6-6b. The modulation pulses are barely visible ($\Delta \lesssim 0.5$ dB), and no distortion was observed. Only slight (acceptable) distortion was found when the antenna was directed at the WT.

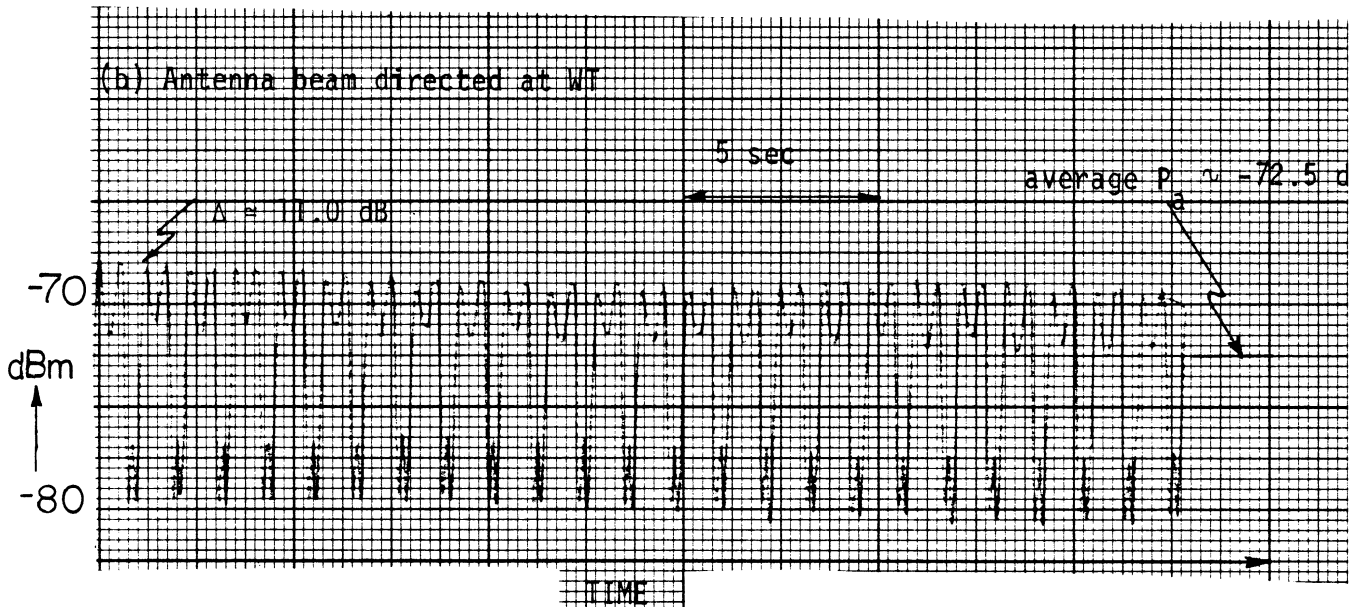
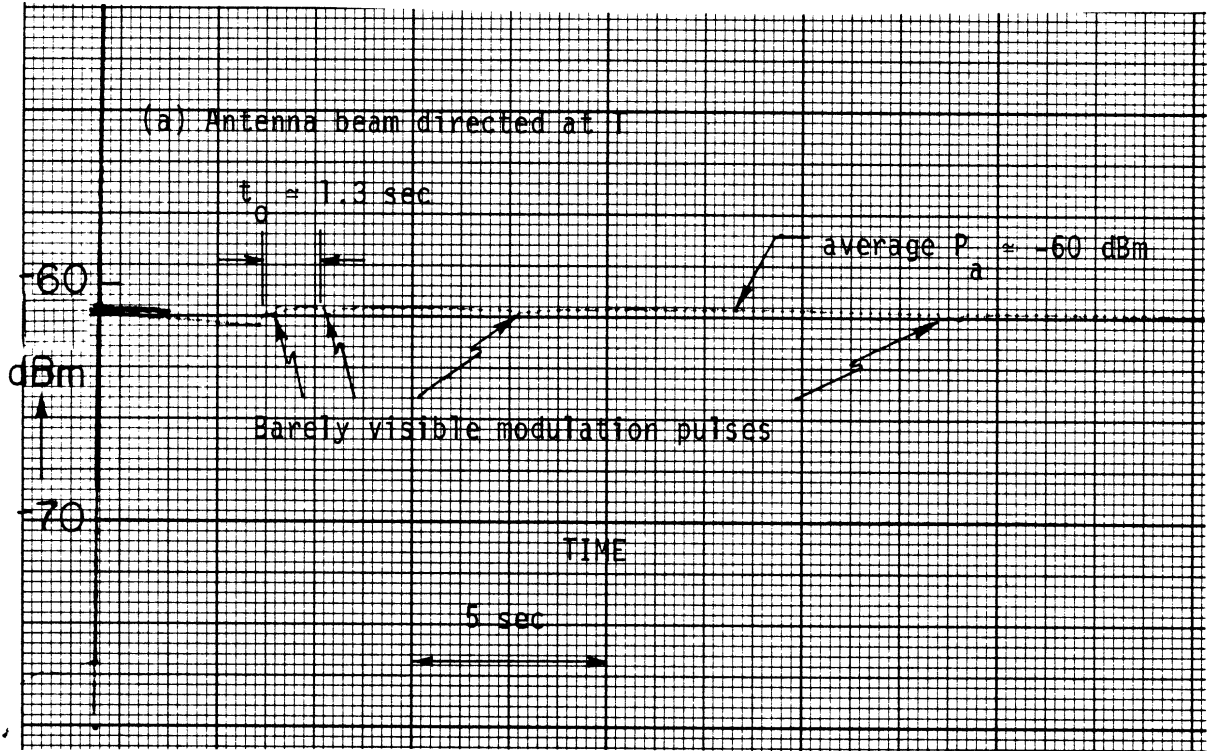


Fig. 6-2 P_a vs. time on Channel 3 at site A. ($\text{rpm} = 23$, $\phi_p = -15^\circ$, nacelle direction = 135° from N)

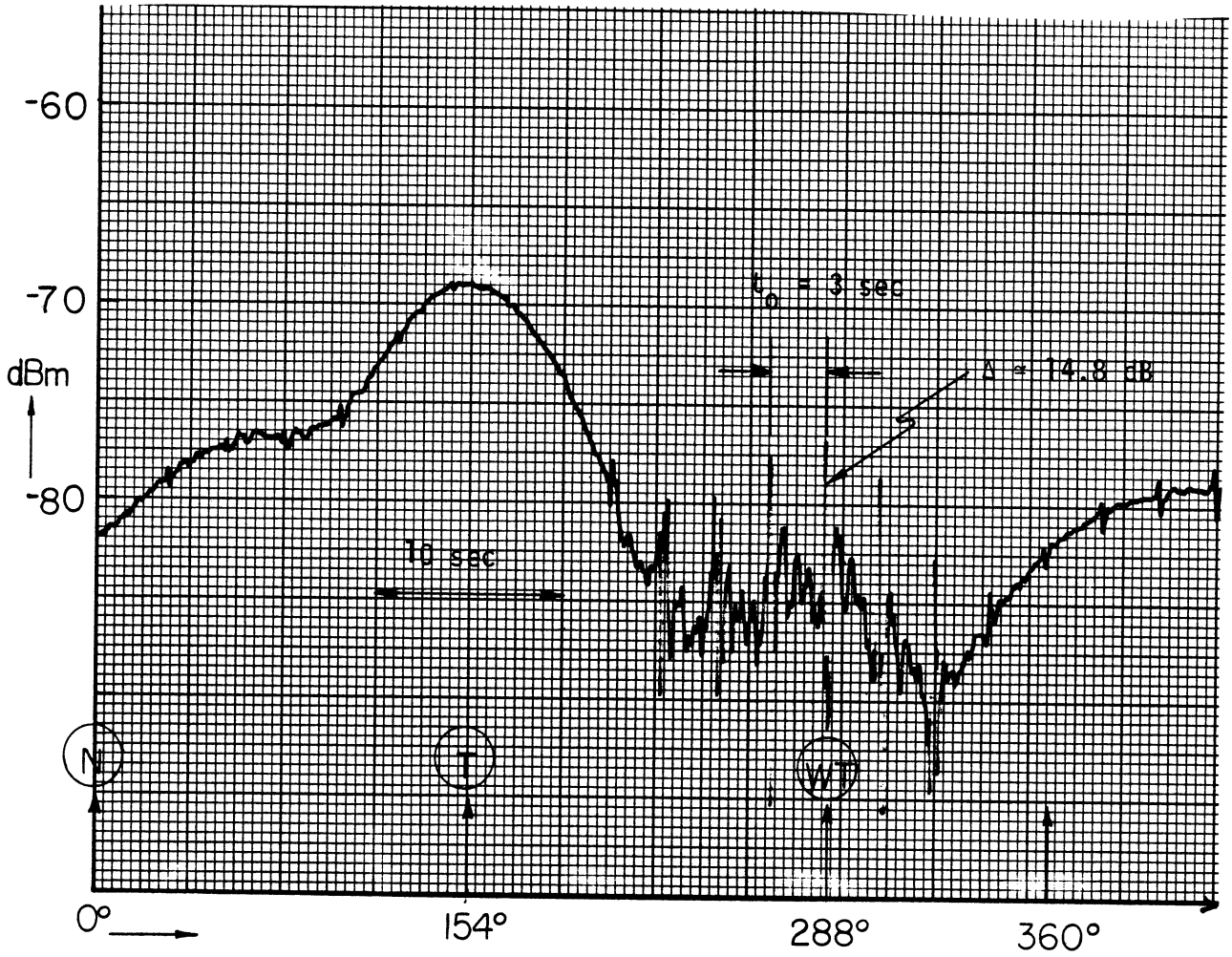


Fig. 6-3 Dynamic response of the Winegard antenna on Channel 3 at site A. (rpm = 10, $\phi_p = -20^\circ$, nacelle direction = 100° from N)

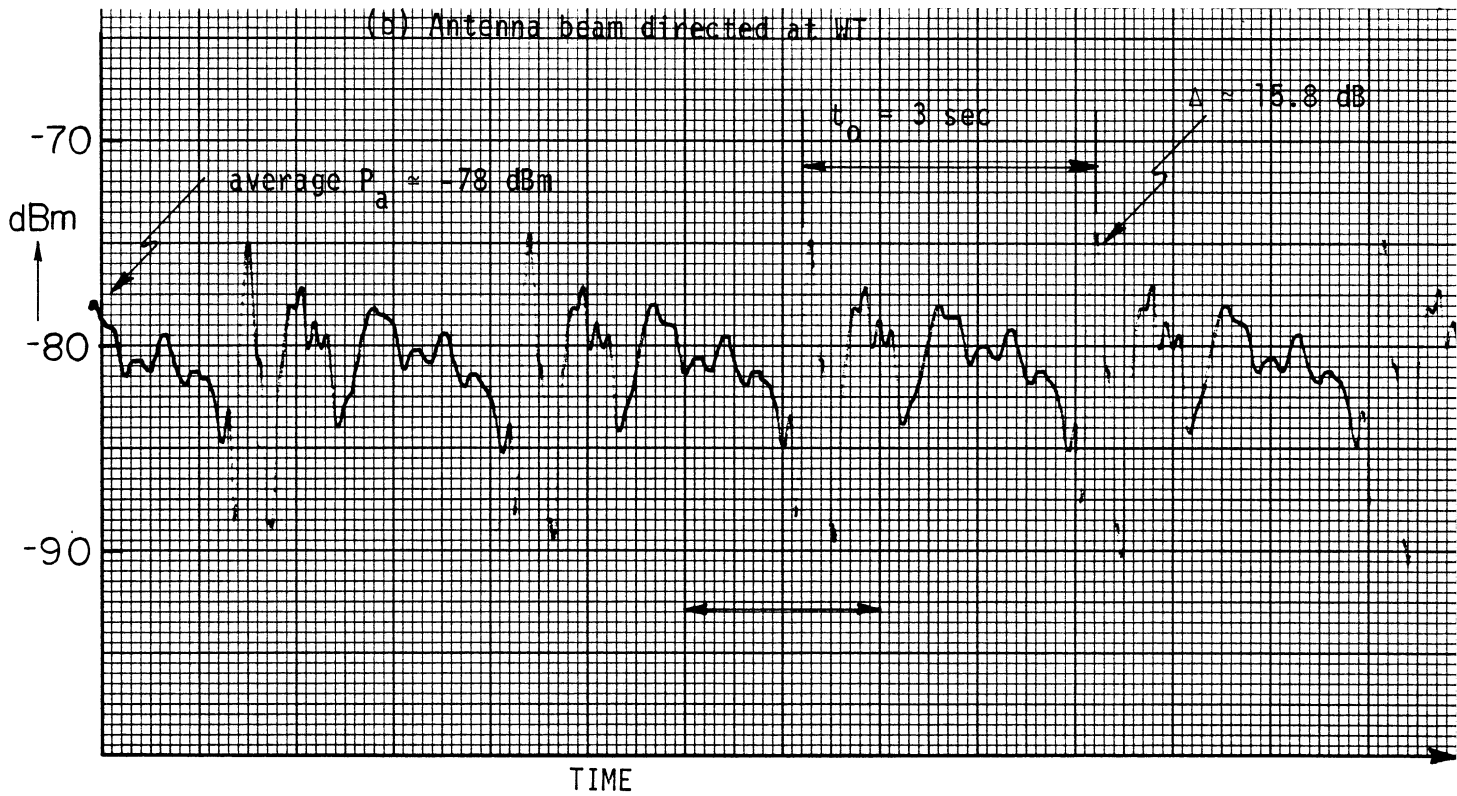
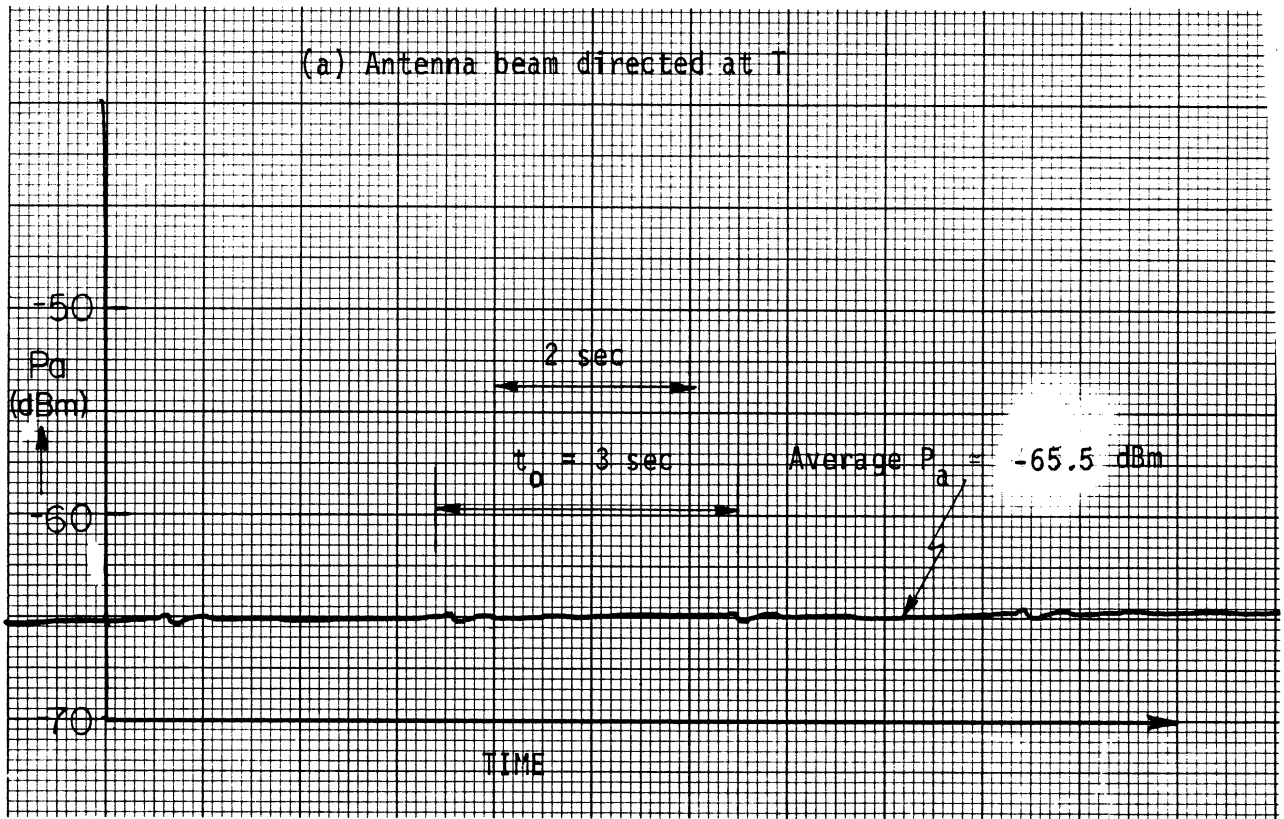


Fig. 6-4 P_a vs. time on Channel 3 at site A. (rpm = 10, $\phi_p = -20^\circ$, nacelle direction = 100° from N)

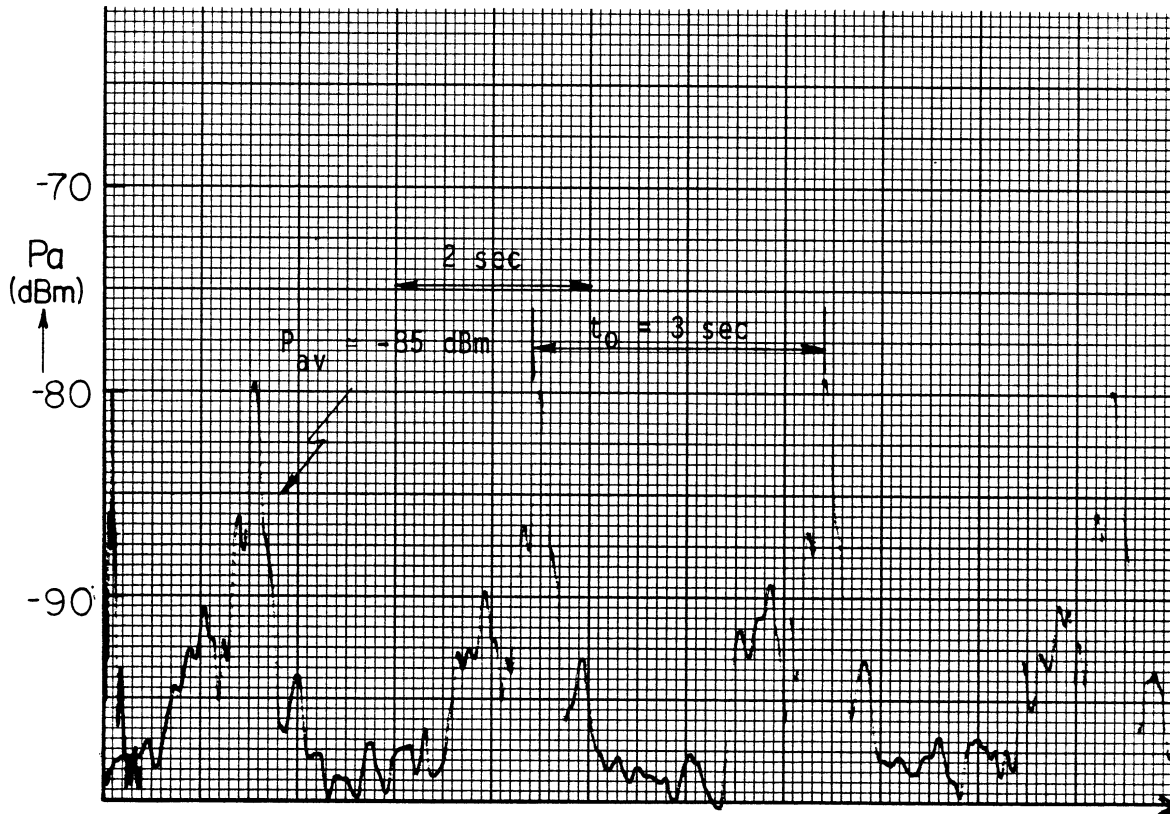


Fig. 6-5 P_a vs. time on Channel 5 at site A. (rpm = 10, $\phi_p = -20^\circ$, nacelle direction = 100° from N)

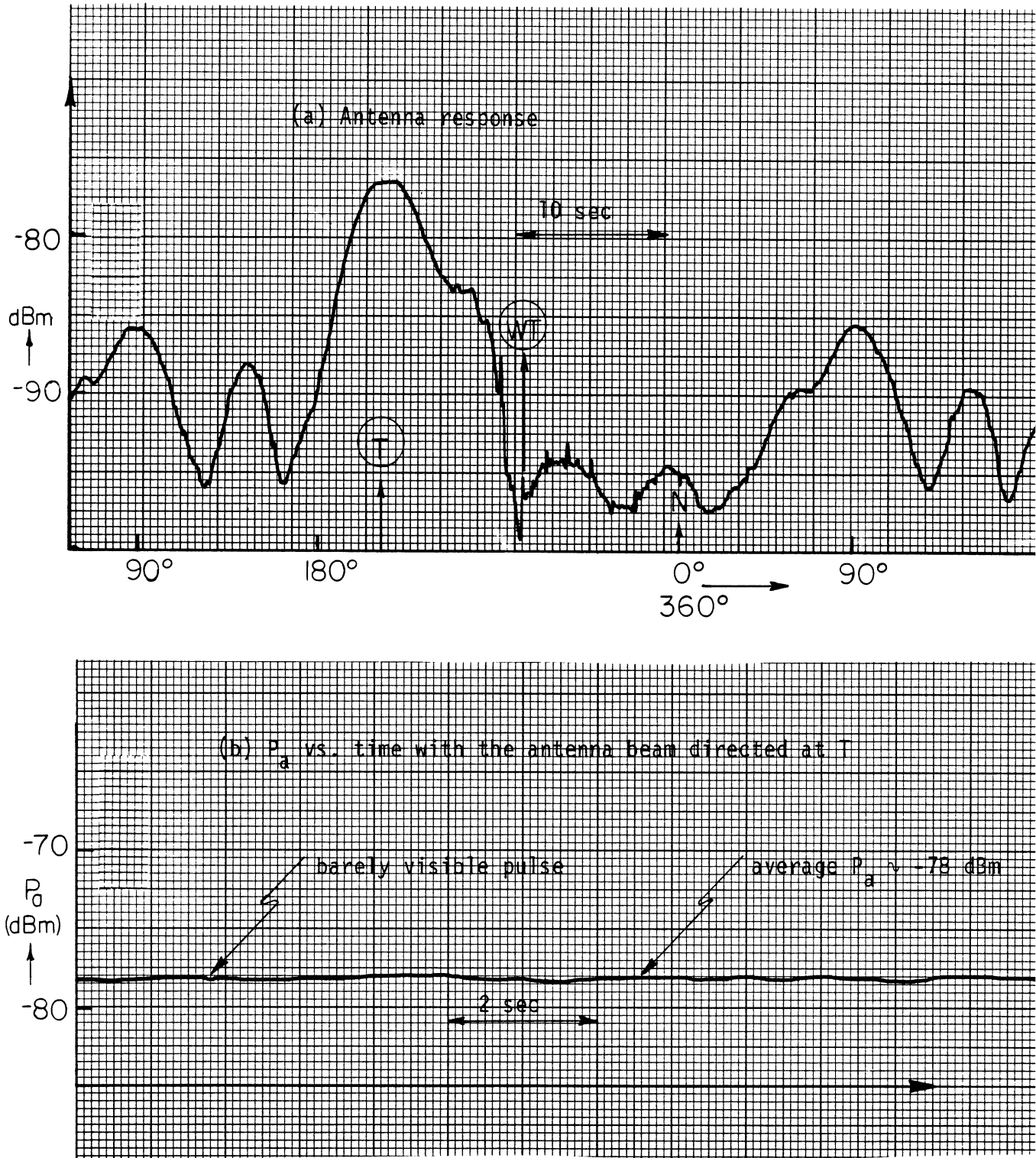


Fig. 6-6 Dynamic response and P_a vs. time on Channel 7 for a Winegard antenna at site A. ($\text{rpm} = 10$, $\phi_p = -20^\circ$, nacelle direction = 100° from N)

The Channel 8 antenna response is shown in Fig. 6-7 and is unusual in that the signal coming from the WT is about 2.5 dB stronger than that from the transmitter. A possible reason for this was discussed in §3.4. The variable amplitude of the modulation pulses confirms that any interference is of the backward region type. Figures 6-8a,b show P_a vs time for the antenna directed at the transmitter and the WT respectively, and in both cases the interference observed was within the acceptable range.

6.1.2 Results Obtained with the Channel Master Antenna. On Channel 3 the antenna response and P_a vs time are shown in Figs. 6-9 and 6-10. When compared with Figs. 6-1 and 6-3 it is found, as expected, that the modulation pulses are larger than were obtained with the Winegard antenna. Some video distortion was observed, but well within the acceptable range.

No tests were made on Channel 5 because of the low signal level, but for Channel 7 the antenna response is shown in Fig. 6-11 (c.f. Fig. 6-6). With the antenna directed at T the modulation pulses were of order 1 dB, and produced some video distortion. The analogous results for Channel 8 are shown in Fig. 6-12. Here also there was some video distortion when the antenna was pointed at the WT, but it was acceptable.

6.1.3 Results Obtained with a Half-Wave Dipole. Data were obtained only for Channel 3. The antenna response and P_a vs time for the dipole oriented to receive the maximum direct signal are shown in Figs. 6-13 and 6-14, respectively. As expected, the average P_a is lower than with the previous two antennas. The signal variation

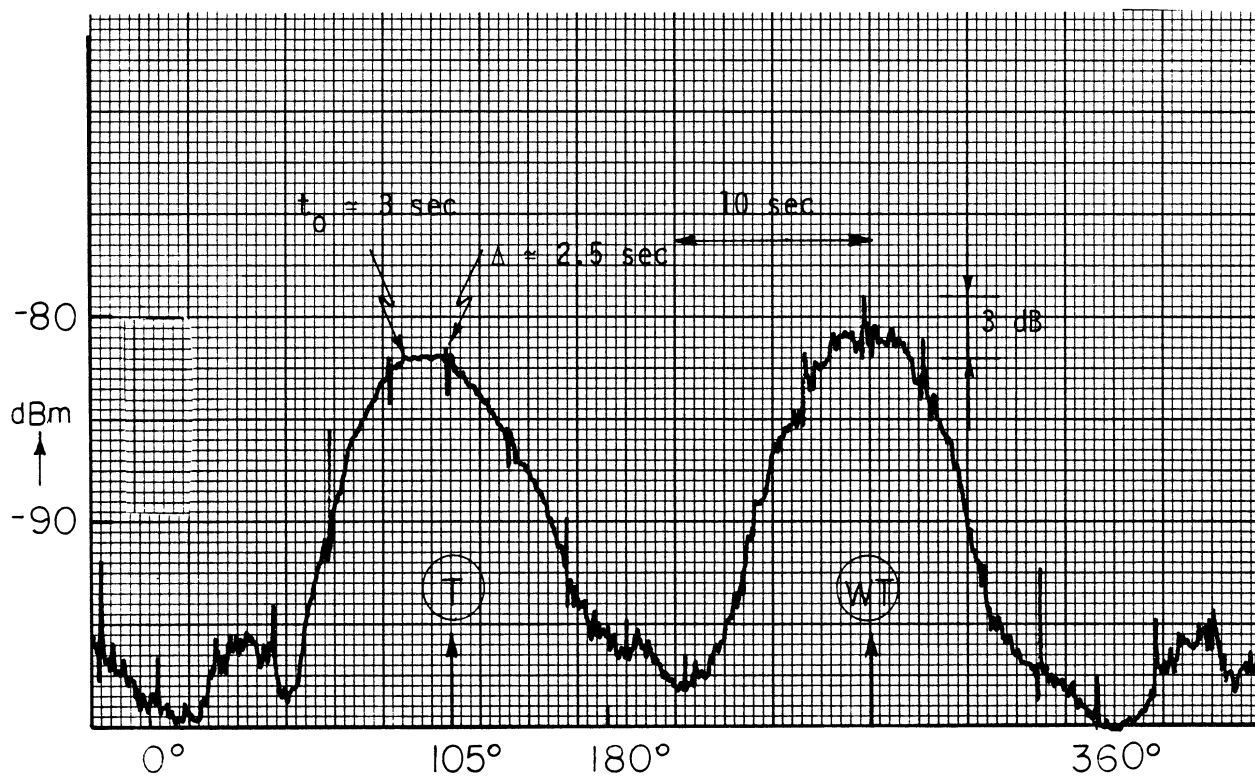


Fig. 6-7 Dynamic response of the Winegard antenna on Channel 8 at site A. (rpm = 10, $\phi_p = -15^\circ$, nacelle direction = 117° from N)

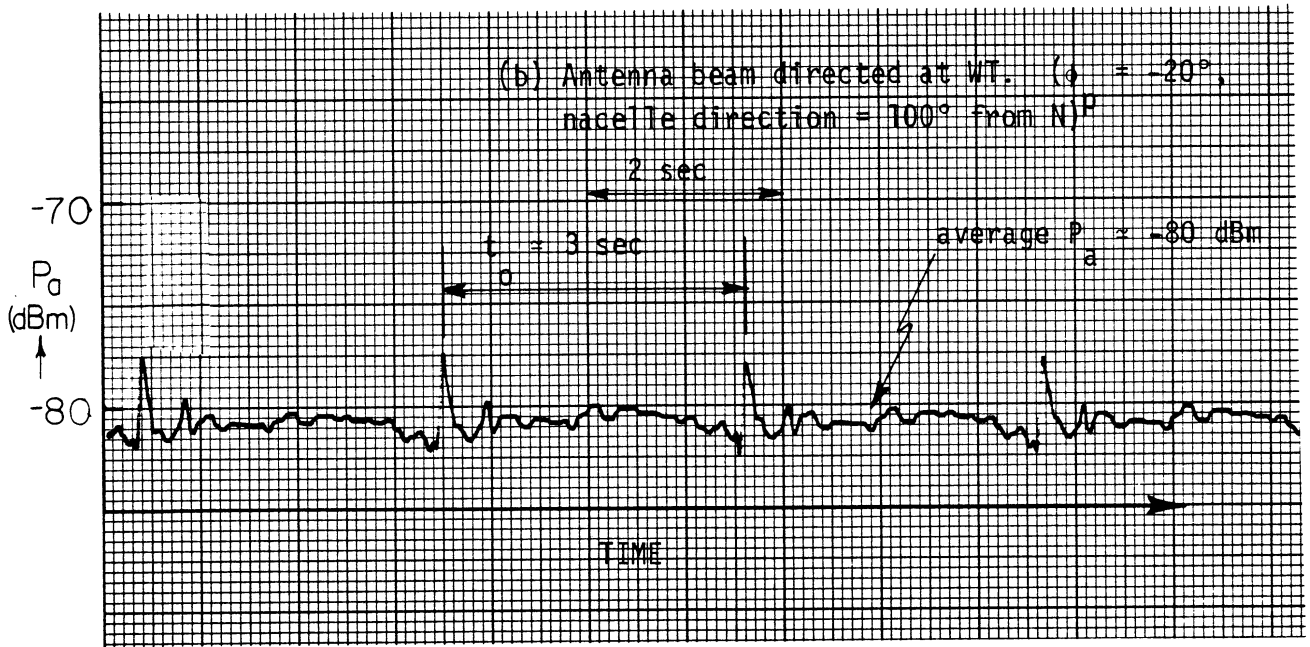
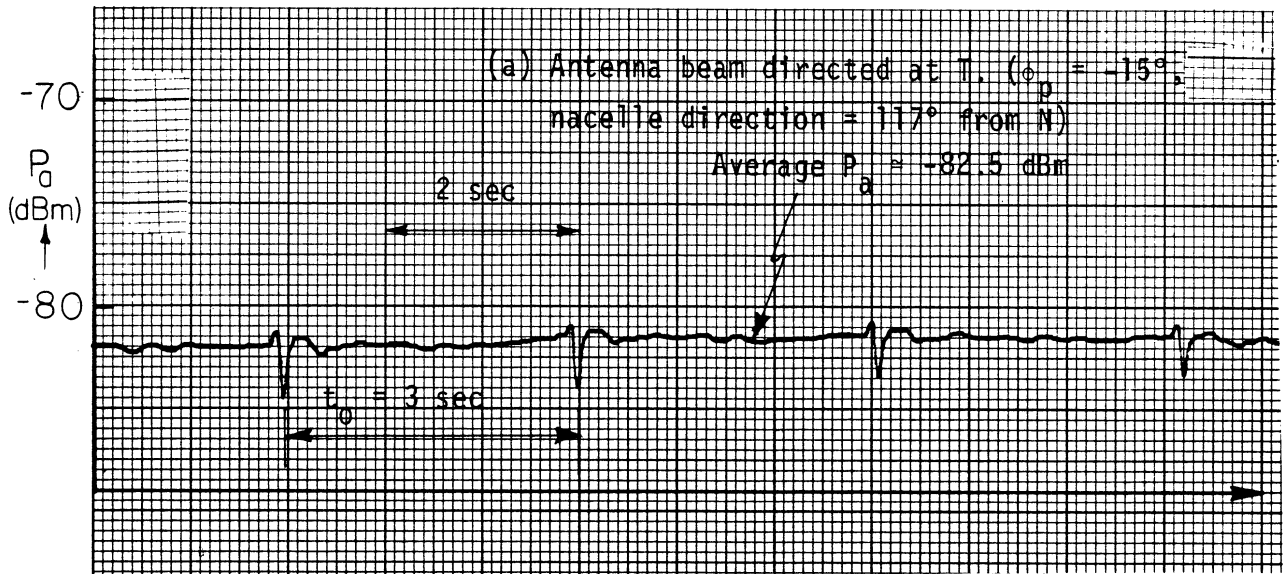


Fig. 6-8 P_a vs. time on Channel 8 at site A.

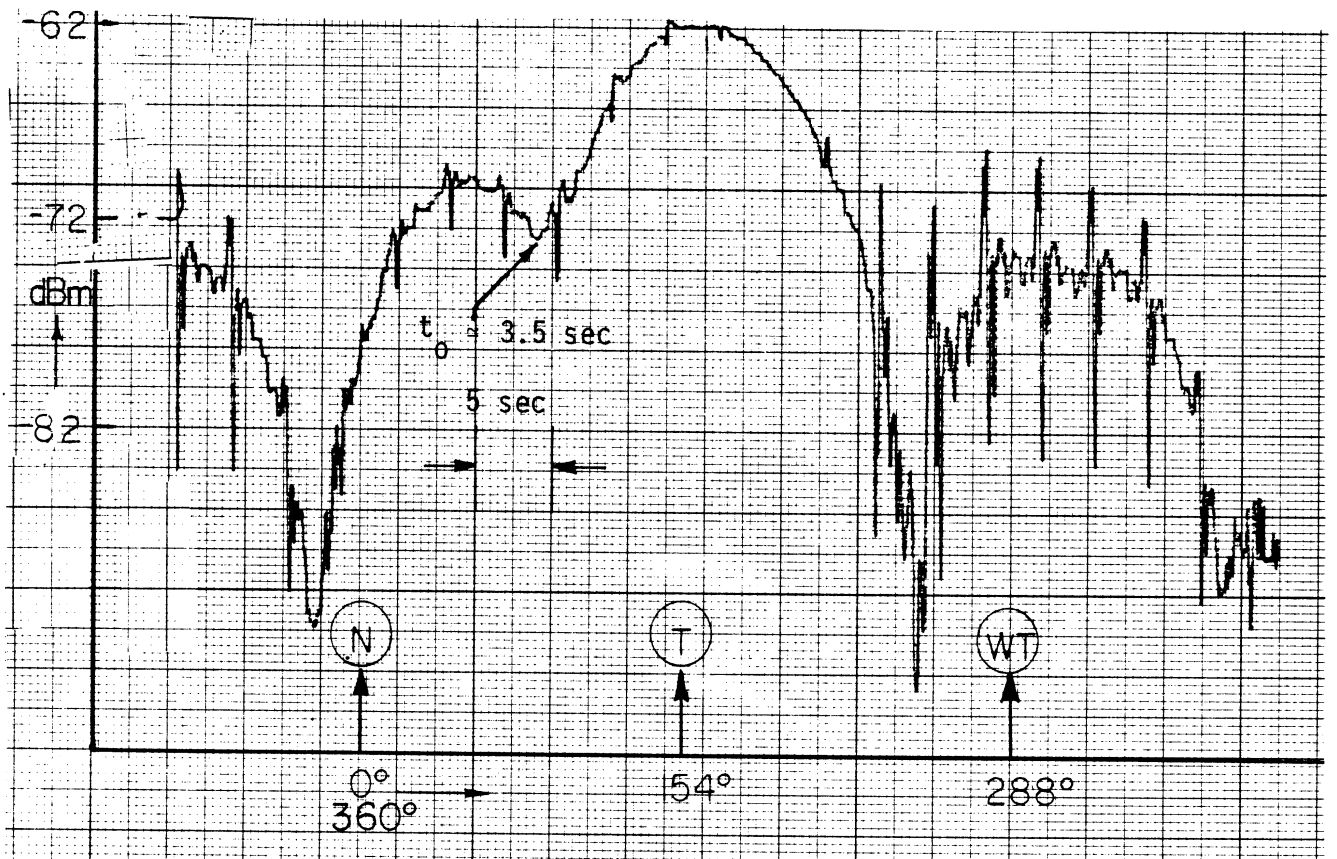


Fig. 6-9 Dynamic response of Channel Master antenna on Channel 3 at site A. (rpm = 9, $\phi_p = -1.5^\circ$, nacelle direction = 135° from N)

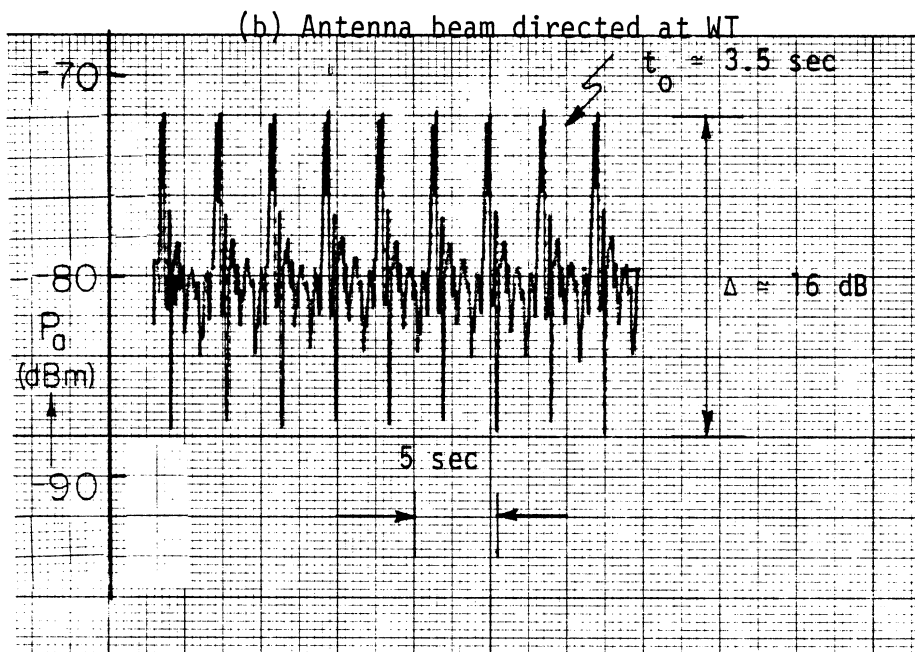
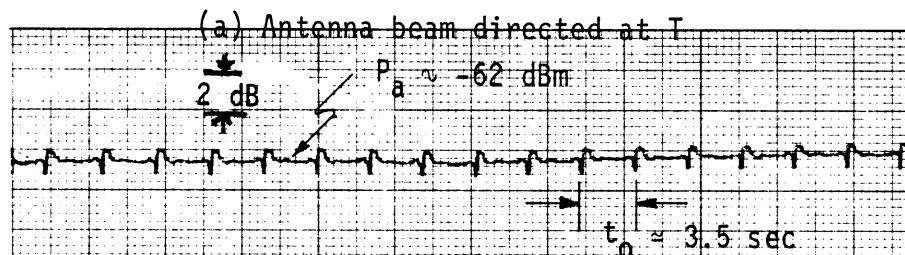


Fig. 6-10 P_a vs. time on Channel 3 with Channel Master antenna at site A. ($\text{rpm} = 9$, $\phi_p = -15^\circ$, nacelle direction = 135° from N)

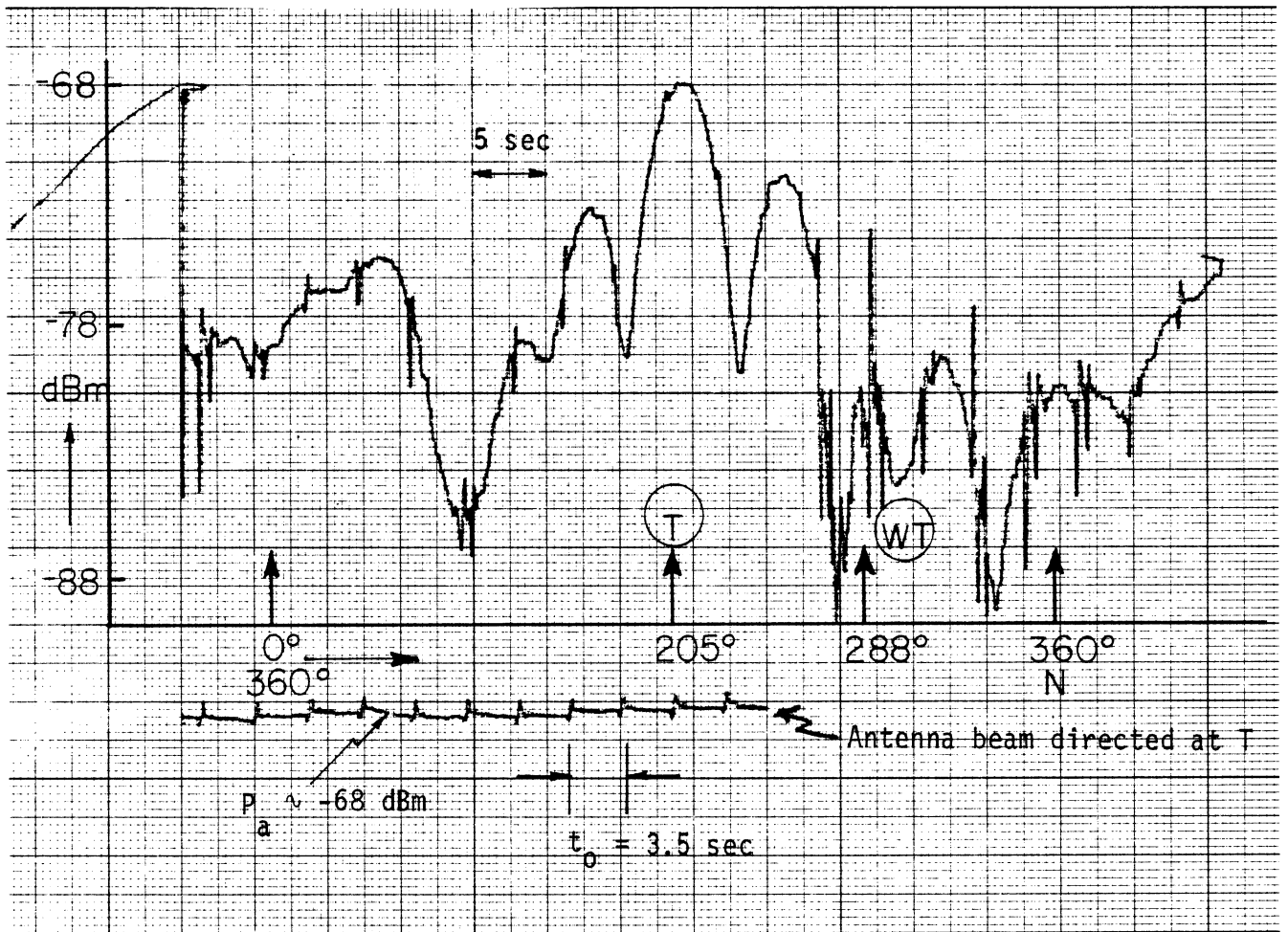


Fig. 6-11 Dynamic response (upper trace) and P_a vs. time (lower trace) on Channel 7 for the Channel Master antenna at site A. (rpm = 9, $\phi_p = -15^\circ$, nacelle direction = 135° from N)

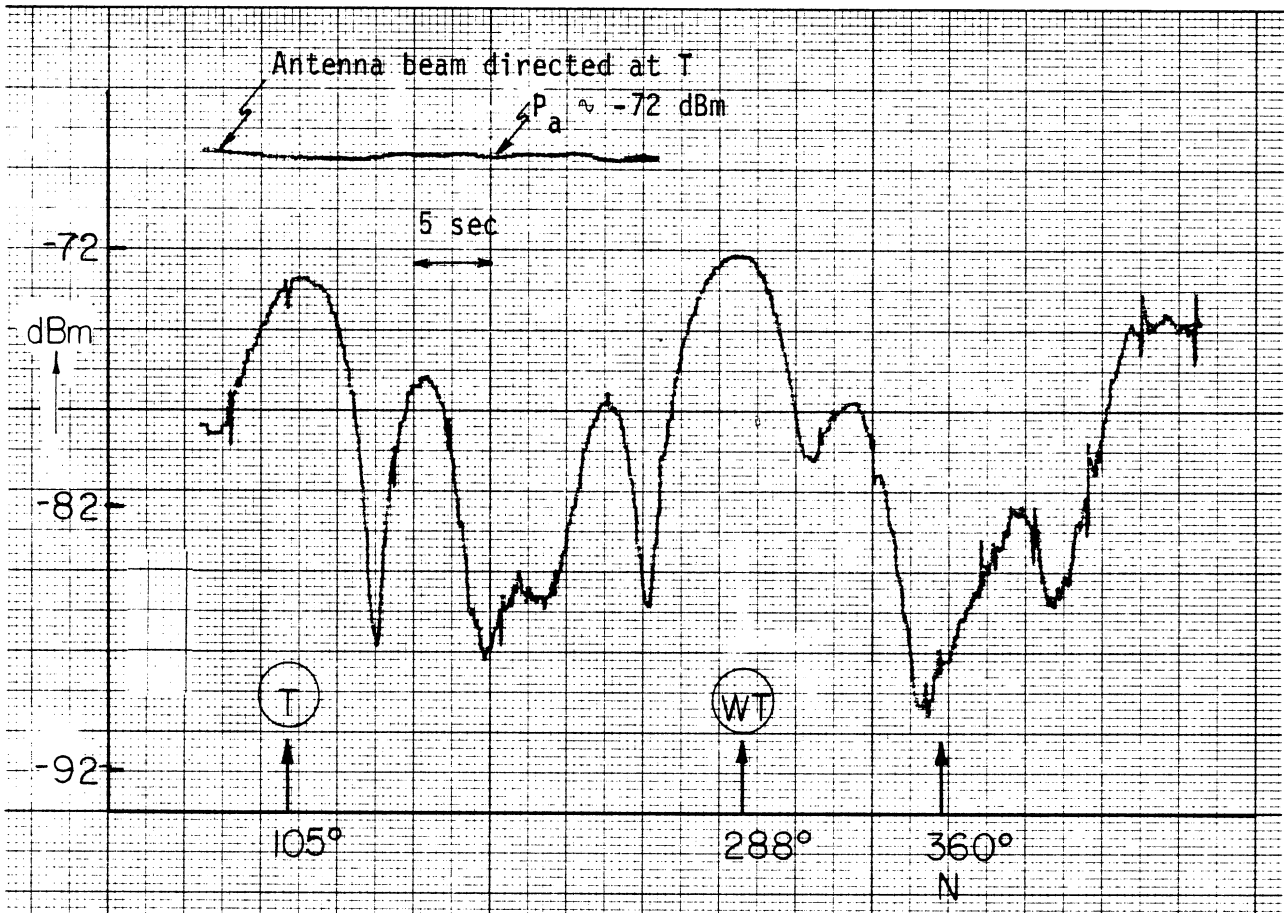


Fig. 6-12 Dynamic response (lower trace) and P_a vs. time (upper trace) on Channel 8 for the Channel Master antenna at site A. ($\text{rpm} = 9$, $\phi_p = -15^\circ$, nacelle direction = 135° from N).

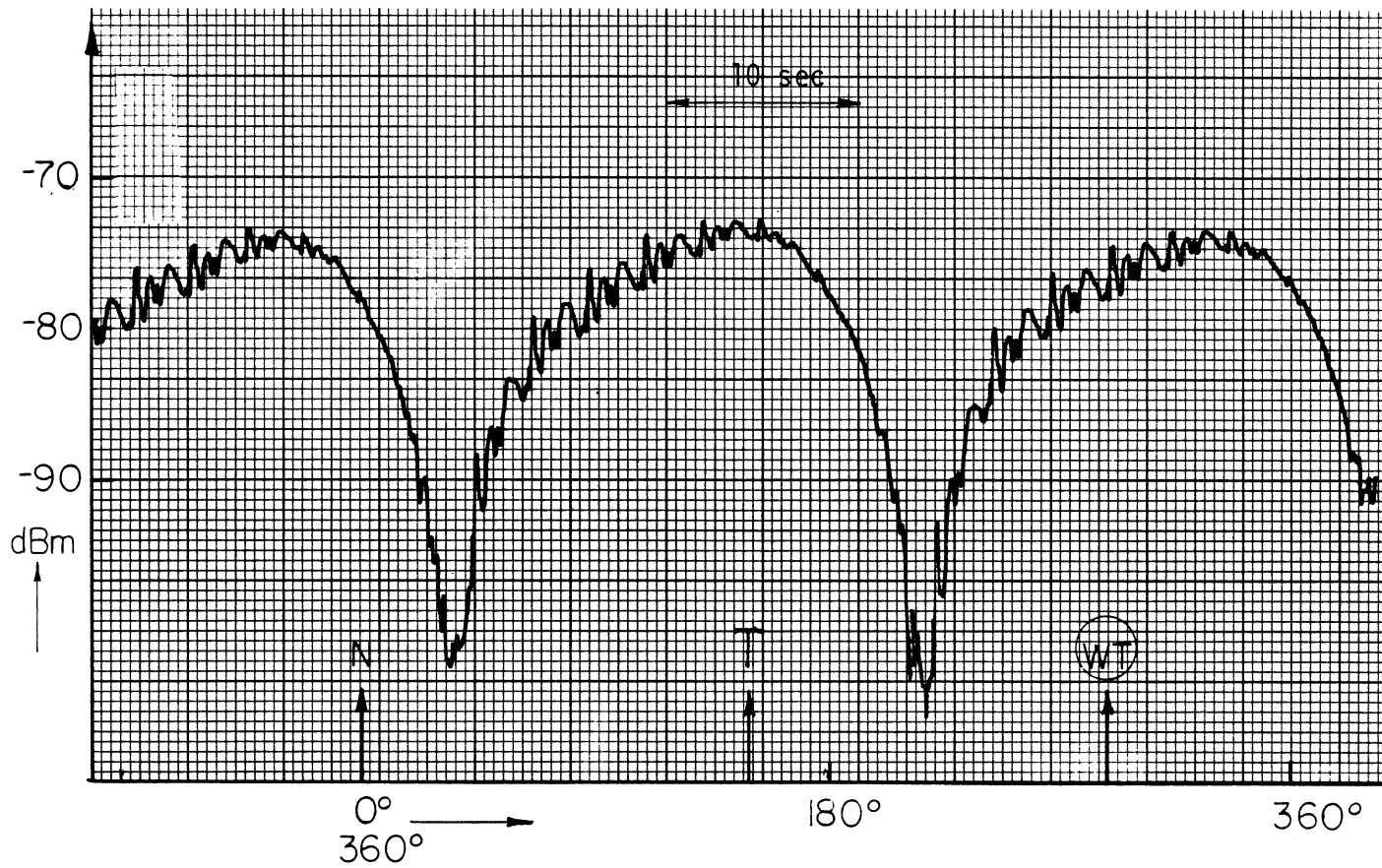


Fig. 6-13 Dynamic response of a $\lambda/2$ dipole antenna on Channel 3 at site A. ($r_{pm} = 10$, $\phi_p = -15^\circ$, nacelle direction = 63° from N)

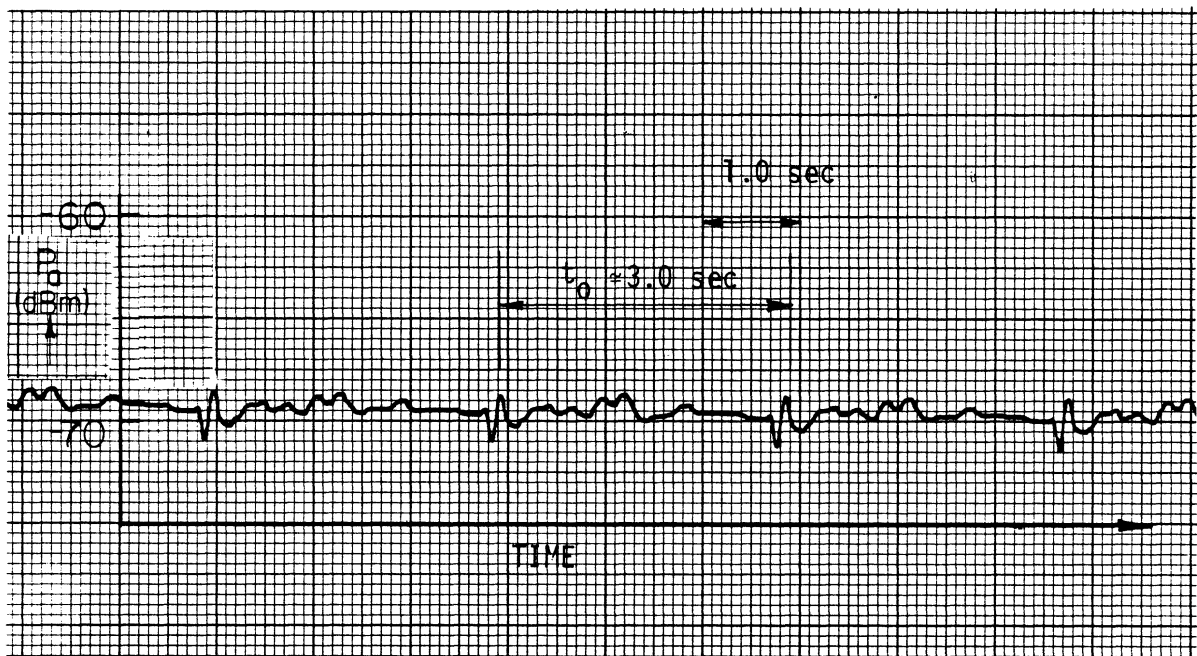


Fig. 6-14 p_a vs. time on Channel 3 at site A with $\lambda/2$ dipole antenna oriented to receive maximum signal from T. (rpm = 10, $\phi_p = 15^\circ$, nacelle direction = 135° from N)

Δ in Fig. 6-14 is about 2.5 dB, which produced significant (but still acceptable) video distortion. It is interesting to note that by properly positioning the sharp null in the antenna pattern (i.e., pointing the end of the dipole at the WT), the TVI effects could be completely eliminated at the expense of a slight reduction in the received signal level.

6.1.4 Data Analysis. The theory outlined in §A.2 will now be applied to calculate the modulation index m and, hence, the total signal variation Δ (in dB) caused by the WT under operating conditions for comparison with the measured values. The symbols are defined in §A.2, and we present the details of the calculation in two of the cases only.

Common Parameters:

$$h_t = 366 \text{ m}, h_a = 6 \text{ m}, D = 975 \text{ m}, r = 1041 \text{ m}$$

$$A = 40 \text{ m}^2, L_1 = 25 \text{ m}, L_2 = 1.6 \text{ m}$$

$$\alpha_c = 9^\circ, \alpha = \tan^{-1} \{(h_t - h_a)/D\} = 20.3^\circ$$

site location 108°

Winegard Antenna Data:

(i) Channel 3 (Set 1: Figs. 6-1 and 6-2)

$$\lambda = 4.56 \text{ m}, \text{ transmitter location } 154^\circ$$

nacelle voltage = 0: nacelle direction = 135° (from Fig. A-2)

$$\text{pitch angle } \phi_p = -15^\circ$$

$$(E_B/E_R)F(B,T) = (33 + 12.5) \text{ dB} = 45.5 \text{ dB} = 188 \text{ (with the antenna beam pointed at the turbine)}$$

$$\phi_o = -(154^\circ - 135^\circ) = -19^\circ, \phi = (135^\circ - 108^\circ) = 27^\circ$$

$$\cos \alpha_c = 0.9877, \cos(\alpha - \alpha_c) = \cos 11.3^\circ = 0.9807$$

$$\cos(\phi - \phi_p) = \cos 42^\circ = 0.7431$$

$$\sin(\phi_o - \phi_p) = -\sin 4^\circ = -0.0698$$

$$\sin(\phi - \phi_p) = \sin 42^\circ = 0.6691$$

$$\sin \equiv \sin\{2\pi h_t h_a / (\lambda r)\} = \sin 166.5^\circ = 0.2334$$

$$\begin{aligned} \text{sinc}_2 &= \text{sinc}[(L_2 / \lambda) \{ \cos \alpha_c \sin(\phi_o - \phi_p) + \cos(\alpha - \alpha_c) \sin(\phi - \phi_p) \}] \\ &= 0.9316 \end{aligned}$$

Use Eq. (A.5) with the first sinc function unity to obtain the modulation index when the antenna is pointed at the WT:

$$\begin{aligned} m(R) &= \frac{2 \times 40 \times 0.743 \times 0.9877}{4.56 \times 1041} \times 0.2334 \times 188 \times 0.9316 \\ &= 0.51 \end{aligned}$$

The corresponding total variation in the received signal is

$$\Delta = 20 \log \frac{1+m}{1-m} = 9.8 \text{ dB} ,$$

compared with the measured value $\Delta \approx 11$ dB obtained from Fig. 6-2b.

With the antenna pointed at the transmitter, use

$$\frac{E_B}{E_R} F(B,T) = (33 - 12.5) \text{ dB} = 20.5 \text{ dB} = 10.6$$

instead of the value 188 above to get $m(R) = 0.029$. The corresponding total variation in the received signal is

$$\Delta = 20 \log \frac{1.029}{0.971} = 0.5 \text{ dB} ,$$

compared with the measured value $\Delta \simeq 0.6$ dB obtained from Fig. 6-2a.

Channel 3 (Set 2: Figs. 6-3 and 6-4)

nacelle voltage = 9: nacelle direction = 100°

$$\phi_p = -20^\circ, \phi_o = -54^\circ, \phi = -8^\circ$$

$$\cos(\phi - \phi_p) = 0.9781, \cos \alpha_c = 0.9877$$

$$\sin = 0.2334, \text{sinc}_2 = 0.9756$$

$$(E_B/E_R)F(BT) = 188$$

For the antenna pointed at the WT, $m(R) = 0.70$ giving $\Delta = 15.1$ dB, compared with the measured value $\Delta \simeq 15.8$ dB obtained from Fig. 6-4b.

For the antenna pointed at the transmitter, $m(R) = 0.04$ giving $\Delta = 0.7$ dB, compared with the measured value $\Delta \simeq 0.8$ dB obtained from Fig. 6-4a.

(ii) Channel 5 (Fig. 6-5)

Site A is in the forward interference region for this Channel and, as noted in §A.2, the interference is greatest when the blades are nearly horizontal and provide in-phase contributions to the scattering. Since this case is different from the ones discussed above, we show the calculations in detail.

$$\lambda = 3.67 \text{ m, transmitter location } 302^\circ$$

nacelle voltage = 0: nacelle direction = 100°

$$\phi_p = -20^\circ, \alpha_c = 9^\circ, \alpha = 20.3^\circ$$

Since the signals are received from the back of the blades, it is convenient to measure the incident and scattered angles ϕ_0 and ϕ from the direction $100^\circ + 180^\circ = 280^\circ$.

Thus, $\phi_0 = -22^\circ$ and $\phi = -188^\circ$.

$$\cos \phi_p = 0.9397, \sin \phi_p = -0.4524$$

$$(E_B/E_R)F(B,T) = (-33 + 85) \text{ dB} = 52 \text{ dB} = 398$$

Blade No. 1 Contribution

$$\cos(\phi - \alpha_c) = -0.9563$$

$$\cos(\alpha - \phi_p) = 0.7397$$

$$\sin(\alpha_0 - \phi_c) = -0.5150, \sin(\phi - \alpha_c) = 0.2924$$

$$\begin{aligned} \text{sinc}_1 &= \text{sinc}[(L_1/\lambda)\{\cos \phi_p \sin(\phi_0 - \alpha_c) + \cos(\alpha - \phi_p)\sin(\phi - \alpha_c)\}] \\ &= -0.0919 \end{aligned}$$

$$\sin \phi_p = -0.3420, \sin(\alpha - \phi_p) = 0.6730$$

$$\cos \alpha_c = 0.9877, \sin \alpha_c = 0.1564$$

$$\cos \phi_0 = 0.9272, \cos \phi = -0.9903, \cos(\alpha - \phi_p) = 0.7397$$

$$\begin{aligned} \text{sinc}_2 &= \left[\text{sinc} (L_2/\lambda) [\{\sin \phi_p - \sin(\alpha - \phi_p)\} \cos \alpha_c \right. \\ &\quad \left. - \{\cos \phi_p \cos \phi_0 + \cos(\alpha - \phi_p)\cos \phi\} \sin \alpha_c \right] \\ &= 0.7029 \end{aligned}$$

Use (A.7) to obtain

$$\begin{aligned} m_1 &= \frac{2 \times 40 \times 0.9563 \times 0.9397}{3.67 \times 1041} \times 0.0919 \times 0.7029 \times 0.4524 \times 398 \\ &= 0.22 \end{aligned}$$

Blade No. 2 Contribution

$$\begin{aligned} \cos(\phi + \alpha_c) &= -0.9999, \cos \phi_p = 0.9397, \cos(\alpha - \phi_p) = 0.7397 \\ \sin(\phi_0 + \alpha_c) &= -0.2250, \sin(\phi + \alpha_c) = -0.0175 \\ \text{sinc}_1 &= \text{sinc}[(L_1/\lambda)\{\cos \phi_p \sin(\phi_0 + \alpha_c) + \cos(\alpha - \phi_p)\sin(\phi + \alpha_c)\}] \\ &= 0.2075 \\ \text{sinc}_2 &= \text{sinc}[(L_2/\lambda)[\{\sin \phi_p - \sin(\alpha - \phi_p)\}\cos \alpha_c \\ &\quad + \{\cos \phi_p \cos \phi_0 + \cos(\alpha - \phi_p)\cos \phi\}\sin \alpha_c] \\ &= 0.7253 \end{aligned}$$

Use (A.7) to obtain

$$\begin{aligned} m_2 &= \frac{2 \times 40 \times 0.9999 \times 0.9397}{3.67 \times 1041} \times 0.2075 \times 0.7253 \times 0.4524 \times 398 \\ &= 0.53 \end{aligned}$$

Thus

$$m(R) = m_1 + m_2 = 0.75$$

and the corresponding total variation in the received signal is

$$\Delta = 20 \log \frac{1.75}{0.25} = 16.9 \text{ dB} ,$$

compared with the measured value $\Delta = 17.5$ to 19.0 dB obtained from Fig. 6-5. It should be noted that the lower signal levels are below the noise level of the spectrum analyzer.

(iii) Channel 7 (Fig. 6-6)

$$\lambda = 1.67 \text{ m, transmitter location } 205^\circ$$

$$\text{nacelle voltage} = 9: \text{nacelle direction} = 100^\circ$$

$$\phi_p = -20^\circ, \phi_0 = -105^\circ, \phi = -8^\circ$$

$$\cos \alpha_c = 0.9877, \cos(\phi - \phi_p) = 0.9744$$

$$\sin = 0.9966, \text{ sinc}_2 = 0.3254$$

$$(E_B/E_R)F(B,T) = (30 - 18)\text{dB} = 12 \text{ dB} = 4.0$$

Then $m(R) = 0.057$ giving $\Delta = 1.0 \text{ dB}$, compared with the measured value $\Delta \approx 0.5 \text{ dB}$ obtained from Fig. 6-6b.

(iv) Channel 8 (Figs. 6-7 and 6-8)

$$\lambda = 1.62 \text{ m, transmitter location} = 105^\circ,$$

$$\sin = 0.9467, \cos \alpha_c = 0.9877$$

The data in Fig. 6-7 show that the average signal level in the direction of the WT is about 2.5 dB higher than in the direction of the transmitter. This peculiar result can be taken into account in the calculation by assuming $F(B,T) \approx 1$, but with the ambient signal level 2.5 dB higher in the direction of the WT.

Antenna beam directed at the transmitter:

$$\text{nacelle voltage} = 9.75: \text{nacelle direction} = 117^\circ$$

$$\phi_p = -15^\circ, \phi_o = 12^\circ, \phi = 9^\circ$$

$$\cos(\phi - \phi_p) = 0.9135$$

$$(E_B/E_R)F(B,T) = 26 \text{ dB} = 20$$

$$\text{sinc}_2 = 0.1865$$

Then $m(R) = 0.15$ giving $\Delta = 2.6 \text{ dB}$, compared with the measured value $\Delta \approx 3 \text{ dB}$ obtained from Fig. 6-8a.

Antenna beam directed at the WT:

$$\text{nacelle voltage} = 9: \text{nacelle direction} = 100^\circ$$

$$\phi_p = -20^\circ, \phi_o = -5^\circ, \phi = -8^\circ$$

$$\cos(\phi - \phi_p) = 0.9781$$

$$(E_B/E_R)F(B,T) = (26 - 2.5)\text{dB} = 23.5 \text{ dB} = 15$$

$$\text{sinc}_2 = 0.6941$$

Then $m(R) = 0.45$ giving $\Delta = 8.4$ dB, compared with the measured value $\Delta \approx 5$ dB obtained from Fig. 6-8b.

Channel Master Antenna Data:

Only the Channel 3 results shown in Figs. 6-9 and 6-10 will be analyzed. Except for $(E_B/E_R)F(B,T)$ and the WT rpm, all the parameters are the same as for the Set 1 results (Figs. 6-1 and 6-2) for the Winegard antenna.

From Fig. 3-6 the gains G_1 and G_2 of the Winegard and Channel Master antennas, respectively, are 9 and 4.5 dB, giving $G_1 - G_2 = 4.5$ dB. From Table 4-1, the average signal level at the blade that would be received with the Channel Master antenna is

$$P_a = (-27-4.5)\text{dB} = -31.5 \text{ dBm},$$

Antenna beam directed at the transmitter:

Use $P_a = -62$ dBm from Fig. 6-10a to obtain

$$E_B/E_R = (-31.5+62.0)\text{dB} = 30.5 \text{ dB} = 33.5 \text{ .}$$

From Fig. 6-9, the antenna discrimination factor $F(B,T) = -10$ dB $\approx 1/3.2$.

Hence

$$\begin{aligned} m(R) &= \frac{2 \times 40 \times 0.7431 \times 0.9877}{4.56 \times 1041} \times 0.2334 \times \frac{33.5}{3.2} \times 0.9316 \\ &= 0.028 \end{aligned}$$

giving $\Delta = 0.5$ dB, compared with the measured value $\Delta \approx 1$ dB obtained from Fig. 6-10a.

Antenna beam directed at the WT:

Use $P_a = -80$ dBm from Fig. 6-10b to obtain

$$(E_B/E_R)F(B,T) = (-31.5+80.0)\text{dB} = 48.5 \text{ dB} = 266 \text{ .}$$

Then

$$\begin{aligned} m(R) &= \frac{2 \times 40 \times 0.7431 \times 0.9877}{4.56 \times 1041} \times 0.2334 \times 266 \times 0.9316 \\ &= 0.72 \end{aligned}$$

giving $\Delta = 15.8$ dB, compared with the measured value $\Delta \approx 16$ dB obtained from Fig. 6-10b.

Half-Wave Dipole Data:

We again analyze only Channel 3 data:

$$\lambda = 4.56 \text{ m, transmitter direction} = 135^\circ$$

$$\text{nacelle voltage} = 8: \text{ nacelle direction} = 63^\circ$$

$$\phi_p = -15^\circ, \phi_o = -91^\circ, \phi = -45^\circ$$

$$\cos(\phi - \phi_p) = 0.8660, \cos \alpha_c = 0.9877$$

Since the gain G_2 of the dipole is 2.15 dB, $G_1 - G_2 = (9-2.15)\text{dB} = 6.85$ dB, and because $F(B,T) \approx 1$,

$$(E_B/E_R)F(B,T) = (-27-6.85+70)\text{dB} = 36.15 \text{ dB} = 64.2$$

$$\sin = 0.2334, \text{ sinc}_2 = 0.6260 \text{ .}$$

Hence

$$\begin{aligned} m(R) &= \frac{2 \times 40 \times 0.8660 \times 0.9877}{4.56 \times 1041} \times 0.2334 \times 64.2 \times 0.6262 \\ &= 0.14 \end{aligned}$$

giving $\Delta = 2.4$ dB, compared with the measured value $\Delta \approx 2.5$ dB obtained from Fig. 6-14.

6.2 Site I

Site I is located about 2.7 km SE of the WT (see Fig. 2-8), and the TV Channels available were 2,3,5,8 and 11. With the WT stationary the quality of reception obtained with the Winegard antenna was fair on Channel 2, fair to poor on Channel 5, and very poor on the other three Channels. As seen from Table 2-2, the site is in the forward interference region for Channels 5 and 11, and in the backward region for the others.

6.2.1 Discussion of the Results. Figure 6-15 shows the antenna response on Channel 2 with characteristic backward region interference, and Fig. 6-16 gives P_a vs time. The upper curve was obtained with the antenna pointed at the transmitter. There is no modulation apparent and no video distortion was observed with the test receiver. The analogous results for Channel 3 are shown in Fig. 6-17a,b where the upper curve is the antenna response and the lower curve is signal vs time for the antenna pointed at the transmitter. The total signal variation Δ is about 3.0 dB and the observed video distortion was close to the threshold level.

The antenna response for Channel 5 is presented in Fig. 6-18, and we recognize the forward region type of interference. The P_a vs time

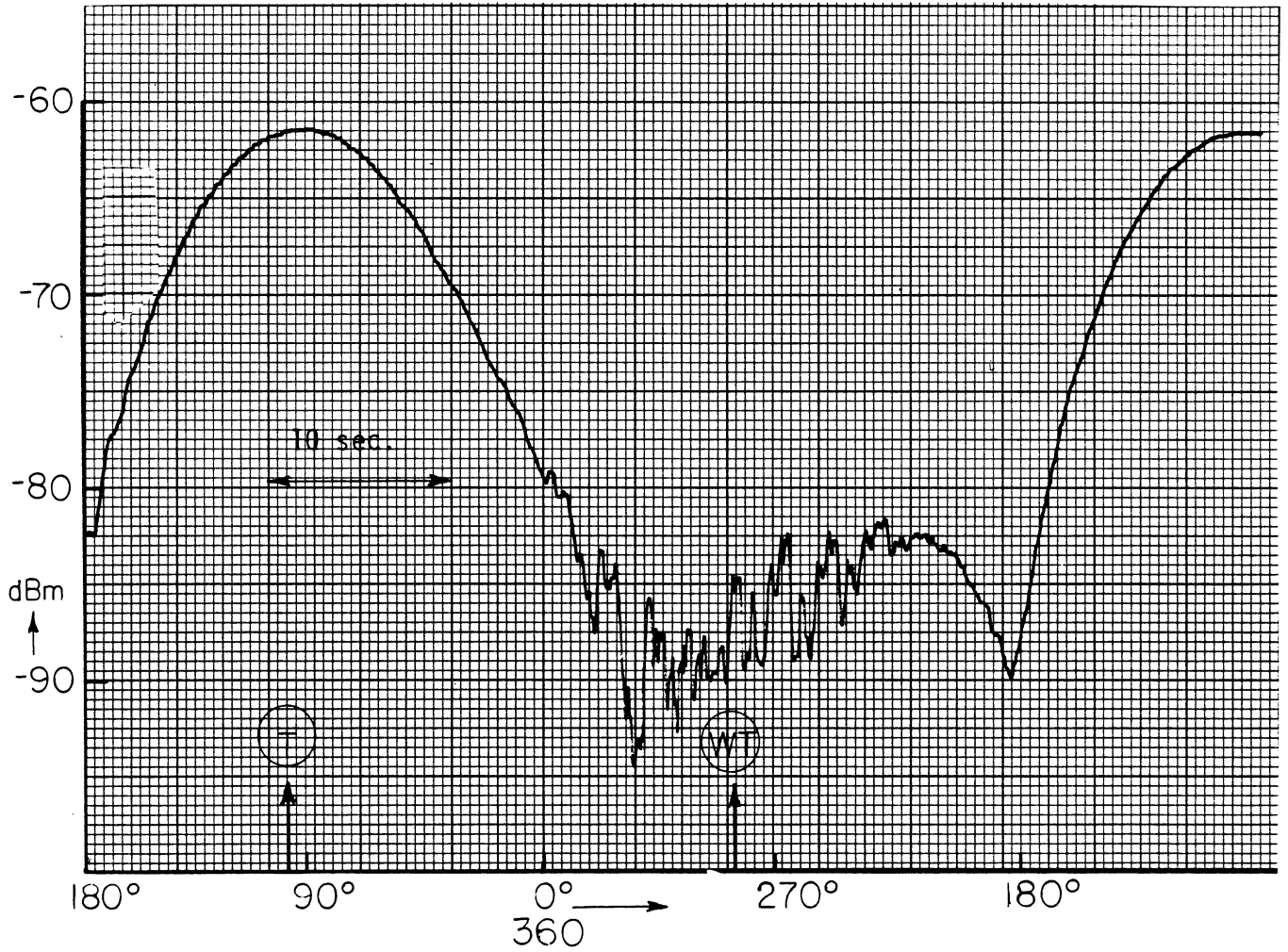


Fig. 6-15 Dynamic response of the Winegard antenna on Channel 2 at site I. (rpm = 12, $\phi_p = -6^\circ$, nacelle direction = 117° from N)

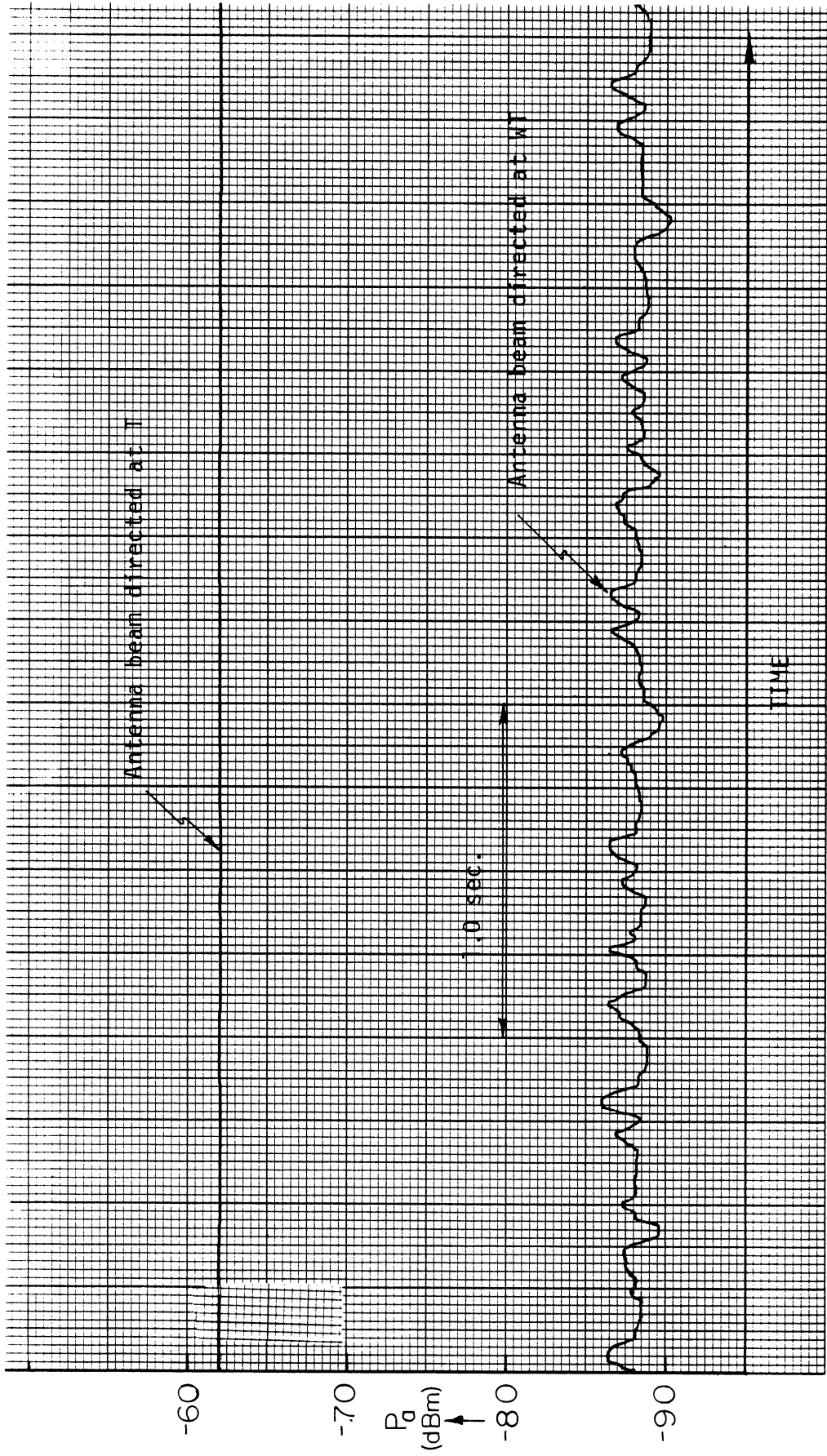


Fig. 6-16 P_a' vs. time on Channel 2 at Site I. (rpm = 12, $\phi_p = -6^\circ$, nacelle direction 117° from N)

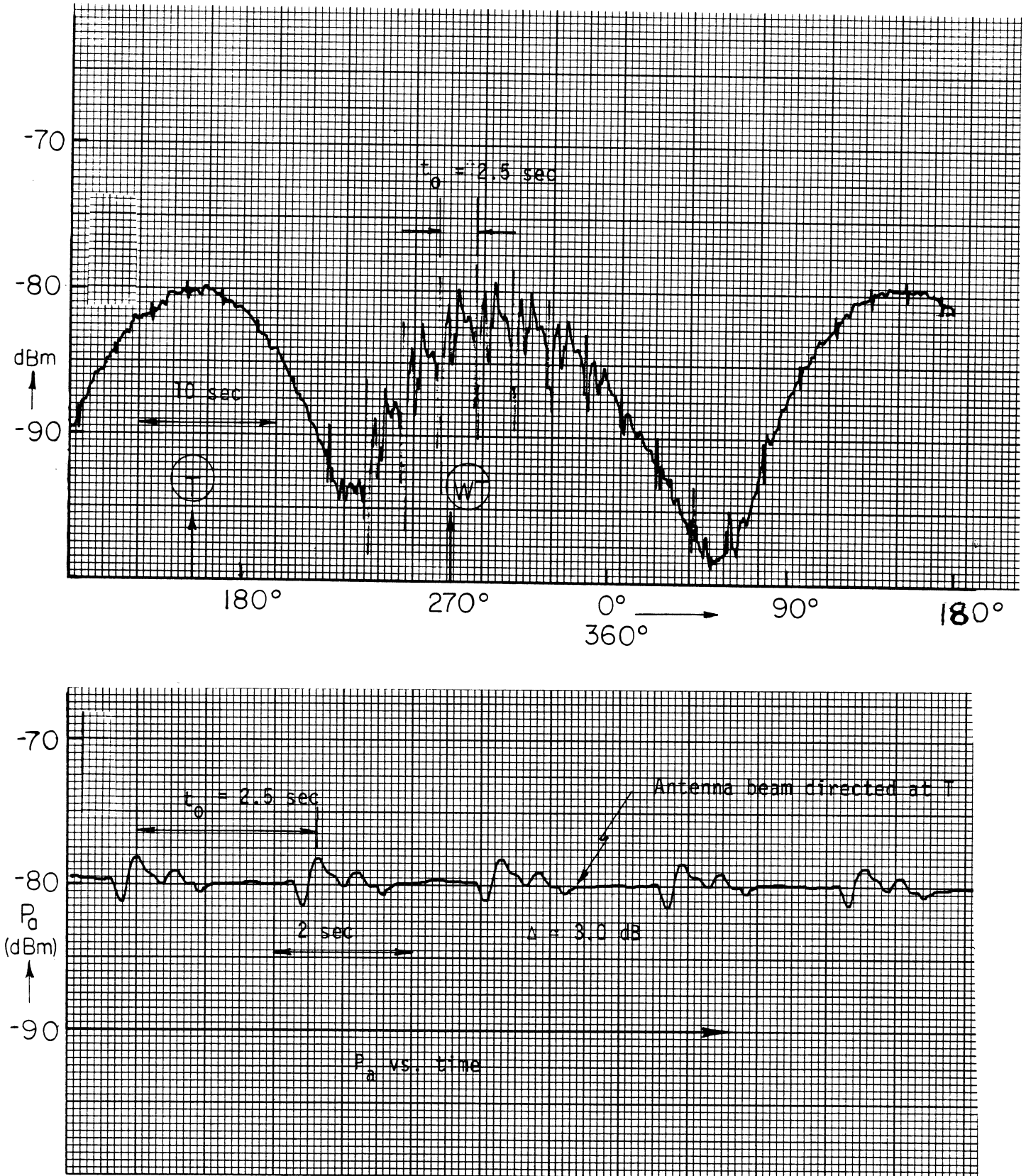


Fig. 6-17 Dynamic response (upper trace) and P_a vs. time (lower trace) on Channel 3 for the Winegard antenna at site 1. (rpm = 12, $\phi_p = -6^\circ$, nacelle direction = 117° from N)

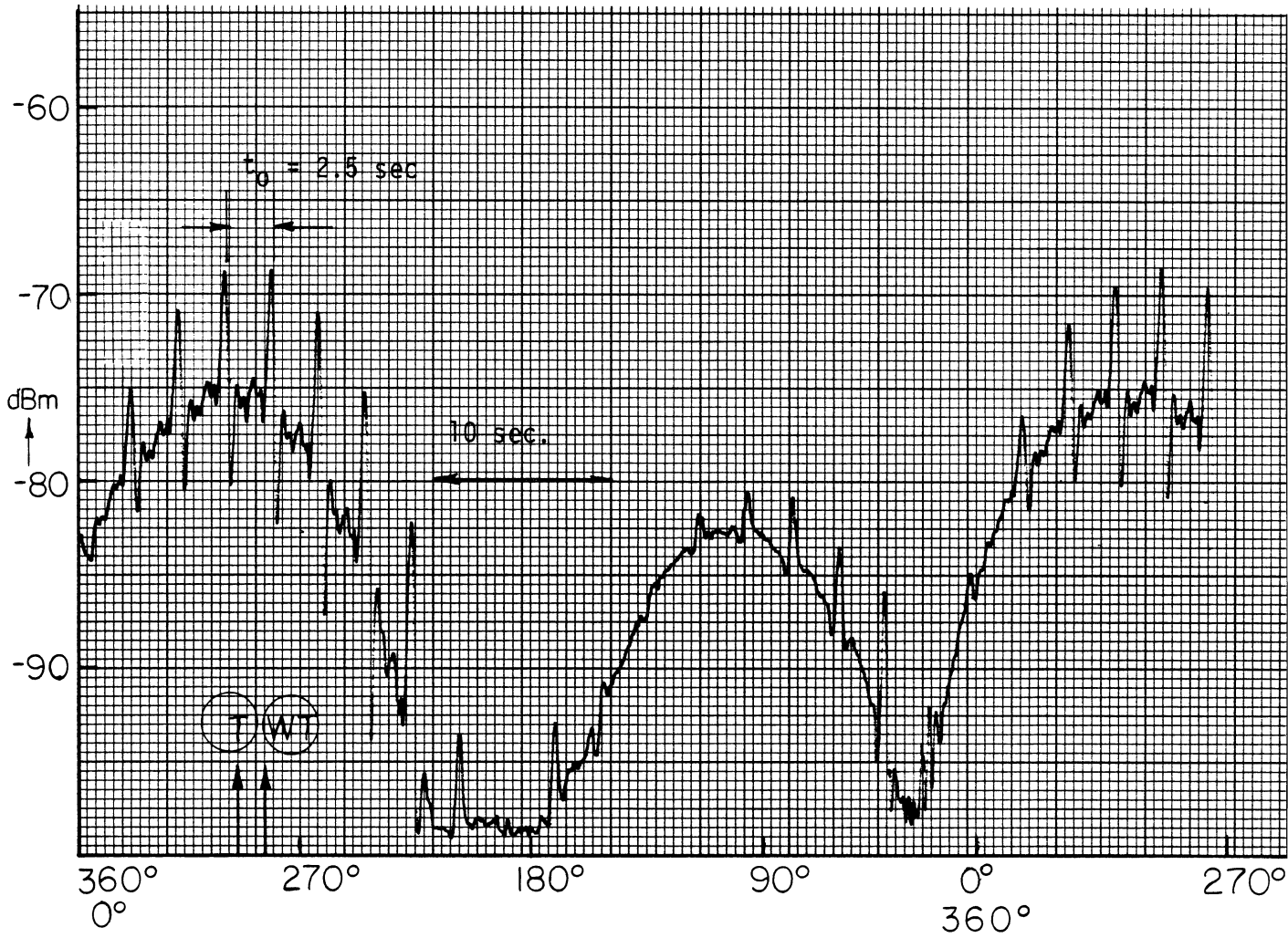


Fig. 6-18 Dyanmic response of the Winegard antenna on Channel 5 at site I. (rpm = 12, $\phi_p = -6^\circ$, nacelle direction = 117° from N)

traces with the antenna directed at the transmitter and at the WT are shown in Fig. 6-19. The total signal variations in the two cases are 7.5 and 13.0 dB, indicating that the site was not precisely in the forward scattering direction. In both instances, the observed video distortion was quite strong and above the level of acceptability.

The results for Channel 8 are shown in Figs. 6-20 and 6-21. As suggested by the latter figure, the video distortion was barely visible when the antenna was pointed at the transmitter (upper trace), but strong when the antenna was pointed at the WT. Figure 6-22 shows the forward region interference for Channel 11. Since $\Delta \approx 7.0$ dB and the average received signal $P_a \approx -80$ dBm, strong video distortion was observed.

6.2.2 Data Analysis. We analyze only the Channel 5 results described above, and since the calculations are similar to those for Channel 5 at site A (see §6.1.4), many of the details are omitted.

key parameters:

$$\lambda = 3.67 \text{ m}$$

$$\text{site location} = 115^\circ; \text{ transmitter location} = 302^\circ$$

$$\text{nacelle direction} = 117^\circ$$

$$\phi_p = -6^\circ, \phi_o = -5^\circ, \phi = -178^\circ$$

$$\alpha = 8.82^\circ, \alpha_c = 9^\circ$$

$$\sin = 0.9996$$

$$\text{sinc}_1 = 0.1870, \text{sinc}_2 = 0.9579 \text{ for blade No. 1}$$

$$\text{sinc}_1 = 0.2548, \text{sinc}_2 = 0.9595 \text{ for blade No. 2}$$

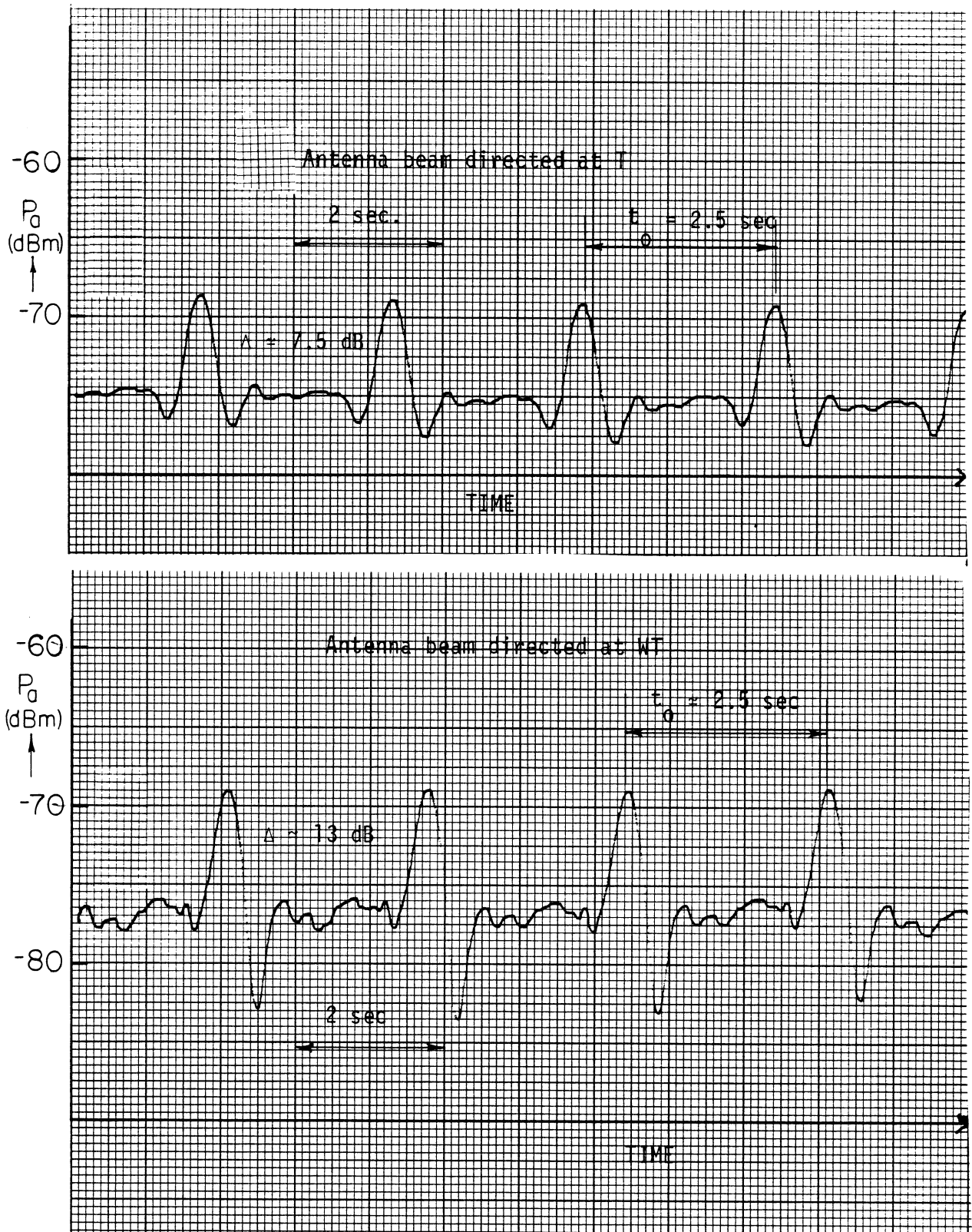


Fig. 6-19 P_a vs time on Channel 5 with the Winegard antenna at site I.
(rpm = 12, $\phi_p = -6$, nacelle direction = 117° from N)

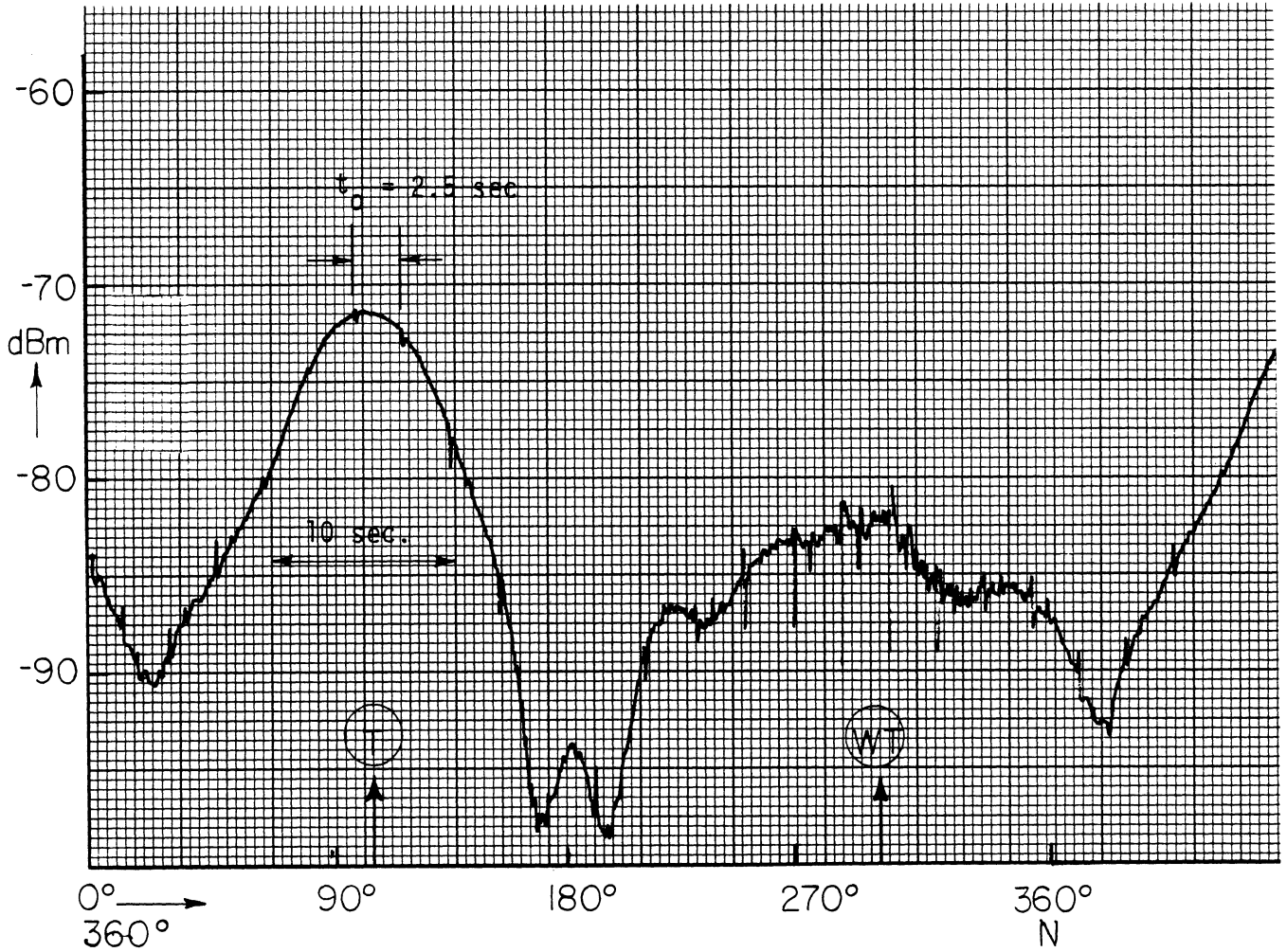


Fig. 6-20 Dynamic response on Channel 8 with the Winegard antenna at site I. (rpm = 12, $\phi_p = -6^\circ$, nacelle direction = 117° from N)

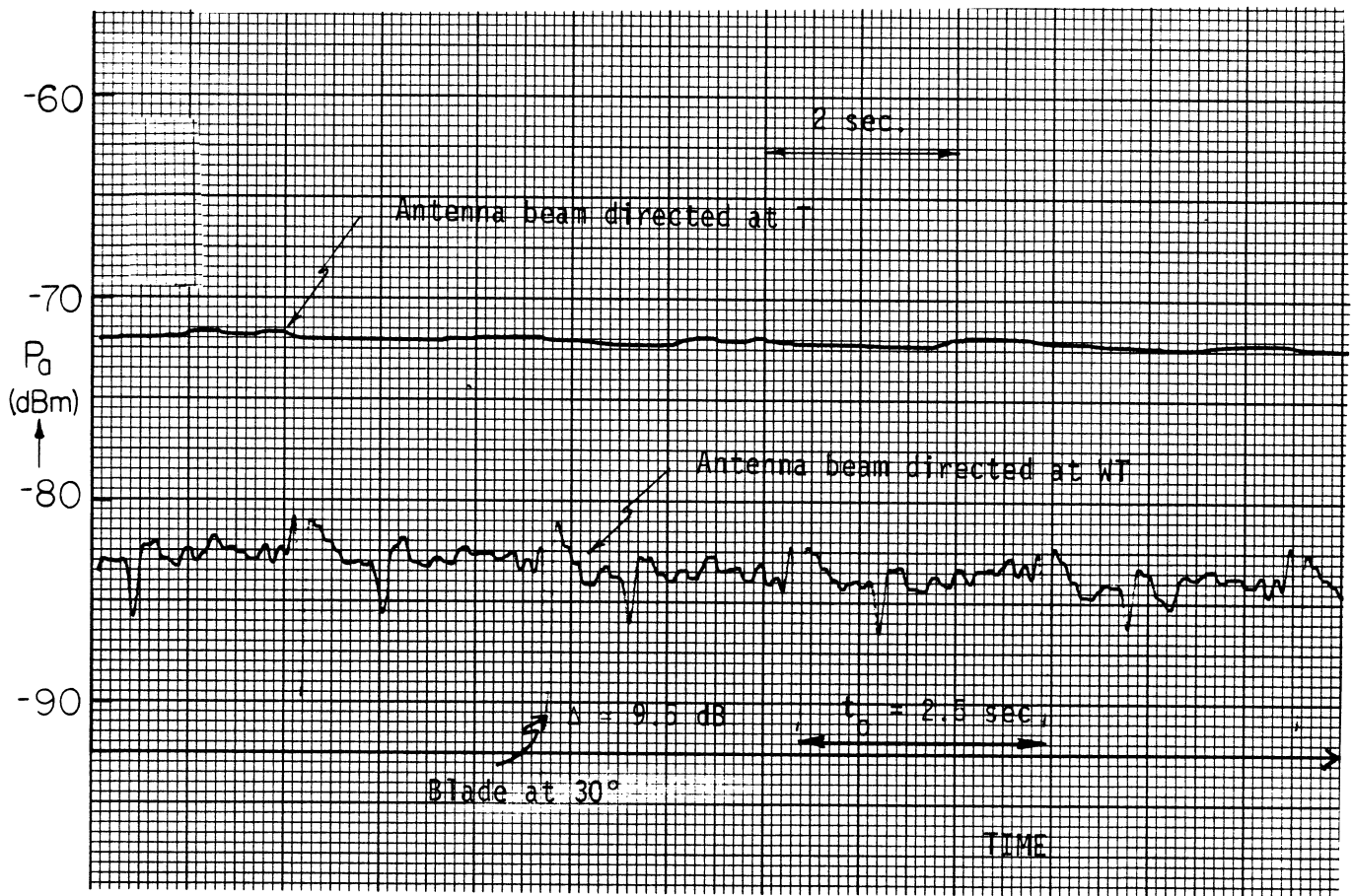


Fig. 6-21 P_a vs time on Channel 8 with the Winegard antenna at site I.
(rpm = 12, $\phi_p = 6^\circ$, nacelle direction = 117° from N)

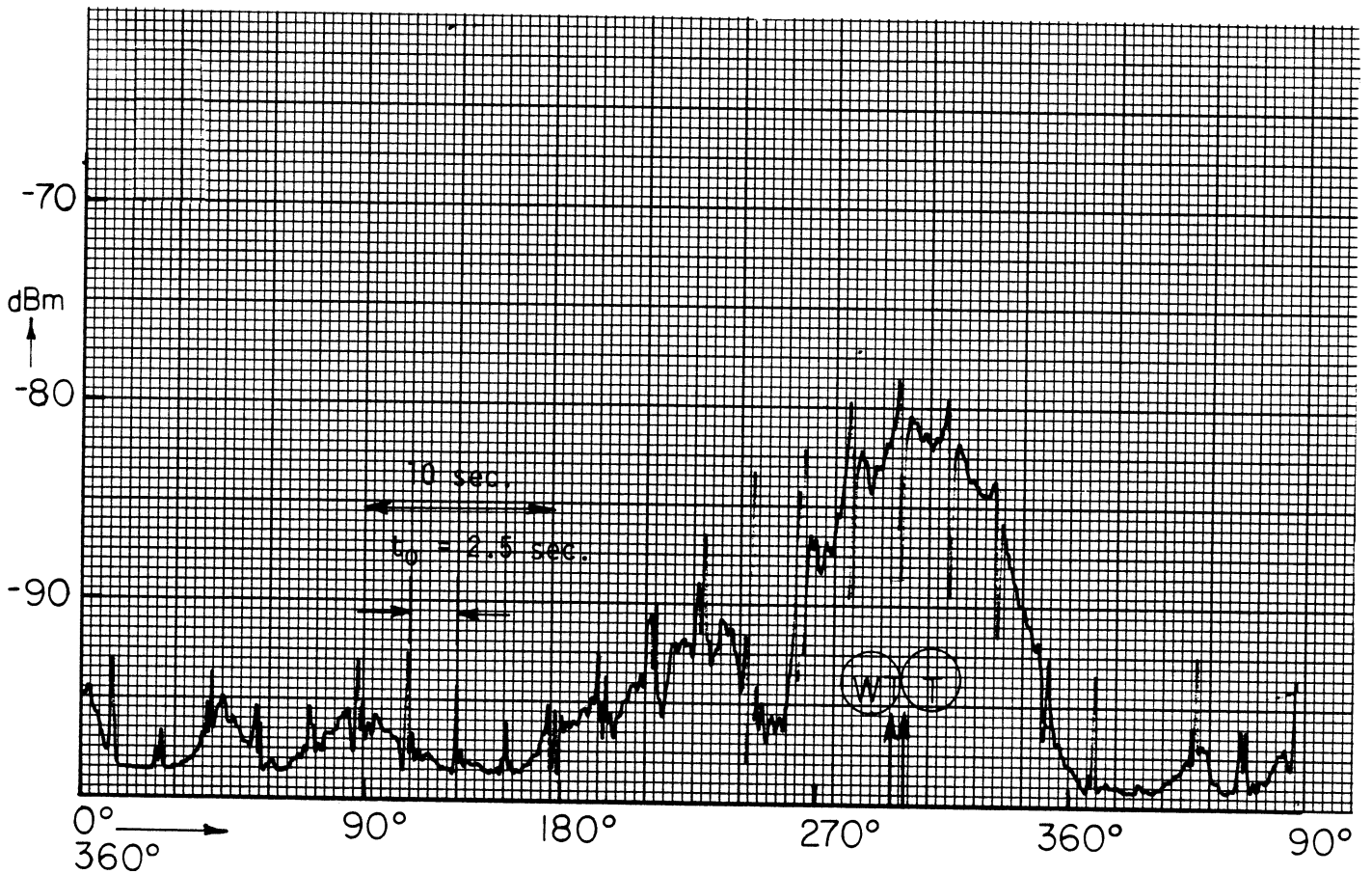
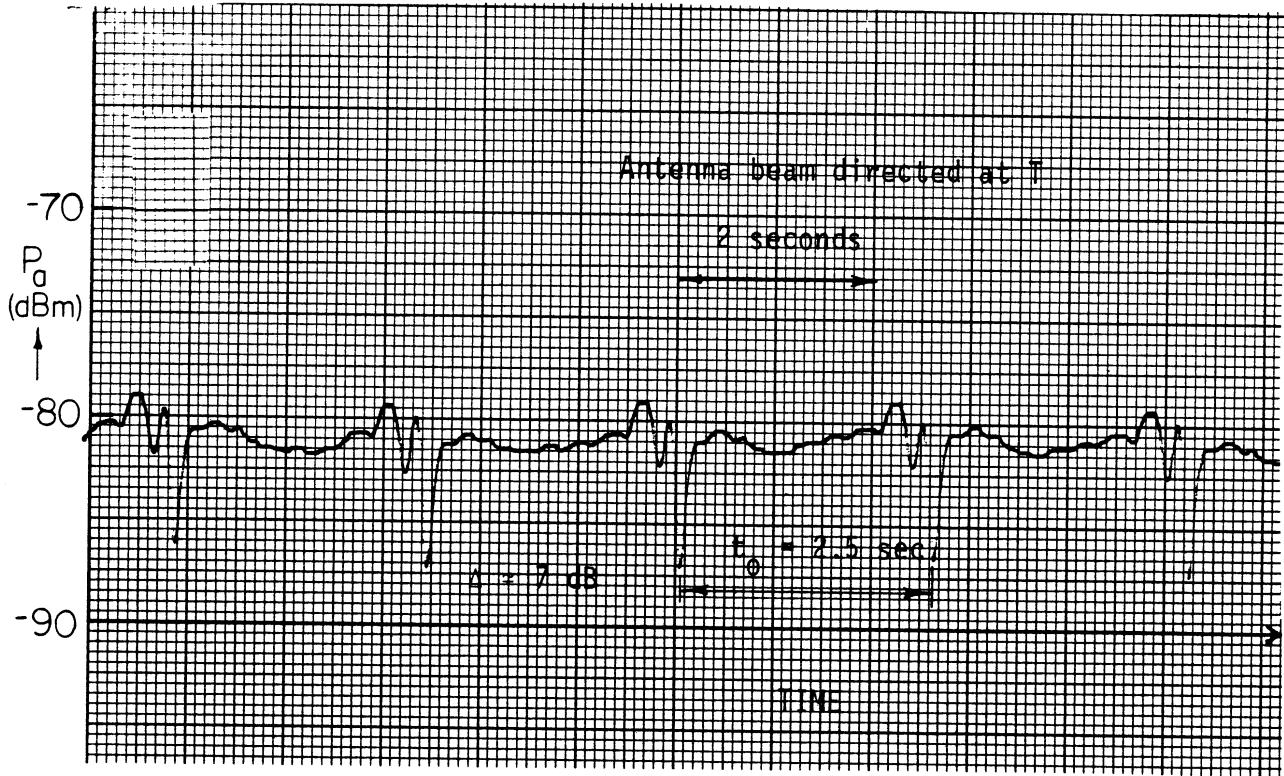


Fig. 6-22 Dynamic response (upper trace) and P_a vs. time (lower trace) on Channel 11 with the Winegard antenna at site I. (rpm = 12, $\phi_p = -6^\circ$, nacelle direction = 117° from N)

For the antenna pointed at the WT,

$$(E_B/E_R)F(B,T) = (-33+77.5)\text{dB} = 44.5 \text{ dB} = 168$$

Using (A.7), $m_1 = 0.23$ and $m_2 = 0.32$ giving $m = 0.55$ from which we have $\Delta = 10.7$ dB, compared with the measured value $\Delta \approx 13$ dB obtained from Fig. 6-19b.

For the antenna pointed at the transmitter

$$(E_B/E_R)F(B,T) = 42.0 \text{ dB} = 126$$

giving $m = 0.31$. Hence, $\Delta = 5.6$ dB compared with the measured value $\Delta \approx 7.5$ dB obtained from Fig. 6-19a.

It is of interest to compare the Channel 5 results at sites A and I. Both sites are in the forward interference region for this Channel in almost the same direction at distances of 1.0 and 2.7 km, respectively, from the WT. With the antenna beam pointed at the transmitter, the modulation indices deduced from the measured data are $m_A = 0.75$ and $m_I = 0.31$. Not surprisingly the observed interference was more severe at site A because of its smaller distance from the WT, but the ratio $m_A/m_I = 2.4$ is actually smaller than the inverse ratio 2.7 of the corresponding distances. This could be due to differences in the WT state (e.g., blade pitch or nacelle direction) at the times of the measurements, or to differences in the propagation conditions at the two sites.

The measurements suggest that the TVI in this direction could remain severe at distances beyond site I. Indeed, if the conditions

(including E_B/E_R) pertaining at site I were the same at sites further out, the interference in the direction 115° from N would exceed the threshold level for which $m = 0.15$ out to a distance of approximately $0.31/0.15 \times 2.7 = 5.6$ km from the WT.

6.3 Summary of Results

Dynamic tests similar to those described above were conducted at all but one of the sites. The pertinent results are summarized in Table 6-1 where, for completeness, we have included the findings for sites A and I as well. At site C the normal ac power was not available, and because of a malfunction in the portable power supply, no dynamic data were collected. Since sites B and C are close to one another, it is expected that the results for site B would also be applicable to C. In the other cases where data are missing from Table 6-1, the desired signals were either not available or were too weak for any meaningful measurements to be made.

At each site and on any Channel the TVI effects are characterized by the following three parameters:

- Δ total variation (in dB) of the received signal P_a caused by the WT blade rotation;
- Q_i quality of video reception of grades $i = 0,1,2$ or 3 under normal conditions, i.e., with the WT stationary;
- D_i video distortion of grades $i = 0,1,2$ or 3 observed in the received picture.

In every instance the parameters were determined from measurements made with the Winegard antenna oriented to receive the maximum signal. The

Table 6-1: Summary of TVI Data

Site	Distance from WT (km)	TVI Parameters								
		Ch. 2	Ch. 3	Ch. 5	Ch. 7	Ch. 8	Ch. 11			
A	1.0	--	0.7 Q ₁ D ₀	18 Q ₃ D ₃	0.5 Q ₂ D ₀	3 Q ₃ D ₂	--	--	--	--
B	0.6	--	3.2 Q ₁ D ₃	0 Q ₀ D ₀	0 Q ₁ D ₀	7 Q ₃ D ₃	--	--	--	--
C	0.8	--	--	--	--	--	--	--	--	--
D	0.9	0.5 Q ₁ D ₀	3.0 Q ₂ D ₂	0 Q ₁ D ₀	--	--	--	0.5 Q ₂ D ₀	--	--
E	0.9	9.0 Q ₃ D ₃	0 Q ₂ D ₀	1.5 Q ₃ D ₁	--	--	--	--	--	--
F	1.6	--	3.5 Q ₂ D ₃	--	6.0 Q ₃ D ₂	7.5 Q ₃ D ₃	--	--	--	--
G	2.0	--	0.5 Q ₁ D ₀	1.0 Q ₂ D ₁	--	3.0 Q ₂ D ₃	--	--	--	--
H	2.3	1.0 Q ₁ D ₁	2.0 Q ₁ D ₁	--	--	3.5 Q ₃ D ₃	--	--	--	--
I	2.7	0 Q ₁ D ₀	3.0 Q ₃ D ₃	7.5 Q ₂ D ₃	--	0.5 Q ₂ D ₀	8.0 Q ₃ D ₃	--	--	--
J	4.0	--	2.0 Q ₃ D ₁	2.5 Q ₁ D ₁	--	--	--	--	--	--

four grades of video reception and observed video distortion were established as follows:

video reception quality:

- Q_0 good
- Q_1 fair (little snowy)
- Q_2 poor (substantial snow)
- Q_3 very poor and unacceptable (extremely snowy)

observed video distortion:

- D_0 none or barely visible
- D_1 visible but below threshold
- D_2 comparable to the threshold
- D_3 above threshold/unacceptable

In general, the four grades of video reception were in accordance with received ambient field levels in the following ranges:

- Q_0 $P_a \geq -56$ dBm
- Q_1 -56 dBm $> P_a \geq -65$ dBm
- Q_2 -65 dBm $> P_a \geq -70$ dBm
- Q_3 -70 dBm $> P_a$

and the four grades of video distortion corresponded to total signal variation Δ as follows:

- D_0 $\Delta \sim 0.0 - 0.5$ dB
- D_1 $\Delta \sim 1.0 - 2.0$ dB
- D_2 $\Delta \sim 2.5 - 3.0$ dB
- D_3 $\Delta > 3.0$ dB

We note that the threshold range is consistent with the previously established value $\Delta_0 = 2.6$ dB discussed in §2.3.

Table 6.1 shows that the WT produced some interference at all sites and on most of the available TV Channels. The degree of observed video distortion depends on the distance of the site from the WT, the state of the WT and, in the case of forward region interference, the ambient signal strength. On those Channels for which a given site was in the backward region, the video distortion was generally found to be acceptable, but the forward region (site A on Channel 5, site B on Channel 8, and site C on Channels 5 and 11) the interference was quite severe and unacceptable.

CHAPTER 7. CONCLUSIONS

The interference to TV reception caused by the MOD-1 WT at Boone has been studied by measuring the ambient field strengths, static (or blade) scattering, and TV interference at a number of sites in the vicinity of the WT. The RF sources were the commercial TV signals available at each site. Using a modified rectangular metal plate model of the WT blade, an approximate theory has been developed to predict the interference levels. The theory is in good agreement with the measured data.

As a result of the measured data and the analyses performed, the following observations are made:

(i) In the city of Boone and the surrounding area, the ambient field strengths are low on all of the available TV Channels. Even with the WT stationary, the quality of reception is poor, and a high performance antenna such as the Winegard cannot suffice to make it good. At the WT site the fields are quite strong, and about 30 to 40 dB higher than at the ten test sites.

(ii) The equivalent blade scattering area A has been determined from the static data. The average of the values obtained using two TV Channels at one site, and one Channel at a second site, is 39.8 m^2 , which is in excellent agreement with the 40 m^2 deduced from laboratory measurements of small scale models. The static measurements also show that under some circumstances the metallic walls of the nacelle

can produce significant amounts of scattering. It is important to take this fact into account in future WT design.

(iii) The main findings of the dynamic measurements of TV interference are: (a) Varying amounts of TVI were found at all sites and on all of the TV Channels. One reason for this is the large increase in ambient field strength on going from a test site to the WT. (b) With a high performance antenna, the backward region interference observed at the test sites was judged to be acceptable, showing that such an antenna can reduce and/or overcome the higher levels of interference that were found with a lower quality antenna. (c) Forward region interference extended furthest from the WT. The interference was judged unacceptable in several instances and, as expected, could not be reduced by using a high performance antenna. (d) For both types of interference, the theoretical results were in good agreement with the measured data. Based on the results obtained at sites A and I, it would appear that the forward region interference on Channel 5 will exceed the level of acceptability out to 5 or 6 km from the WT in a south-easterly direction.

In addition we make the following comments concerning the measurements and prediction of the TV interference produced by horizontal axis WTs:

(i) The equipment setup and the measurement procedures were found to be adequate and can be used for any future TVI measurements on WTs of this (or similar) type.

(ii) The theory constitutes a valid means for predicting the interference, and the information needed to apply the theory is the equivalent scattering area of the WT blade, and the ambient field strengths of all of the available TV Channel signals at the WT and at the receiving sites of interest.

APPENDIX A: THEORETICAL CONSIDERATIONS

It is convenient to collect here some theoretical results which are helpful in interpreting the data obtained from the static (blade scattering) and dynamic (interference) tests. A coordinate system is presented to specify the position of a WT blade at any time relative to the location of the receiving antenna. To describe the electromagnetic scattering properties of a rotating blade, a modified version of the rectangular metal plate model that was used in our earlier studies [6] is introduced, and approximate expressions for the blade-scattered signal are then derived. Finally, the modulation level or index (see §2.3) is discussed, and we show how this important parameter can be obtained from the measured data.

A.1 WT Blade Model and the Coordinate Systems

The scattered field of concern to us is that produced by a single WT blade. Our previous studies [1,6] indicated that the scattering can be simulated using a rectangular metal plate of length L_1 and width L_2 , and the equivalent scattering area of the blade is then $A = L_1 L_2$. The electromagnetic model of the WT therefore consists of a pair of coned plates of these dimensions.

In most circumstances and certainly in the case of the WT at Boone, any receiver location will be lower in elevation than the WT. At a given instant, let the upper blade of the WT be oriented as shown in Fig. A-1. B is the origin of a Cartesian coordinate system x,y,z

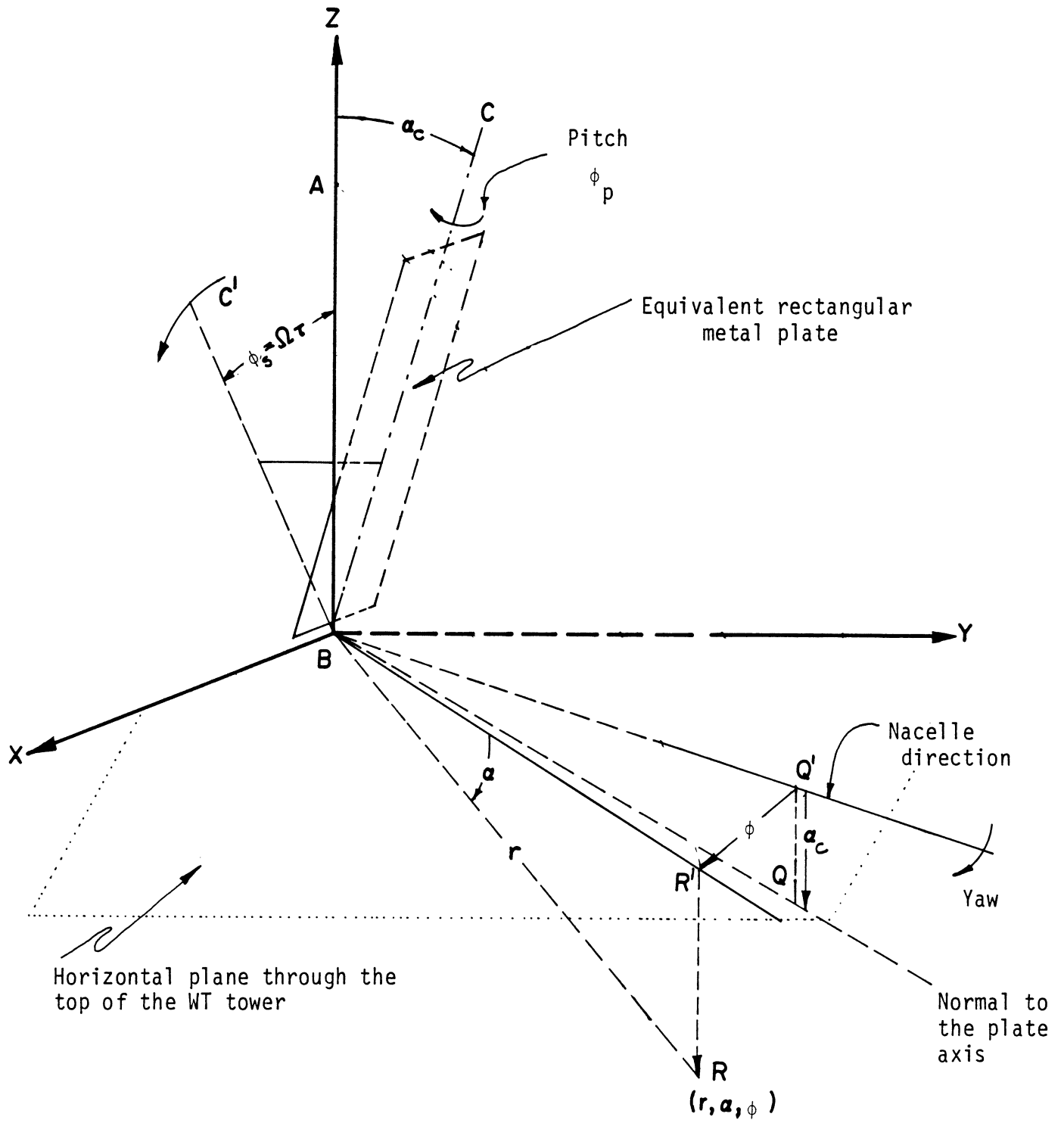


Fig. A-1 Rectangular plate model of the upper blade of the WT and the coordinate system used.

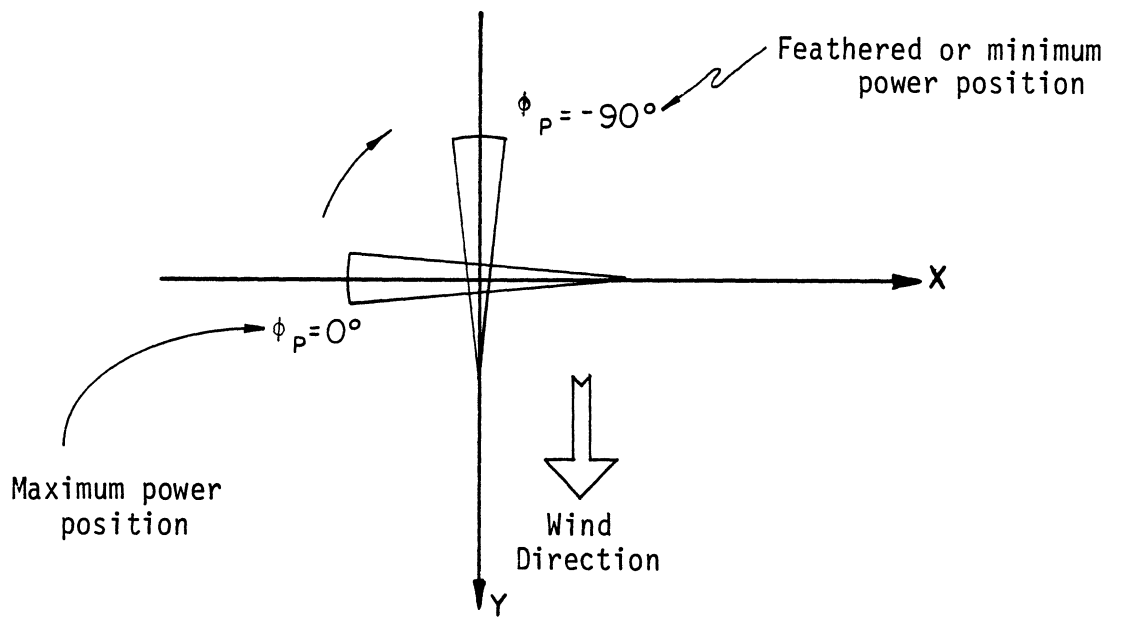


Fig. A-2 Horizontal cross-sectional views of the vertically oriented blade showing the sign convention for pitch.

whose z axis is perpendicular to the rotor axis and is also the polar axis of a spherical coordinate system. The angle α_c between the plate axis BC and the z axis is the coning angle of the actual WT blade.

The lower blade, not shown in Fig. A-1, would be located similarly at an angle $\pi - \alpha_c$. The blade can be rotated clockwise (as viewed from the top) about its axis BC through an angle ϕ_p representing the blade pitch which, in the actual WT, controls the power output. Assuming the blade is vertical with zero pitch as in Fig. A-1, the convention used to define the pitch angle is shown in Fig. A-2, where the feathered position is the usual one when the WT is not operating.

The wind direction is assumed horizontal as indicated by the line Q'B in Fig. A-1. At any instant the WT nacelle will point into the wind, i.e., in the direction BQ' and will yaw in azimuth (about the z axis) as the wind shifts. The WT can also be yawed mechanically when not in operation. The azimuthal position is measured in nacelle volts. The calibration curve for the MOD-1 WT relating nacelle volts to azimuthal angle (degrees from N) is given in Fig. A-3 from which the axis of blade rotation follows. At a time t later than that depicted in Fig. A-1, the projection BC' of the blade axis BC on the xz plane makes an angle θ_s with the z axis, where $\theta_s = \Omega t$, Ω being the angular frequency of blade rotation.

When a rectangular plate is illuminated by a plane electromagnetic wave, the scattered field is symmetric about the line perpendicular to the plate in its two principal planes. Because of the blade coning, the normal to the plate through the origin B lies below the horizontal plane, and in Fig. A-1 where $\phi_p = 0$, the normal

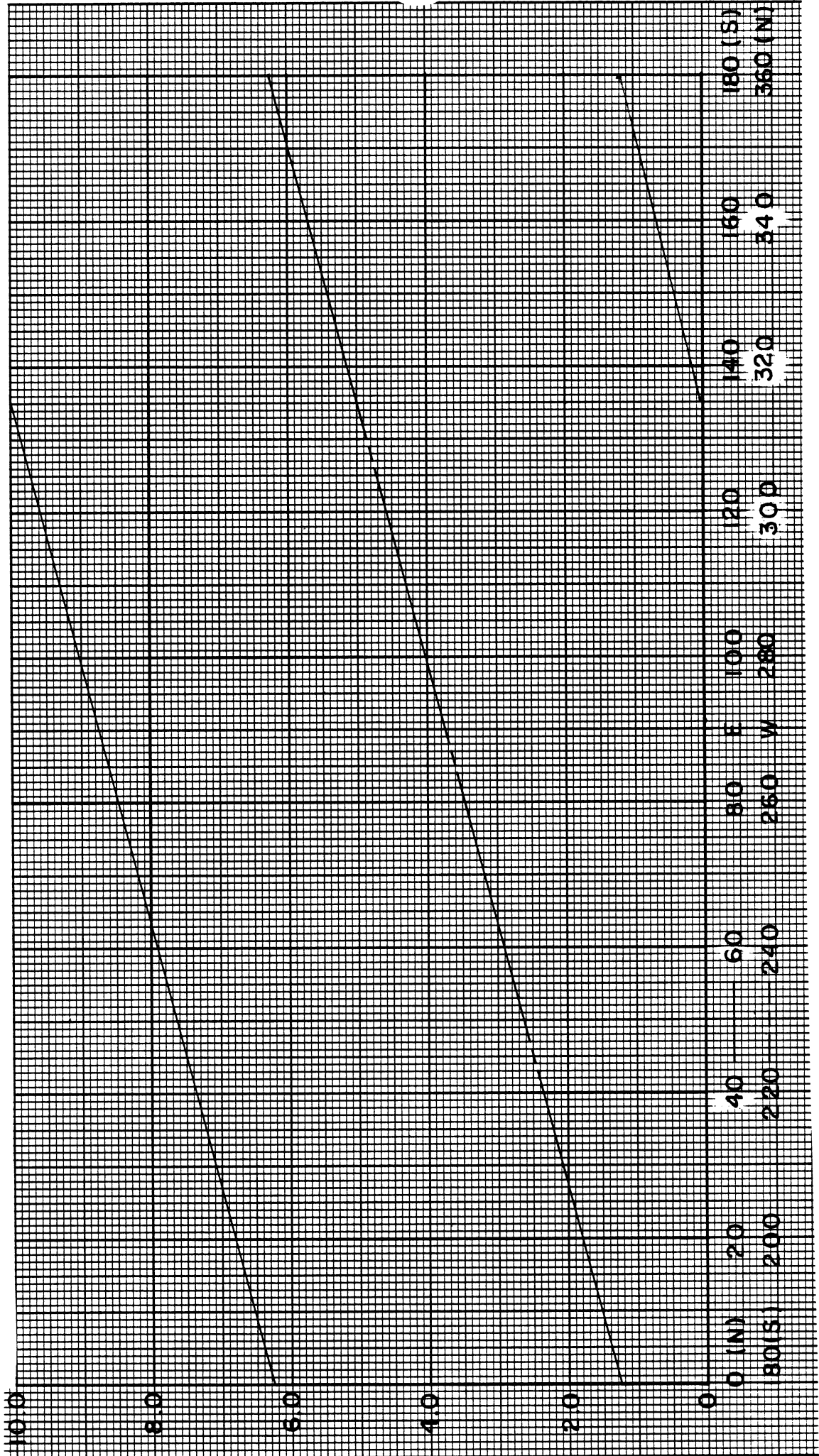


Fig. A-3 The calibration curve for MOD-1 WT relating nacelle volts to azimuthal angle (degrees from N)

is the line BQ. To compute the scattering from a blade it is convenient to reference the location of the receiving point R to the origin B (which can be considered to be the phase center of the two blades taken together) and to the nacelle direction BQ' in the horizontal plane. The coordinates of R are therefore r, α, ϕ where r is the distance from B, α is the depression angle below the horizontal, and ϕ is the azimuthal angle in the horizontal plane measured from BQ'.

Since the above angles differ from those of a usual spherical coordinate system, the following sign convention will be adopted: (i) 'elevation' angles α and α_c are considered positive for points below the horizon, and (ii) azimuthal angles ϕ, ϕ_p , etc are positive when measured anticlockwise as viewed from above. According to this convention, any compass bearing (from N) associated with the on-site tests must be treated as a negative quantity in our analysis of the scattered field.

A.2 Received Scattered Field

With the aid of our plate model, expressions for the maximum blade-scattered field relative to the direct field can be obtained by a trivial extension of our previous analyses [6,13]. For simplicity, the distant TV transmitter is assumed to lie in the horizontal (xy) plane of Fig. A-1 in a direction $(0, \phi_0)$ which is therefore the direction of the incident, horizontally polarized field. The receiving antenna is at $R(r, \alpha, \phi)$, and elevation and azimuthal (horizontal) plane diagrams of the incident and scattering directions are given in Figs. A-4a,b, where the blade is shown

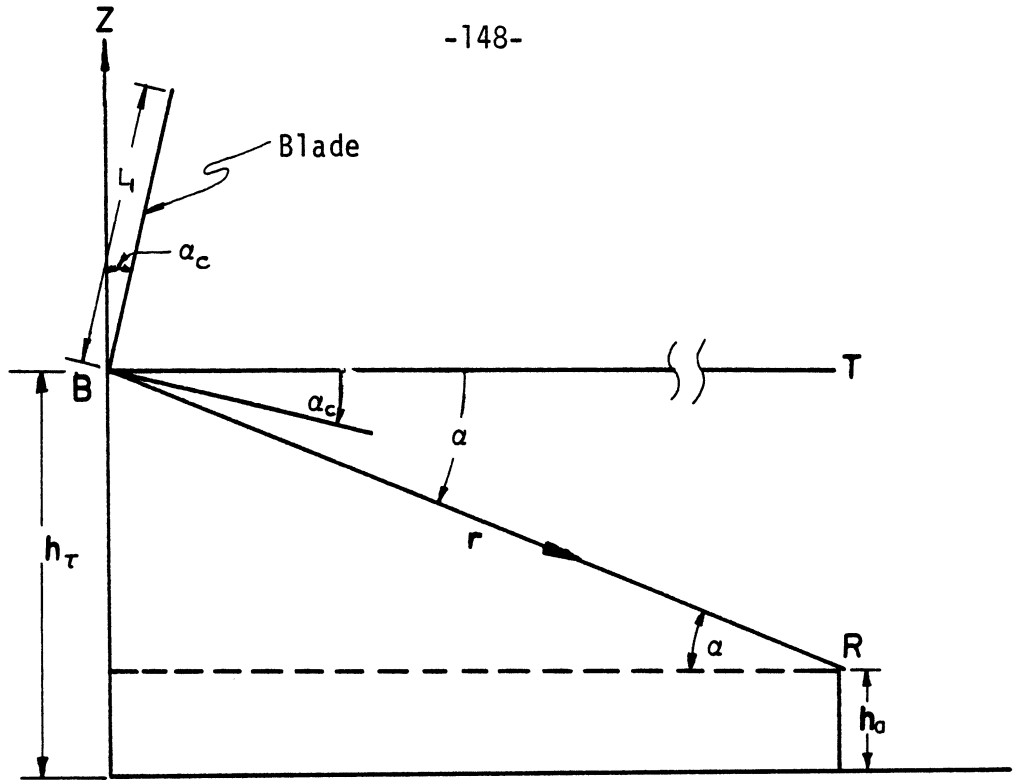


Fig. A-4a Elevation plane geometry of the blade, receiver, the incident and scattered field directions.

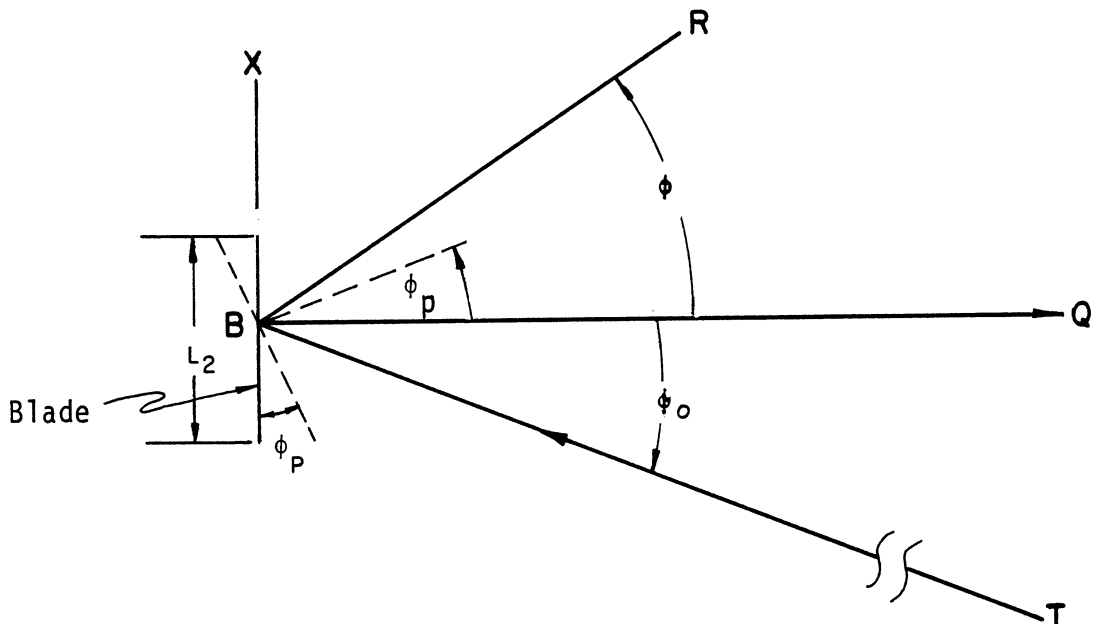


Fig. A-4b Azimuth plane geometry of the blade, receiver, the incident and scattered field directions.

vertical ($\theta_s = 0$). h_t and h_a are the heights of B and R respectively above the horizontal plane defined by ground level at the receiving site. For a blade in the vertical position, the magnitude of the horizontal component of the scattered electric field at R is

$$E^S(R) = E_B \frac{A}{\lambda r} |\cos(\phi - \phi_p) \cos \alpha_c| S_1 S_2 \quad (A.1)$$

with

$$S_1 = \left| \text{sinc} \left[\frac{L_1}{\lambda} \left\{ \sin \alpha_c - \sin(\alpha - \alpha_c) \right\} \right] \right| \quad (A.2)$$

$$S_2 = \left| \text{sinc} \left[\frac{L_2}{\lambda} \left\{ \cos \alpha_c \sin(\phi_0 - \phi_p) + \cos(\alpha - \alpha_c) \sin(\phi - \phi_p) \right\} \right] \right| \quad (A.3)$$

where E_B is the magnitude of the incident field at B,

λ is the wavelength,

A is the equivalent scattering area of the blade,

L_1, L_2 are the length and width, respectively, of the blade,

and

$$\text{sinc } x = \frac{\sin \pi x}{\pi x} \quad (A.4)$$

The other parameters are as defined before. The analogous expression for the field at R produced by the lower blade is obtained by replacing α_c by $\pi - \alpha_c$.

The modulation index or level $m(R)$ of the total received field is the ratio of the amplitudes of the scattered and incident (ambient) fields at R . For a perfectly conducting flat ground,

$$m(R) \equiv \frac{E^S(R)}{E_R}$$

$$= \frac{A}{\lambda r} \left| \cos(\phi - \phi_p) \cos \alpha_c \left[S_1 S_2 \right]^2 \left| \sin \left(\frac{2\pi h_a h_t}{\lambda r} \right) \right| \right| \frac{E_B}{E_R} F(B,T) \quad ,$$

(A.5)

where E_R is the magnitude of the incident field at R , and

$$F(B,T) = \frac{f(B)}{f(T)}$$

is a voltage response factor associated with the polar diagram of the receiving antenna, and depending on the antenna and its orientation. By definition, for an antenna whose beam is directed at T , $f(T) = 1$. Similarly, for $f(B)$. Both quantities are positive and, in general, $f(T), f(B) \leq 1$.

For the static tests it will be assumed that the blades are locked in the position $\theta_s = 0$ with $\phi_p = 0$. With the antenna beam directed at the WT, the received signal is recorded as the machine is yawed in azimuth. Under these conditions, the maximum value of $m(R)$ is obtained when the nacelle is pointed such that $\phi \approx -\phi_0$, and the resulting expression for the modulation index attributable to the front face of the upper blade is

$$\begin{aligned}
 m(R) = & \frac{2A}{\lambda r} \left| \cos \phi_0 \cos \alpha_c \right| \left| \operatorname{sinc} \left[\frac{L_1}{\lambda} \left\{ \sin \alpha_c - \sin(\alpha - \alpha_c) \right\} \right] \right| \\
 & \cdot \left| \operatorname{sinc} \left[\frac{L_2}{\lambda} \sin \phi_0 \left\{ \cos \alpha_c - \cos(\alpha - \alpha_c) \right\} \right] \right| \left| \sin \left(\frac{2\pi h_a h_t}{\lambda r} \right) \right| \frac{E_B}{E_R} F(B,T) .
 \end{aligned}
 \tag{A.6}$$

This is used in §5.2 to analyze the static test data. The analogous result for the front face of the lower blade is obtained by replacing α_c by $\pi - \alpha_c$, and if the nacelle pointing direction is reversed, the corresponding expression for the rear face contribution is obtained by replacing α_c by $2\pi - \alpha_c$ for the upper blade, and by $\pi + \alpha_c$ for the lower blade.

In a dynamic situation with the blades rotating, the derivation of expressions for the scattered field and modulation levels as functions of time is quite involved. However, our previous results [6,12] showed that for reception in directions away from the specularly reflected and forward scattering directions, the scattered field is a maximum when $\theta_s = 0$, and if this is still true, the maximum modulation index attributable to the upper plate is given by (A.5). Because of the blade coning, the effect of the lower blade (obtained by replacing α_c by $\pi - \alpha_c$) is negligible away from the specular and forward directions.

In or near the forward direction $\phi = \pi + \phi_0$, the maximum scattered signal is obtained when the blade is horizontal ($\phi_s = \pi/2$). The modulation indices attributable to the blades are

$$\begin{aligned}
 m_{1,2} &= \frac{2A}{\lambda r} \left| \cos(\phi_0 \mp \alpha_c) \cos \phi_p \right| \left| \operatorname{sinc} \left[\frac{L_1}{\lambda} \left\{ \cos \phi_p \sin(\phi_0 \mp \alpha_c) \right. \right. \right. \right. \\
 &+ \left. \left. \left. \cos(\alpha - \phi_p) \sin(\phi \mp \alpha_c) \right\} \right] \right| \left| \operatorname{sinc} \frac{L_2}{\lambda} \left[\sin \phi_p - \sin(\alpha - \phi_p) \right] \right| \\
 &\cos \alpha_c \mp \left\{ \cos \phi_p \cos \phi_0 + \cos(\alpha - \phi_p) \cos \phi \right\} \sin \alpha_c \left| \right. \\
 &\cdot \left| \sin \left(\frac{2\pi h_a h_t}{\lambda r} \right) \right| \frac{E_B}{E_R} F(B,T) \quad , \quad (A.7)
 \end{aligned}$$

where the suffix 1 and the upper signs apply to the 'upper' blade, and the suffix 2 and the lower signs to the 'lower' blade. Since the two blades now provide in-phase contributions to the scattered field, the total modulation level in the forward region is

$$m(R) = m_1 + m_2 \quad . \quad (A.8)$$

A.3 Modulation Level

The amount of video distortion observed at any site is determined by the modulation level (or index) m of the received signal, and this can be obtained from dynamic measurements of the

signal versus time. Under certain conditions, the maximum possible modulation can also be derived from static measurements and then used to obtain the equivalent scattering area of a blade (see §5.2).

For the static and dynamic tests the spectrum analyzer is tuned to the audio carrier frequency of the TV Channel. This is done because the audio signal is frequency modulated and, after first (or envelope) detection by the spectrum analyzer, is noise-like and ideally constant. Extraneous amplitude modulation is then easy to identify in the strip chart recorder output. It is assumed that the modulation suffered by the video signal is approximately the same as that of the audio signal P_a .

The dynamic tests yield recordings of P_a (in dBm) versus time. Any extraneous modulation shows up as fluctuations in dB above and below the ambient level, and from the total dB variation Δ , the modulation index can be deduced using the relationship

$$\Delta = 20 \log_{10} \frac{1+m}{1-m} \quad , \quad (A.9)$$

which is plotted in Fig. A-5. The modulation threshold m_0 is the largest value of m for which the video distortion is still judged to be acceptable, and has been established as 0.15 (i.e., $\Delta = 2.6$ dB) in the backscattering direction, increasing uniformly with angle to 0.35 (i.e., $\Delta = 6.3$ dB) in the forward direction. The latter is for a strong ambient signal ($P_a \gtrsim -60$ dBm), and could be as small as 0.15 in a weak signal area.

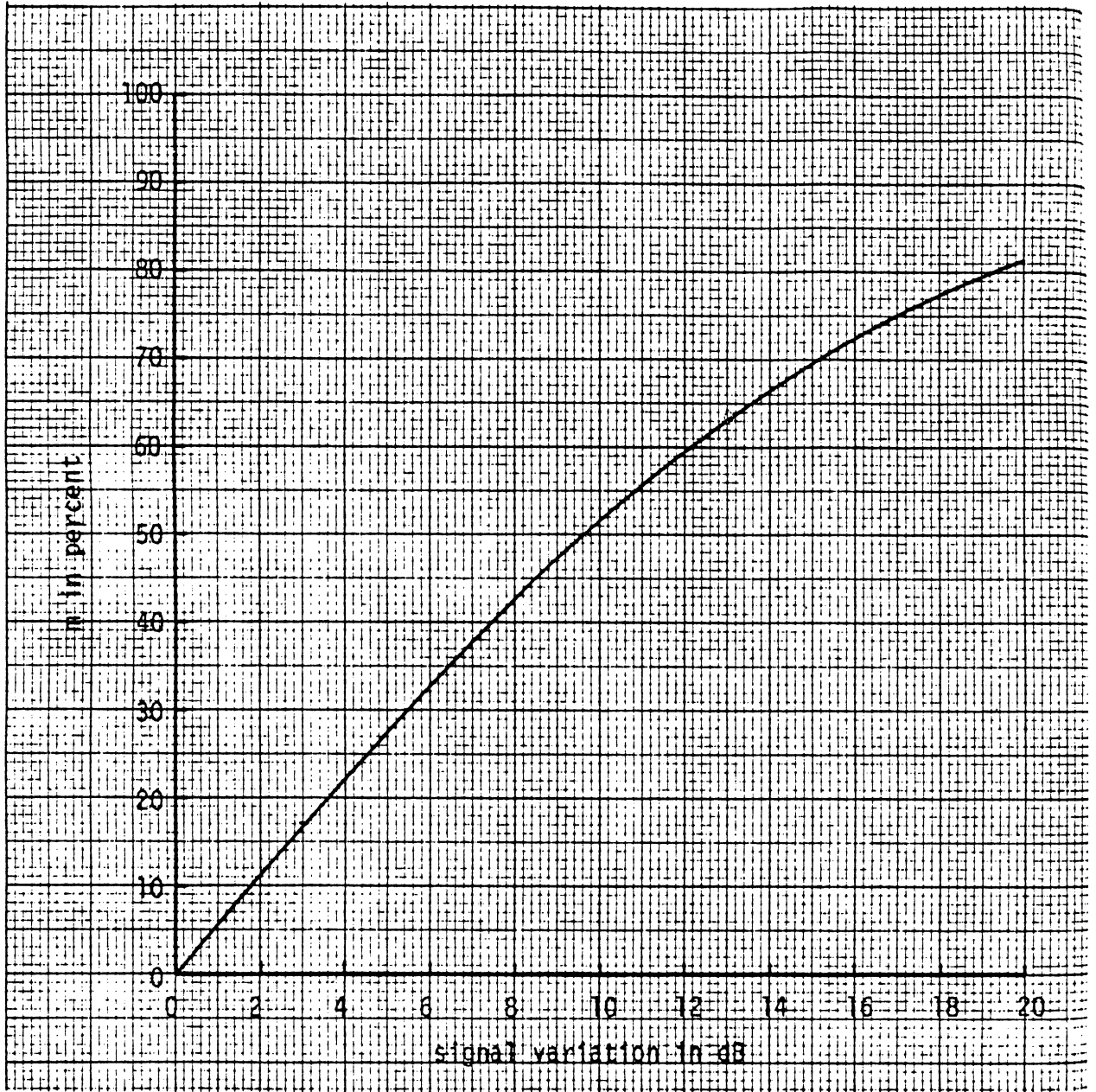


Fig. A-5 Percent modulation as a function of the total dB variation of the observed signal.

APPENDIX B: TEST PLAN

For the benefit of those who may wish to perform tests of the type described, it may be helpful to present our test plan. To the extent possible and appropriate, the entire sequence was followed at each of the sites A through J, and for all of the TV Channels of interest.

The equipment required is as follows:

- spectrum analyzer (S.A.)
- x-y recorder
- video recorder
- television receivers (2, identical)
- antenna
- antenna tower (minimum height 15 ft)
- antenna rotor and control box
- *portable power supply
- *line conditioner
- compass
- portable radio transceivers ('walkie-talkies') (2)
- 75-ohm coaxial cable
- 50-ohm coaxial cable
- AC power cord

*Not needed if commercial power is available.

The steps required to set up the equipment are:

- 1.1 Assemble the antenna, rotor and mast to position the antenna at least 15 ft above the ground.
- 1.2 Interconnect the antenna rotor and rotor control box.
- 1.3 Interconnect the antenna, S.A. and x-y recorder.
- 1.4 Calibrate the S.A. and x-y recorder.

The following measurements are carried out with the WT stationary and are needed to determine the ambient fields and the antenna response in the local environment.

- 2.1 Position the antenna so its main beam is in the computed direction of the TV transmitter of the Channel of interest.
- 2.2 Adjust the frequency response of the S.A. to display and record the video and audio spectra.
- 2.3 Rotate the antenna to give maximum signal.
- 2.4 Record the audio and video spectra using the x-y recorder, noting the following information on the recording:
 - compass heading of the antenna's main beam
 - TV Channel number
 - date and time
- 2.5 Readjust the frequency of the S.A. to coincide with that of the maximum signal level of the audio spectrum.
- 2.6 Record a power versus time plot, noting the following information on the recording:
 - power level of the audio spectrum
 - WT nacelle pointing direction
 - TV Channel number
 - date and time

A complete sequence of static tests is as follows:

- 3.1 Set the pitch of the WT blades for maximum power, lock the blades in a vertical position with respect to the ground, and repeat step 2.3.
- 3.2 Adjust the frequency response of the S.A. to coincide with that of the maximum signal level of the audio spectrum.
- 3.3 Yaw the WT through 360° and record a power versus time plot, noting the following information on the recording:
 - power level of the audio spectrum
 - compass heading of the antenna's main beam
 - TV Channel number
 - date and time
- 3.4 Rotate the WT blades to 45° from the vertical, and repeat steps 3.1 through 3.3.
- 3.5 Rotate the WT blades to position them horizontal, and repeat steps 3.1 through 3.3.
- 3.6 Rotate the WT blades a further 45° to position them 135° with respect to the vertical and repeat steps 3.1 through 3.3.
- 3.7 Repeat steps 3.1 through 3.6 with the main beam of the antenna pointed at the WT.

The dynamic tests to measure the actual interference are carried out with the WT blades rotating, and are as follows:

- 4.1 Repeat steps 2.5 and 2.6, noting also the pitch and rpm of the blades.
- 4.2 Record a pattern of the antenna, noting the following information on the recording:
 - power level of the audio spectrum
 - WT nacelle pointing direction

TV Channel number

date and time

4.3 Interconnect the antenna, TV receiver and video recorder.

4.4 Make a 30 second video recording of the TV program being viewed, noting the following information in a log book:

perceived degree of video distortion identifiable with the

WT blade rotation

WT nacelle pointing direction

wind direction

WT rpm

TV Channel number

date and time

4.5 Interconnect the antenna, S.A. and x-y recorder.

4.6 Rotate the antenna to point its main beam at the WT.

4.7 Repeat steps 2.6 and 2.6.

The above tests are performed on each TV Channel of interest at all of the sites. Re-ordering is possible in the light of weather and/or other conditions.

REFERENCES

1. _____, "2000-kilowatt wind-turbine project," NASA Lewis Research Center Report, January 1980.
2. _____, "Reference data for radio engineers," Howard W. Sans & Co., Inc., Indianapolis, 1975; pp. 28-9 to 28-11.
3. loc. cit., p. 30-18.
4. G. W. Bartlett, Editor, National Association of Broadcasters Engineering Handbook, Sixth Edition, National Association of Broadcasters, Washington, D.C., 1975, pp. 377-378.
5. T.B.A. Senior, D. L. Sengupta and J. E. Ferris, "TV and FM interference by windmills," University of Michigan Radiation Laboratory Report 014438-1-F, February 1977.
6. D. L. Sengupta and T.B.A. Senior, "Electromagnetic interference by wind turbine generators," University of Michigan Radiation Laboratory Report 014438-2-F, March 1978 (TID-28828).
7. D. L. Sengupta and T.B.A. Senior, "Electromagnetic Interference to Television Reception Caused by Horizontal Axis Windmills," Proc. IEEE, Vol. 67, No. 8, pp. 1133-1142, August 1979.
8. D. L. Sengupta and T.B.A. Senior, "Wind turbine generator interference to electromagnetic systems," University of Michigan Radiation Laboratory Report 014438-3-F, August 1979.
9. D. L. Sengupta, T.B.A. Senior and J. E. Ferris, "Television interference tests on Block Island, RI," University of Michigan Radiation Laboratory Report 014438-3-T, January 1980.

10. T.B.A. Senior and D. L. Sengupta, "Wind turbine generator siting handbook," University of Michigan Radiation Laboratory Report 014438-2-T, December 1979.
11. _____, Reference Data for Radio Engineers, Howard W. Sams & Co., Inc., Indianapolis, 1975, pp. 30-13, 30-15.
12. D. L. Sengupta and T.B.A. Senior, Wind Turbine Interference to Television Reception, University of Michigan Radiation Laboratory Report No. 014438-4-F, September 1980.
13. I. J. LaHaie and D. L. Sengupta, "Scattering of Electromagnetic Waves by a Slowly Rotating Rectangular Metal Plate," IEEE Trans., Vol. AP-27, No. 1, pp. 40-46, January 1979.